PMEL Tsunami Forecast Series: Vol. 067

A Tsunami Forecast Model for Santa Monica, California

Diego Arcas[1,2]

[1]Joint Institute for the Study of the Atmosphere and Ocean (JISAO), University of Washington, Seattle, WA

[2]NOAA/Pacific Marine Environmental Laboratory (PMEL), Seattle, WA

June 2, 2014

Contents

List of Figures

List of Tables

Foreword

Tsunamis have been recognized as a potential hazard to United States coastal communities since the mid-twentieth century, when multiple destructive tsunamis caused damage to the states of Hawaii, Alaska, California, Oregon, and Washington. In response to these events, the United States, under the auspices of the National Oceanic and Atmospheric Administration (NOAA), established the Pacific and Alaska Tsunami Warning Centers, dedicated to protecting United States interests from the threat posed by tsunamis. NOAA also created a tsunami research program at the Pacific Marine Environmental Laboratory (PMEL) to develop improved warning products.

The scale of destruction and unprecedented loss of life following the December 2004 Sumatra tsunami served as the catalyst to refocus efforts in the United States on reducing the tsunami vulnerability of coastal communities, and on 20 December 2006, the United States Congress passed the "Tsunami Warning and Education Act" under which education and warning activities were thereafter specified and mandated. A "tsunami forecasting capability based on models and measurements, including tsunami inundation models and maps." is a central component for the protection of United States coastlines from the threat posed by tsunamis. The forecasting capability for each community described in the PMEL Tsunami Forecast Series is the result of collaboration between the NOAA office of Oceanic and Atmospheric Research, National Weather Service, National Ocean Service, National Environmental Satellite Data and Information Service, the University of Washington's Joint Institute for the Study of the Atmosphere and Ocean, National Science Foundation, and United States Geological Survey.

NOAA Center for Tsunami Research

Abstract

The present study documents the development of a tsunami forecast model for Santa Monica, California. Santa Monica is a highly populated major resort town with extensive entertainment areas along the beach, visited every year by thousands of local residents and tourists. Santa Monica is 8 miles north of Los Angeles International Airport (LAX), a critical facility in the event of a natural disaster. The forecast model grid therefore includes the cities of Venice Beach, Marina del Rey, and El Segundo in order to encompass LAX. In addition, special attention was given to ensure the Channel Islands, offshore of Santa Monica Bay, were represented with enough resolution in the forecast model grids, so that the correct tsunami wave dynamics between the various islands and the main coast were adequately captured by the model. In order to guarantee the accuracy, robustness, and stability of the forecast model in an operational environment, 13 historical events have been simulated and results compared with tide gauge observations whenever data were available. In addition, the robustness of the model to very large events has been tested by simulating 19 synthetic, Mw=9.3 events originating in different subduction zones throughout the Pacific Ocean. Results from both the historical and synthetic simulations show that Santa Monica has been relatively free from major tsunami impact in recent history. However, tsunamigenic earthquakes in certain areas of the Pacific Ocean can generate large tsunamis in the Santa Monica region. Contrary to intuition, the areas that pose the highest tsunami risk to Santa Monica do not seem to be the nearby Cascadia or Mexican coasts, but rather the Manus oceanic convergence boundary, in the Melanesia area of the southwest Pacific.

Chapter 1

Background and Objectives

The NOAA Center for Tsunami Research (NCTR) has developed a tsunami forecasting capability for operational use by NOAA's two Tsunami Warning Centers located in Hawaii and Alaska (Titov et al., 2005). The system is designed to efficiently provide basin-wide warning of approaching tsunami waves. The system, termed Short-term Inundation Forecast of Tsunamis (SIFT), combines real-time tsunami event data with numerical models to produce estimates of tsunami wave arrival times and amplitudes at one or more coastal communities of interest. The SIFT system integrates several key components: deep-ocean, real-time observations of tsunamis, a basin-wide pre-computed propagation database of water level and flow velocities based on potential seismic unit sources, an inversion algorithm to refine the tsunami source based on deep-ocean observations during an event, and optimized tsunami forecast models.

The objective of the present work is to construct a tsunami inundation model for Santa Monica, California, that can be used by the Tsunami Warning Centers to assess, in real time, the local impact of a tsunami generated anywhere in the Pacific Ocean. The city of Santa Monica is located on the western oceanfront edge of the city of Los Angeles, just 16 miles from the heart of downtown Los Angeles, and 8 miles from Los Angeles International Airport. The city of Santa Monica is located on the western oceanfront edge of Los Angeles, just 16 miles from the city center and 8 miles from Los Angeles International Airport. The population is 88,050 residents (U.S. Census Bureau, 2006 estimates). The population density is 10,170 per square mile (U.S. Census Bureau 2000 estimates).

One of the city's major centers of attraction is its renowned Third Street Promenade, a three-block outdoor shopping mall that opened in the late 1980s and draws an estimated 7,000 daily visitors. The northern part of the city's coastline is separated from the shoreline by an approximately 300-m-wide stretch of sandy beach and a 20-m-high bluff of unconsolidated sediments, which protects the city from tsunami impact. The structure most vulnerable to tsunami attack in the northern part of the city is the pier, which is also one of the city's main attraction centers, featuring an amusement park, an aquarium, and a multitude of restaurants. The Santa Monica pier is patronized on a daily basis by hundreds of tourists and visitors.

The bluff, protecting the city from tsunami impact along the Northern shoreline, disappears approximately south of the point where Interstate 10 reaches the coastline. South of this point, a slightly narrower (approximately 150 m wide) sandy beach is the only protection from tsunami inundation. An aerial view of Santa Monica can be found in Figure 1 showing the location of the the Santa Monica pier, Interstate 10, and the beach that separates the city from the ocean.

The most relevant bathymetric feature offshore of Santa Monica is the presence of the Channel Islands, which historically seems to have provided protection from tsunamis rather than trapping and focusing the waves.

Even though the present study is concerned with the development of a tsunami forecast model for seismically generated tsunamis, the morphology of the coastline along Santa Monica Bay, with extensive areas occupied by bluffs and cliffs of unconsolidated sediments, pose a considerable risk for landslide generated tsunamis. This is particularly evident to the south of the study area (Borrero et al., 2002), where submarine landslide scars are evident along the Palos Verdes Peninsula as seen in Figure 2.

Due to the strategic importance of Los Angeles International Airport and its proximity to the study site, the inundation model generated in the present work was designed to include not only Santa Monica, but also Venice Beach, Marina del Rey, and El Segundo, in the study area. This grid extension will provide tsunami forecasts for the seaward side of the airport while still satisfying the requirements of computational speed.

The existence of a National Ocean Service (NOS)-operated tide gauge on the Santa Monica pier, which was established on 29 May 1950, is crucial to the development of a tsunami forecast model since it provides historical data for model validation and the possibility of quantitative assessment of model accuracy in future events. The high population density in the vicinity of Santa Monica, together with its regional economic importance, offer ample justification for the development a tsunami forecast model of the site.

This report details the development of a high-resolution tsunami forecast model for Santa Monica, California, including development of the bathymetric grids, model validation with historical events, and stability testing with a set of synthetic mega-tsunami events (Mw 9.3). Inundation results from such artificial events are presented in later sections.

Chapter 2

Forecast Methodology

A high-resolution inundation model was used as the basis for an operational forecast model in order to provide an estimate of wave arrival time, height, and inundation immediately following tsunami generation. Tsunami forecast models are run in real time while the tsunami in question is propagating across the open ocean. These models are designed and tested to perform under very stringent time constraints, given that time is generally the single limiting factor in saving lives and property. The goal is to maximize the amount of time that an at-risk community has to react to a tsunami threat by providing accurate information quickly. To this end, the tsunami propagation solution in deep water is pre-computed in the linear wave regime and used to force the inundation forecast models during the last stage of tsunami propagation and runup.

The tsunami forecast model, based on the Method of Splitting Tsunami (MOST), emerges as the solution in the SIFT system by modeling real-time tsunamis in minutes while employing high-resolution grids constructed by the National Geophysical Data Center. Each forecast model consists of three telescoped grids with increasing spatial and temporal resolution for simulation of wave inundation. The forecast model utilizes the most recent bathymetry and topography available to reproduce the correct wave dynamics during the inundation computation. Forecast models are constructed for populous at-risk coastal communities in the Pacific and Atlantic Oceans. Previous and present development of forecast models in the Pacific (Titov et al., 2005; Titov, 2009; Tang et al., 2009; Wei et al., 2008) have validated the accuracy and efficiency of the forecast models currently implemented in the SIFT system for real-time tsunami forecast. The model system is also a valuable tool in hind-cast research. Tang et al. (2009) provide forecast methodology details.

Chapter 3

Model Development

Modeling of coastal communities is accomplished by development of a set of three nested grids that telescope down from a large spatial extent to a grid that finely defines the bathymetric and topographic features of the community under study. The basis for these grids is a high-resolution digital elevation model constructed by either NCTR or, more commonly, by the National Geophysical Data Center (NGDC) using best available bathymetric, topographic, and coastal shoreline data for an at-risk community. For each community, data are compiled from a variety of sources to produce a digital elevation model referenced to Mean High Water in the vertical and to the World Geodetic System 1984 in the horizontal (http://ngdc.noaa.gov/mgg/in undation/tsunami/inundation.html). From these digital elevation models, a set of three high-resolution reference models are constructed which are then "optimized" to run in an operationally specified period of time. Due to the necessary subsampling of grid resolution that takes place during the optimization process, some small bathymetric and topographic features may disappear from the grids. Some of these features, such as breakwaters and jetties, may have a significant impact on local tsunami wave dynamics, and their disappearance from the grids may impact the quality of the forecast significantly. Therefore, it is important to ensure that these sub-grid features are present in the operational models. To this end, their size should be increased by manually adding dry grid-nodes to guarantee that their presence will be reflected in the forecast grids. Increasing their size will have a very limited effect on tsunami dynamics, but their absence will have a major impact on the simulation.

The bathymetry and topography used in the development of this forecast model was based on a digital elevation model provided by the National Geophysical Data Center, and the author considers it to be an adequate representation of the local topography/bathymetry. As new digital elevation models become available, forecast models will be updated, and report updates will be posted at *http://nctr.pmel.noaa.gov/forecast_reports*.

3.1   Forecast area

Santa Monica is a city along the shores of Santa Monica Bay in Southern California. It was incorporated into Los Angeles County in 1886. The Santa Monica municipal territory includes the stretch of coastline between 34.025° N, 118.517° W and 33.995° N, 118.484° W, as indicated by the highlighted area in Figure 3. The forecast area covered by the present forecast model extends beyond the limits of the City of Santa Monica, encompassing the stretch of coastline

4

between Temescal Canyon north of Santa Monica and El Segundo Boulevard to the south, next to Los Angeles International Airport. Santa Monica is of vital importance to the local economy. Even though the city was eclipsed as the port of Los Angeles by San Pedro (Encyclopedia Britannica), Santa Monica remains a prime beach and vacation resort due to its mild climate and its proximity to Los Angeles. In addition to its entertainment venues, the city has motion-picture, biotechnology, software, communications and aerospace industries. Several state parks often crowded with local residents and visitors are located in close proximity to Santa Monica and are included in the forecast grids developed here.

3.2 Historical Events and Data

The Santa Monica tide gauge is located at the offshore end of the Santa Monica pier at 118.5000° W, 34.0075° N. Figure 4 shows the location of the tide gauge within the inundation grid (Grid C). The Santa Monica pier, at the end of which the tide gauge is located, has been eliminated from Grid C, since it stands on piles and does not affect wave dynamics underneath. Tidal time series reveal that the tidal range in Santa Monica is approximately 2 m. This is an important piece of information to keep in mind, since the stage of the tide during a tsunami event is vital in determining the actual amount of flooding. Data for historical tsunamis at the tide gauge were compiled in order to validate model calculations. Of the 13 historical tsunami events modeled in this study (see Table 1), data recorded by this tide gauge has been located for 11 of the 13 cases: 1994 Kuril Islands, 1996 Andreanof, 2003 Rat Island, 2006 Tonga, 2006 Kuril Islands, 2007 Kuril Islands, 2007 Solomon Islands, 2007 Peru, 2010 Chile and 2011 Japan.

Within historical records, Santa Monica has not been severely impacted by large tsunamis of seismic origin. Significant events (exceeding 1 m wave height) include: 1964 Alaska, 1.6 m; 2010 Chile, 1.3 m; and 2011 Japan, 1.6 m. These values reflect both tide gauge observations and model results. (All observed wave height values have been filtered for tidal effects.). Lacking reliable source data for Kamchatka 1952 and Chile 1960, these events have been excluded from the historical validation series. Nevertheless these 2 tsunamis, with wave heights of 1.6 m and 1 m respectively (California Geological Survey and NDGC data base), are among the events that have most severely affected Santa Monica in the past 50 years. The Chile 1960 event generated inundation up to 91 m inland (NGDC based on eyewitness observation). To the knowledge of this author, no inundation was reported at Santa Monica from either the 1964 Alaska or the 2011 Japan events. Because the tidal range in Santa Monica is larger than the maximum wave amplitude recorded for any of the historical tsunami events, the tsunami inundation extent would be largely determined by the level of the tide at the time of peak tsunami arrival.

3.3 Model Setup

Setup of the computational grids for the MOST code (Titov et al., 1998) requires a total of 3 nested grids, for which the outer Grid A has the lowest spatial resolution but covers the largest area, and the inner grid C has the highest spatial resolution, but covers a reduced geographical area. The code makes use of an additional intermediate Grid B with medium resolution and spatial coverage. Each interior grid area is completely enclosed in the coverage area of the immediate exterior grid, and inundation is computed only in the most interior grid (Grid C). The set of three nested grids ensures that, as the tsunami wavelength shrinks when it travels

from deep to shallow waters, the model maintains an approximately constant number of grid nodes per wavelength. As mentioned earlier in Chapter 2.0, this set of 3 nested grids is forced by a pre-computed solution on an ocean-wide grid at lower resolution.

This set of telescoping grids is designed to simulate the last stage of tsunami propagation in shallow water and inundation onto dry land. The onset of non-linear behavior in wave propagation prevents us from obtaining the solution of tsunami propagation in shallow water from a linear combination of unit sources extracted from the pre-computed propagation database. The appearance of non-linear effects is associated with the elevated values of wave amplitude and reduced values of water depth encountered in shallow waters. When the ratio of wave amplitude to local depth is not negligible, the solution can be expected to exhibit non-linear features. In practice, one can expect non-linear effects to appear quite close to the shoreline. Although nonlinearities and the appearance of high-frequency waves both require the use of higher resolution grids, it is the latter that manifests in deeper water, thereby determining the offshore extent of the outer forecast model grid (Grid A). Consequently, it is standard practice to extend the offshore boundary of the forecast model grids to waters beyond the continental shelf.

During the development of an operational forecast model, a higher resolution set of grids referred to as the reference model is generated first. The purpose of the reference model is to evaluate grid convergence between a high-resolution model and the forecast model, ensuring that the solution obtained with the lower-resolution forecast model is consistent with that of the high-resolution reference model.

In the case of Santa Monica, two factors determined the design of the model grids. The first one is the presence of a wide continental shelf that interacts with the oncoming tsunami wave, causing it to slow down and reduce its wavelength. It is important that, after the wavelength reduction takes place, the model maintains enough grid nodes per wavelength in order to minimize numerical dispersion and dissipation (Burwell et al., 2007). To achieve this, the largest grid (Grid A) was designed to extend beyond the continental shelf into waters with a depth larger than 1500 m. This ensures that the wave is transferred from the lower resolution ocean-wide grid to the finer resolution outer grid (Grid A) of the forecast model for Santa Monica before it reaches the shallow waters of the continental shelf, i.e., before its wavelength begins to shrink. For this same reason, grid coverage has remained constant between the reference and forecast models.

The second factor to take into consideration in grid design is the presence of the Channel Islands offshore of Santa Monica. It is not immediately clear how tsunamis will be affected as they pass the islands; the Channel Islands may shield Santa Monica Bay from the force of the waves, or reflection and interference of the waves interaction with the islands may intensify the waves' power. These high frequency waves necessitate the modification of the grid boundaries to account for the influence of offshore islands. The A grid was therefore extended to include the Channel Islands; similarly, the intermediate B grid was designed to include Santa Catalina Island.

The fine resolution inundation grid (Grid C) was extended south to include not only the city of Santa Monica, but also Venice Beach, Marina del Rey and El Segundo, so that the southern part of the grid would also cover Los Angeles International Airport.

Figure 3 shows an orthographic projection of the city of Santa Monica and surrounding areas and Figures 5 and 6 show identical grid area coverage and relative grid position with respect to the community and local bathymetric features, for the reference and forecast models, respec-

tively. Table 2 summarizes the parameters and model set up for each set of grids.

Even though the non-linear shallow water equations solved by MOST do not explicitly contain frequency dispersion terms, the resolution of the propagation grid has been selected to match the inherent numerical dispersion of the numerical solution to the physical dispersion specified by linear theory. Since the behavior of tsunami waves in deep water is highly linear, this approximation should provide an accurate representation of dispersive effects in deep water. In shallow water, this approximation of numerical dispersion to the linear dispersion relation is not as valid, but the solutions computed with MOST will still exhibit a certain amount of both numerical and amplitude dispersion. Amplitude dispersion is mainly associated with non-linear effects in shallow water when tsunami wave amplitudes and current speed are non-negligible compared to the local water depth and wave propagation speed.

The original bathymetric and topographic grid data used in the development of the Santa Monica model were provided, under PMEL contract, by NGDC. Details of data gathering and grid construction techniques, used by NGDC in the generation of the original grid are provided by Caldwell et al., (2011).

Chapter 4

Results and Discussion

Three types of tests were performed to assess the forecast model convergence, accuracy and robustness characteristics. To assess model convergence, results obtained with the reference model were compared with those obtained with the forecast model to confirm consistency of results at least for the leading tsunami waves. This type of test is not, strictly speaking, a grid convergence test in the sense used in computational science, since the solution is compared on grids with varying resolution, coverage and bathymetric information; however, it provides a good estimate of the similarities and discrepancies between the solutions of a more accurate, high resolution model of the area and that of a coarser resolution run-time optimized forecast model.

The accuracy of both the reference and the forecast models is evaluated by comparing modeled and recorded data for a set of historical events.

Robustness tests include the simulation of 19 tsunamis generated by Mw 9.3 earthquakes throughout the Pacific basin. Figures 7 and 8 show the epicenter of the historical events and center of the rupture segment for each of these artificial mega-events, respectively. The forecast model proved to run smoothly and without instabilities during 24 hours of simulation for each of these synthetic mega-events.

4.1 Model Validation

Model validation using historical events is accomplished by comparing the modeled time series at the location of the tide gauge with that recorded by the instrument during several tsunami events. The tidal level is assumed to be at Mean High Water (MHW) as specified in Caldwell et al., (2011) . In the case of Santa Monica, the site has not been seriously impacted by any of the 13 historical cases under investigation here (or by either of the other two large Pacific tsunamis of the last century: 1960 Chile and 1964 Alaska). Contributing to this may be the fact that most of the large historical events have arrived during low tide at Santa Monica, therefore, there are no guarantees that future events will not have a larger impact on the area. Consequently for a couple of the tsunamis for which comparison results are presented here, the tsunami signal was below the noise level of the recorded tide gauge signal. Such is the case for 1994 Kuril Islands and 2003 Rat Island. Although a comparison between the observed waveform and model results is not possible in these cases, results of the model runs reveal that, the predicted tsunami amplitude at Santa Monica during those two events was below the noise level of the tide

gauge, which is also extremely valuable information from an emergency management stand-point. There are two tested historical cases in which the tsunami signal is just barely above the tide gauge noise level, the 2007 Kuril and 2007 Solomon events. In both of these cases, the predicted tsunami signal also falls very close in amplitude to the observed signal, however, because of the low signal-to-noise ratio in these cases, a waveform comparison is not possible here either. For seven of the historical events both the observed and the modeled signals are above the noise level of the tide gauge and waveform comparison is feasible:

1. 1964 Alaska: Even though there is approximately 10 minutes of mismatch between the predicted and the recorded arrival time of the tsunami, model results show very good agreement with observations particularly during the first two hours of wave activity and even beyond. Model results reflect the maximum wave height and wavelength quite accurately for this event.

2. 1996 Andreanof: The forecasted tsunami model here fails to capture the full amplitude of the tsunami waves during this event. A possible reason for this discrepancy in tsunami magnitude between forecast model and observations is probably found in the source definition for this event, since the forecast model and the observed data seems to correlate better in all the other cases.

3. 2006 Kuril Islands: For the this event, the forecasted results seem to capture well the overall magnitude of the event based on the observed data. However, the model fails to capture some peak values reflected in the observed time series. In this case, also, the forecasted waveform decays faster than the observed data shows.

4. 2006 Tonga: In this case, a good comparison in amplitude between the forecast model and the measured data can be observed. The forecasted tsunami, however, seems to decay faster than the observations indicate. A possible cause for this can be the presence of trapped waves in Santa Monica Bay between the coast and the Channel Islands not being captured by the model.

5. 2007 Peru: In this case the predicted results forecast the correct overall magnitude of the tsunami, although with peak and trough values slightly below the measured signal. A slight shift in model arrival time is also observed in this case.

6. 2010 Chile: The Chile 2010 event is the second largest historical tsunami tested here. Comparison with the observed waveform exhibits an excellent correlation during the first hour of tsunami activity with the overall magnitude of the event being captured correctly throughout. A slight early arrival of the model can also be observed in this case.

7. 2011 Japan: This is the largest historical event tested in this series with a peak-to-trough amplitude of 1.4 m correctly captured by the forecasted time series. Model signal arrival seems to occur approximately 10 minutes earlier than observations which results in the forecasted and observed wave forms being out of phase by almost 1/4 period. The tsunami decay rate seems to be captured correctly in this case.

Although a formal study of the simulation of trapped and leaky wave modes on the continental shelf in the southern California area (Munk et al., 1964) is beyond the scope of this study and a

formal power spectrum analysis is not included in this report. It appears obvious from the results presented above, that the model is moderately successful at capturing the energy trapped in edge waves after arrival of the first tsunami waves. In most cases with a high signal to noise ratio, namely 2010 Chile and 2011 Japan, the initial maximum amplitudes are well captured by the model. However, the modeled signal seems to decay faster than observations in most cases except in the case of 2011 Japan where the decay rates of modeled and observed amplitudes are quite similar. The results seem to point to the correct capturing of resonant behavior on the shelf by the model for large events. However, reproduction of this resonant behavior may not be guaranteed for smaller tsunami events.

Comparison results at the tide station for the reference and forecast models are presented in Figures 9–21 with Figures 10–18 and 19–20 also displaying tide gauge data.

Comparisons between reference and forecast model time series (blue and red lines in Figures 9–21) reveal good agreement between both time series from tsunami arrival to almost 2 hours into the simulation for all computed cases with some minor discrepancies being observed during the simulation of the later waves.

Of the thirteen historical events simulated during the validation process, only three resulted in significant variations of the sea level in Santa Monica: 1946 Unimak Island, 2010 Chile and 2011 Japan. In the case of the last two events, tide-gauge data are available and agreement with modeled results is quite good. In the case of the 2010 Chile tsunami, the model-predicted maximum wave height is 1.3 m while the recorded value was 1.1 m. In the case of the 2011 Japan event, the maximum, modeled wave height is 1.4 m, which is basically the same as the recorded value. However, these maximum values are reached at different instants in each time series.

A thorough investigation of the reasons behind the deficient comparison between model and observations for some of the tested events is beyond the scope of this report. Many are the reasons that affect the accuracy of the results of any particular simulation; some of the most relevant sources of errors are listed below.

- Uncertainties in source definition: The definition of an accurate tsunami source for a particular seismic event is a complicated task. In general, it requires the solution of an inversion problem either from observation of seismic signals or from sea level observations. The most reliable inversions are those based on data provided by deep-water DART systems. These observations are direct sea-level measurements of tsunami waves during the linear regime of wave propagation. Consequently, inversion from DART gauges requires the solution of a linear inversion problem, as opposed to inversion from tide gauges, which requires the inversion of non-linear time series. In the absence of direct sea-level measurements of tsunami waves, a seismic inversion solution can be used as the initial condition for hydrodynamic calculations under the assumption that the sea-surface is identical to the sea-floor deformation.

-Deficiencies in grid resolution: It has been mentioned earlier that the resolution of the forecast models, although designed to produce fast results during operations, should be able to reproduce the main characteristics of most tsunamis. In order to do this, a minimum number of grid nodes per wavelength should be maintained. The frequency spectrum may change from one tsunami to another, with some tsunamis exhibiting higher energy density at higher frequencies than others. When this happens, the grid resolution of the forecast model may have difficulty in reproducing the correct characteristics for that particular event, which will result in the deterioration of the quality of the forecast.

-Bathymetric data errors: Inaccuracies in the bathymetric and topographic digital elevations models used in the construction of the numerical grids will have a direct impact on the accuracy of the computed tsunami prediction. It is essential to periodically assess the availability of bathymetric and topographic data for a particular site and to update the forecast models on a regular basis.

-Limitations of the mathematical model: Occasionally, a tsunami may have to be modeled for which the choice of mathematical model describing its behavior is not the most appropriate. In the case of MOST, the non-linear shallow water (NSW) equations are used. These equations are known to not have explicit terms to reproduce the physical behavior of frequency dispersion. When a tsunami occurs with wavelengths and amplitudes more appropriate to be described by a dispersive model, it is expected that some deficiencies in the solution computed with a non-dispersive model will appear.

In addition to tide gauge comparisons, the maximum sea-level elevation at each point on the inundation grid (Grid C) for every historical event simulated was computed and compared between the reference and forecast models. The main purpose here is to make sure that the distribution of the maximum wave height and inundation areas do not differ substantially between the reference and the forecast model. Figures 22–34 show this comparison with the reference model results exhibiting slightly higher maximum amplitudes over the forecast models for almost every historical event, except in the cases of the 2007 Solomon and 2011 Japan events, in which the forecast model results very slightly exceeded the reference model. Since there was no significant flooding from any of these historical events in the Santa Monica area, flooding areas where not compared, but forecast models correctly predicted the absence of inundation in Santa Monica for the tested historical events.

4.2   Model Stability Testing Using Synthetic Scenarios

During model stability testing, 19 mega-tsunamis (earthquake Mw 9.3) were simulated using the forecast model. Details of the 19 synthetic events tested can be found in Table 3. Each of these extreme synthetic events is constructed along a 1000-km-long and 100-km-wide fault plane with uniform slip amount of 25 m along the fault (Gica et al., 2008). The output from the code at every time step was visualized and inspected for instabilities. The cause of any instability was corrected and a final set of forecast grids emerged from the process. During development of the forecast model, some instabilities associated with lack of resolution were corrected to resolve small bathymetric and topographic features. These instabilities were not present in simulations conducted at higher resolution with the reference model. The instabilities occurred mainly in two areas:

1. The breakwater at the entrance of Marina del Rey boat harbor and canal: The solution here was to thicken the jetty by adding a few dry grid nodes along the offshore side of the jetty, which will allow for a better resolution of this feature in the forecast grid, without any major impact on the local tsunami dynamics.

2. The various waterways of Marina del Rey small boat harbor: The inner waterways of Marina del Rey harbor leading to the boat slips were widened, by adding a few wet grid nodes along the wet side of the waterways, which should only have an effect on the high frequency tsunami dynamics inside the marina.

11

The effect of both modifications above can visually be observed in the comparison of maximum water elevation plots for the reference and forecast model results for the historical cases shown in Figures 22–34. As in the case of historical events, the maximum water elevation at every point (Figures 35–53) in the computational grid (Grid C) and the time series of each synthetic scenario (Figures 54–58) at the Santa Monica tide gauge were recorded. Maximum and minimum values of the water surface elevation at the tide gauge for each synthetic scenario can be found on Table 3. Although the original purpose of the robustness tests is not to assess the tsunami risk on the study site, it is important to note in Figures 54–58 that the maximum wave height falls below 4 m for all synthetic scenarios simulated here, except for synthetic scenario case 16 featuring a tsunami originating in the Manus oceanic convergence boundary, where the maximum computed wave height at the tide gauge is approximately 13.5 m (note the range in the vertical axis of synthetic case 16 in Figure 57). The extreme values in synthetic scenario 16 can be understood by examining the series of plots in Figures D1–D5 in Appendix D, which shows the intensity of the tsunami throughout the ocean basin. The intensity of the tsunami throughout the ocean basin is depicted in those images. Of the 19 synthetic scenarios computed here, scenario 16 directs energy focused towards the Southern California area, and Santa Monica in particular. The result is peak offshore wave amplitudes about 0.5 m, and shallow water wave heights greater than 13 m (as shown in the tide gauge time series plot of Figure 57). This extreme case causes flooding well beyond the predictions of the state of California's current tsunami inundation map of the area (particularly in the Marina del Rey / El Segundo area where LAX is located). Three images showing the tsunami inundation zone, as estimated by the California Emergency Management Agency, the University of Southern California and the California Geological Survey can be found in Figures D6–D8 of Appendix D (State of California, 2009). However, this does not imply inaccuracy of the State's current inundation map for Southern California since the seismic scenarios used for stability testing of the model in this study are designed strictly for testing of grid stability and may not represent a credible seismic scenario. It is also unclear what the vertical sea level datum used in the study by the State of California was, although it is standard practice to take a conservative approach by using MHW (Mean High Water) for the vertical datum. Tsunami inundation can be expected to be less extensive if the stage of the tide is below MHW.

In addition to the 19 Mw=9.3 synthetic events, one micro-tsunami (Mw=6.2, slip amount = 0.01 m) was tested to ensure that there are no artificially growing instabilities in the grid. A standard mid-size Mw=7.5 was also included in the set of simulations. The maximum sea surface elevation in the inundation grid can be seen for these two cases in Figures 59 and 60, respectively.

4.3   Summary and Conclusions

A set of tsunami forecast grids has been developed for operational use by the Tsunami Warning Centers utilizing the Method of Splitting Tsunami code. Two sets of grids were developed: a high-resolution set intended to provide reference values, and a forecast set designed to minimize processor run time and to provide real-time tsunami estimates for Santa Monica.

Unique geographic features of the Santa Monica region. e.g., the Channel Island on the continental shelf just offshore, as well as significant population centers and infrastructure, e.g., LAX, were given special consideration during the design of the Grids.

Examination of observed and modeled data for the several historical events simulated in this study reveals that Santa Monica Bay has been relatively protected from the impact of large

tsunami waves during the tsunami events of the last century. However, the study also identifies the Melanesia (Manus Oceanic Convergence Boundary) area of the Pacific Ocean as having the potential to direct tsunami energy towards the Southern California area in general, and to Santa Monica in particular, as evidenced in synthetic scenario 16.

Local tsunami events immediately to the north and south of Southern California, such as synthetic scenario 9 from the Cascadia subduction zone and synthetic scenario 10 from the Pacific Mexican coast, seem to have a limited impact on Santa Monica, despite their proximity (see figures D1 through D5 in Appendix D).

The design of the forecast model grids, which includes the Channel Islands in the intermediate resolution grid (Grid B) and the decision to extend the inundation grid south in order to encompass the Los Angeles International Airport has some impact in processor run time. The forecast model, however, is still capable of simulating 4 hours of tsunami activity in 7 minutes of wall clock time on an Intel Xeon E5670 2.3 processor.

Chapter 5

Acknowledgments

Chapter 6

References

Borrero, J.C., S. Cho, S. Gordon, J. Moore, H.W. Richardson, and C. E. Synolakis. (2002). Natural Disasters and California: The Regional Economic Cost of a Tsunami Wave Generated by the Palos Verdes Slide. *Report to the USC Zumberge Research and Innovation Fund*, August, 2002

Burwell, D. , E. Tolkova, H. A. Chawala, J. (2007). Diffusion and dispersion characterization of a numerical tsunami model. *Ocean Modelling*, Vol. 19, Issues 1-2, ISSN 1463-5003.52

Caldwell, R.J., L.A. Taylor, B.W. Eakins, K.S. Carignan, P.R. Grothe,, E. Lim and D.Z. Friday. (2011). Digital Elevation Models of Santa Monica, California: Procedures, Data Sources and Analysis National Geophysical Data Center. Boulder, Colorado, 2011.

California Geological Service. http://http://www.consrv.ca.gov/cgs/geologic_hazards/Tsunami. Historic Tsunamis in California (Table). /Pages/About_Tsunamis.aspx

Dartnell, P., J.V. Gardner. (1999). Sea-foor images and data from multibeam surveys in San Francisco Bay, southern California, Hawaii, the Gulf of Mexico, and Lake Tahoe, California-Nevada US Geological Survey Digital data Series DDS-55, version 1.0. (1999).

Encyclopedia Britannica. http://www.britannica.com/EBchecked/topic/523067/Santa-Monica

Gica, E., M. Spillane, V.V. Titov, C. Chamberlin, and J. C. Newman, (2008). Development of the forecast propagation database for NOAA's Short-term Inundation Forecast for Tsunamis (SIFT). *NOAA Tech. Memo*, OAR PMEL-139, NTIS: PB2008-109391, 89 pp (2008).

López, A. M. and E. Okal (2006). A seismological reassessment of the source of the 1946 Aleutian 'tsunami' earthquake. *Geophysical Journal International*, Vol. 165, Issue 3. DOI: 10.1111/j.1365-246X.2006.02899.x

Munk, W., F. Snodgrass, and F. Gilbert (1964). Long waves of the continental shelf: an experiment to separate trapped and leaky modes. *J. Fluid. Mech*, Vol. 20, part 4, pp. 529-554.

State of California (2009). Tsunami Inundation Map for Emergency Planning, Venice Quadrangle, County of Los Angeles; produced by California Emergency Management Agency, California Geological Survey, and University of Southern California-Tsunami Research Center; dated March 1, 2009, mapped at 1:24,0000 scale.

Tang, L., V.V. Titov, and C.D. Chamberlin (2009). Development, testing, and applications of site-specific tsunami inundation models for real-time forecasting. *J. Geophys. Res*, Vol.114, C12025, doi: 10.1029/2009JC005476, ISSN 1463-5003.52.

Titov, V.V., and C.E. Synolakis (1998). Numerical modeling of tidal wave runup. *J. Waterw. Port Coast. Ocean Eng*, 124(4), 157-171.

Titov, V.V., F.I. González, E.N. Bernard, M.C. Eble, H.O. Mofjeld, J.C. Newman, and A.J. Venturato (2005). Real-time tsunami forecasting: Challenges and solutions. *Nat. Hazards.*, 35(1), 41-58.

Titov, V.V. (2009). Tsunami forecasting. In *The Sea*, Vol. 15, Chapter 12, Harvard University Press, Cambridge, MA and London, England, 371-400.

U.S. Census. http://quickfacts.census.gov/qfd/states/06/0670000.html

Wei, Y., E. Bernard, L. Tang, R. Weiss, V. Titov, C. Moore, M. Spillane, M. Hopkins, and U. Kânoğlu. (2008). Real-time experimental forecast of the Peruvian tsunami of August 2007 for U.S. coastlines. *Geophys. Res. Lett.*, L04609, doi: 10.1029/2007GL032250.

FIGURES
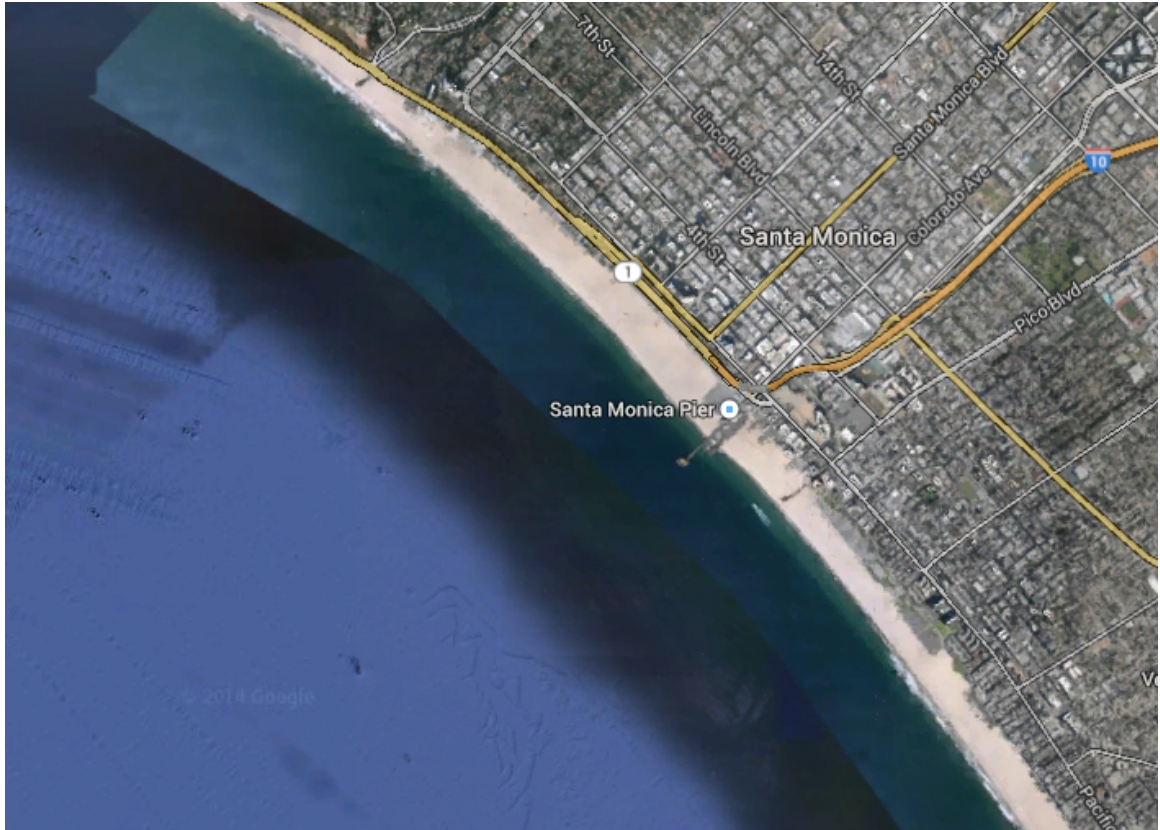
Figure 1: Aerial view of Santa Monica showing the location of the the Santa Monica pier, Interstate 10, and the beach that separates the city from the ocean.
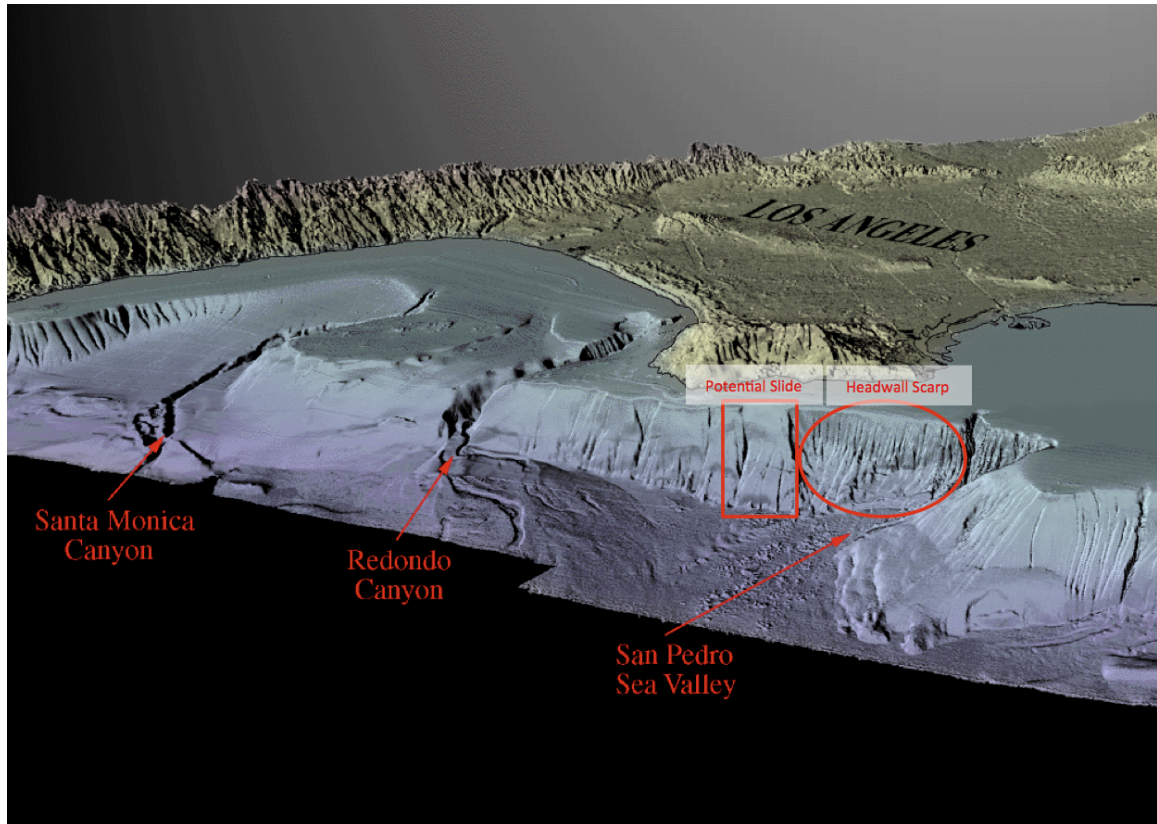
Figure 2: Multibeam shaded-relief of the Palos Verdes submarine debris slide in Southern California from Dartnell and Gardner (1999). The site of a potential slope failure next to the scar is also indicated in the image.

Figure 3: Orthographic view of the Santa Monica area and neighboring communities. The highlighted area indicates the municipal extent of the City of Santa Monica.
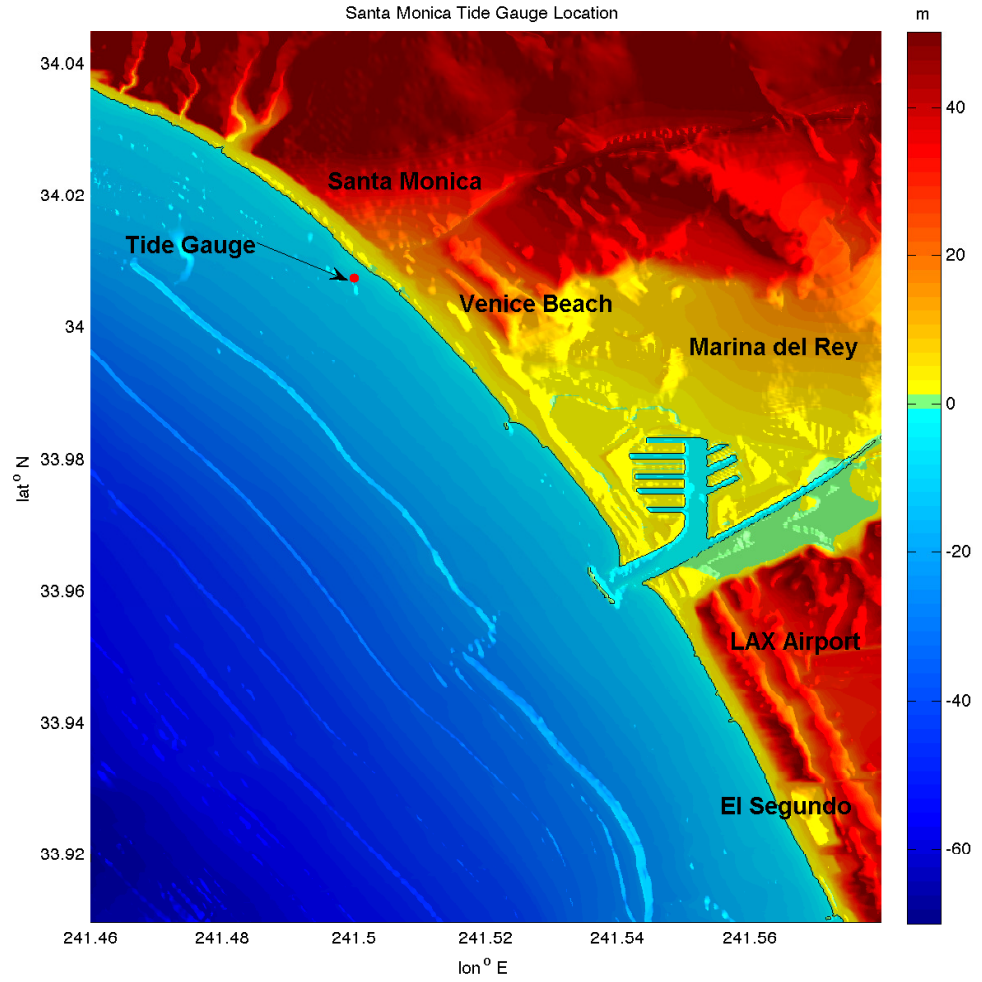
Figure 4: Bathymetric and topographic relief of Santa Monica and neighboring communities. Relief data are taken from NGDC Digital Elevation Model (DEM) used in the study. The Santa Monica and Venice Beach piers have been removed from the DEM since they stand on piles and do not affect wave propagation. The red dot indicates the location of the Santa Monica tide gauge on the Santa Monica pier (not shown on the image).
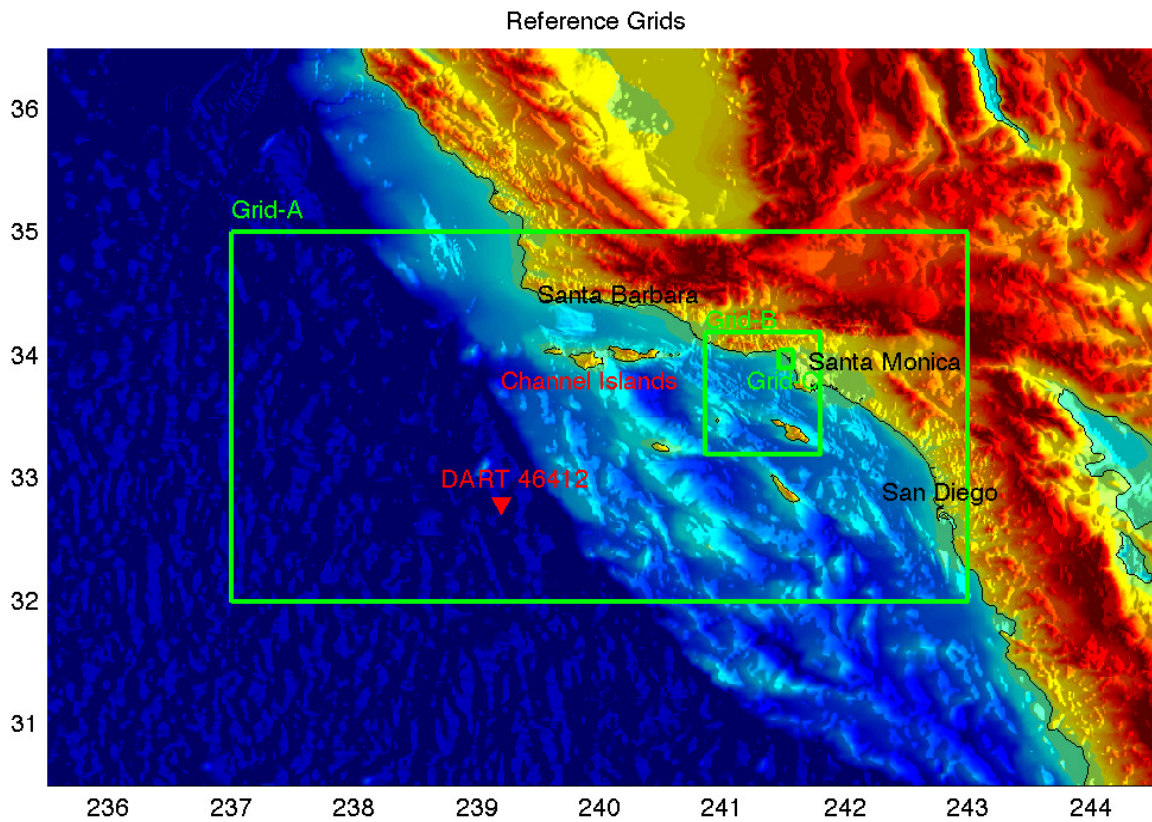
Figure 5: Map of the Southern California area showing the relative position of the reference model grids relative to Santa Monica Bay and to the Channel Islands.
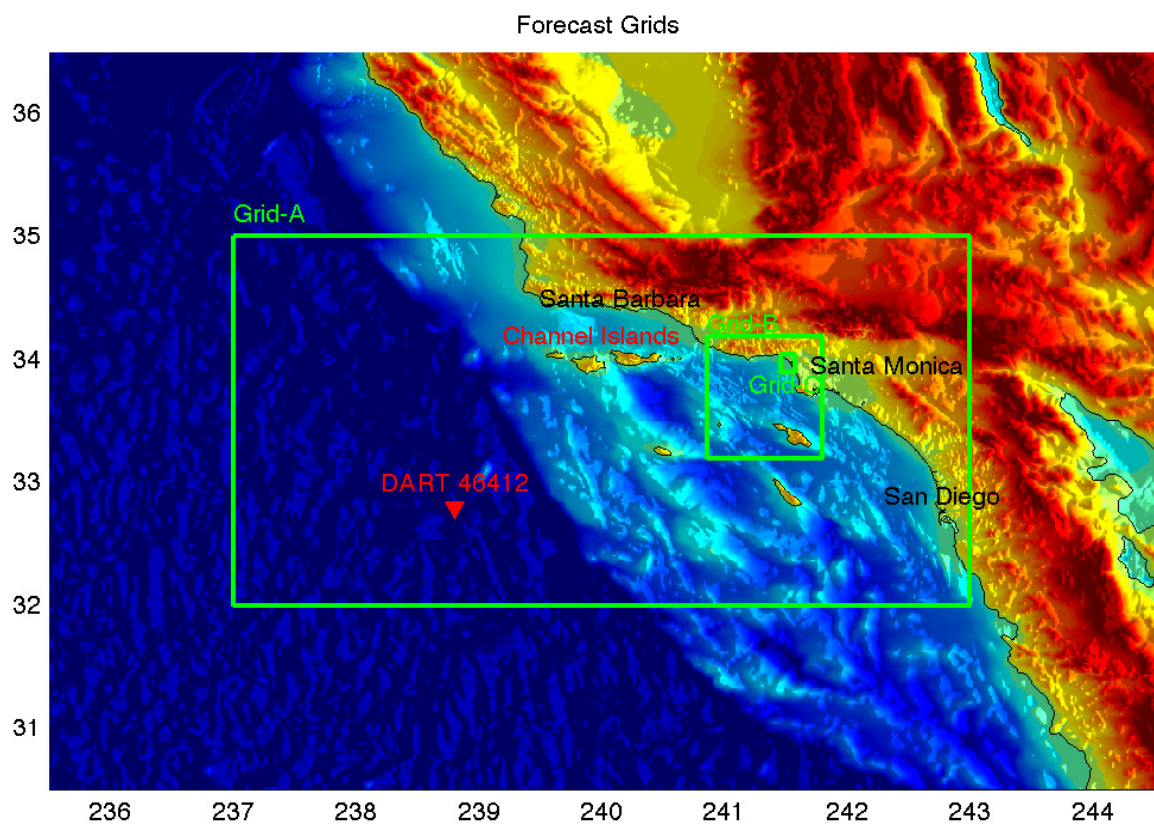
Figure 6: Map of the Southern California area showing the relative position of the forecast model grids relative to Santa Monica Bay and to the Channel Islands.
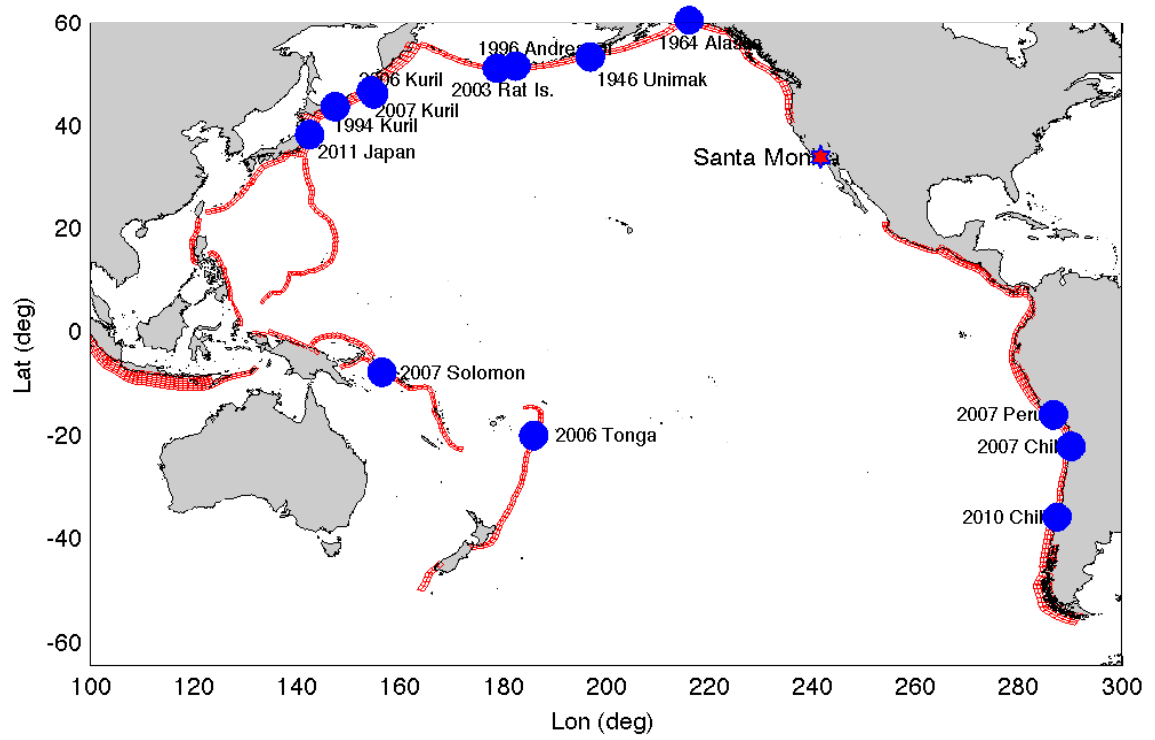
Figure 7: Location of the 13 historical events used in the model validation tests, showing the position of Santa Monica relative to the epicenter locations.
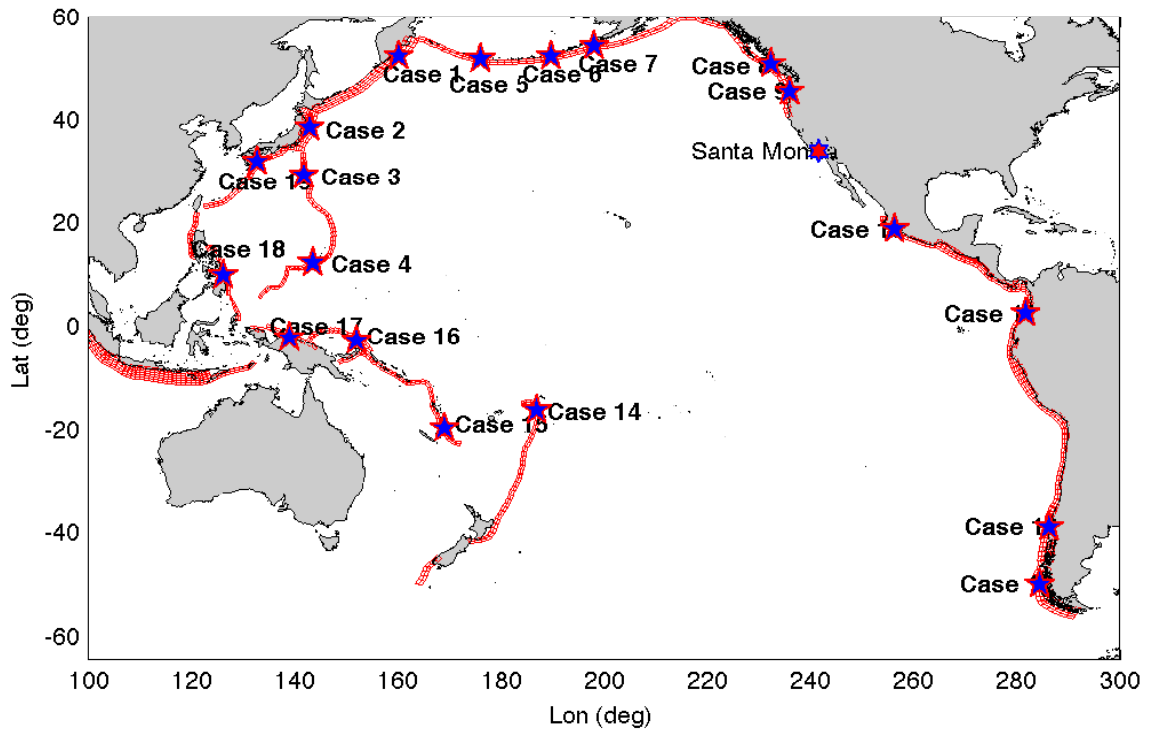
Figure 8: Location of the mid-rupture point of the 19 synthetic (Mw=9.3) events used in the model robustness tests, showing the position of Santa Monica relative to the epicenter locations.
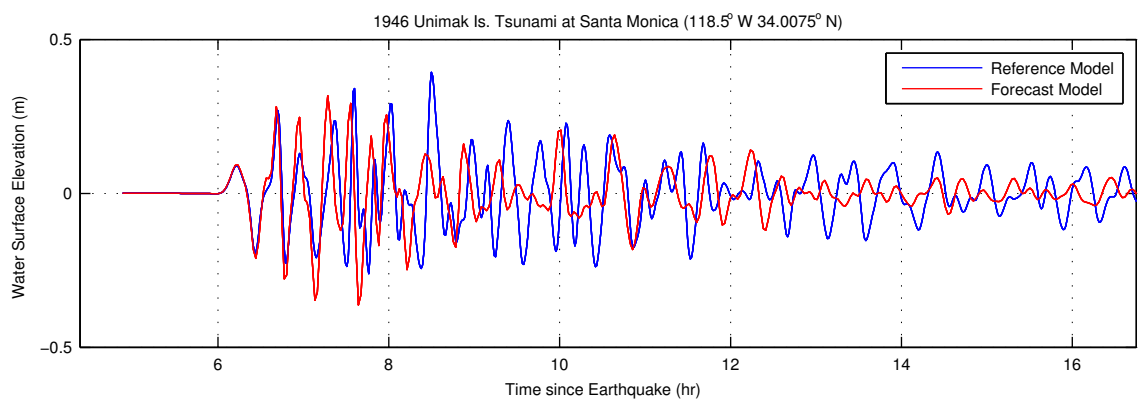
Figure 9: Comparison at the Santa Monica tide gauge of the forecast and reference models for the 1946 Unimak Island tsunami.
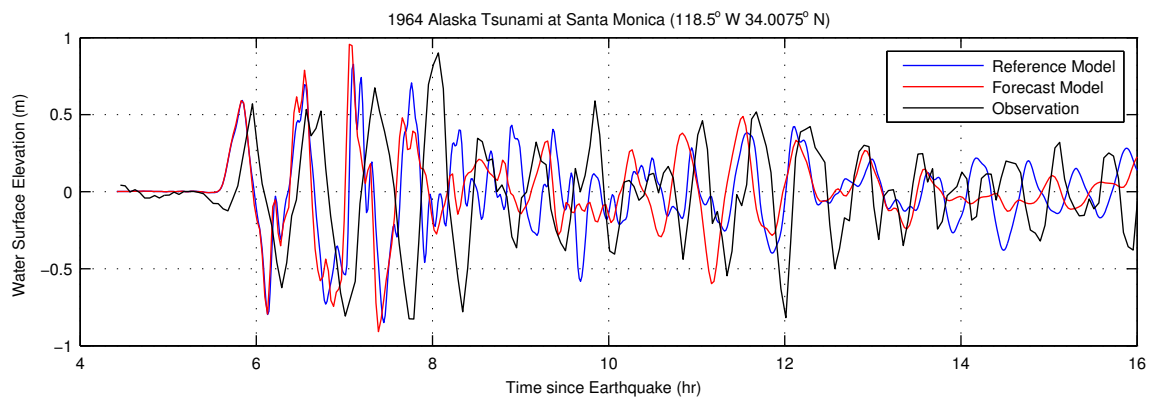
Figure 10: Comparison at the Santa Monica tide gauge of the forecast and reference models for the 1964 Alaska tsunami.
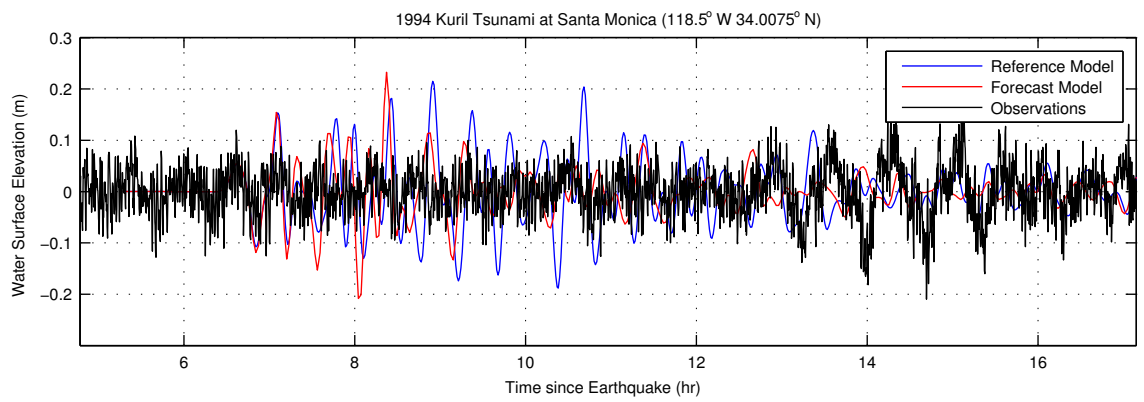
Figure 11: Comparison at the Santa Monica tide gauge of the forecast and reference models for the 1994 Kuril Island tsunami with observed data.
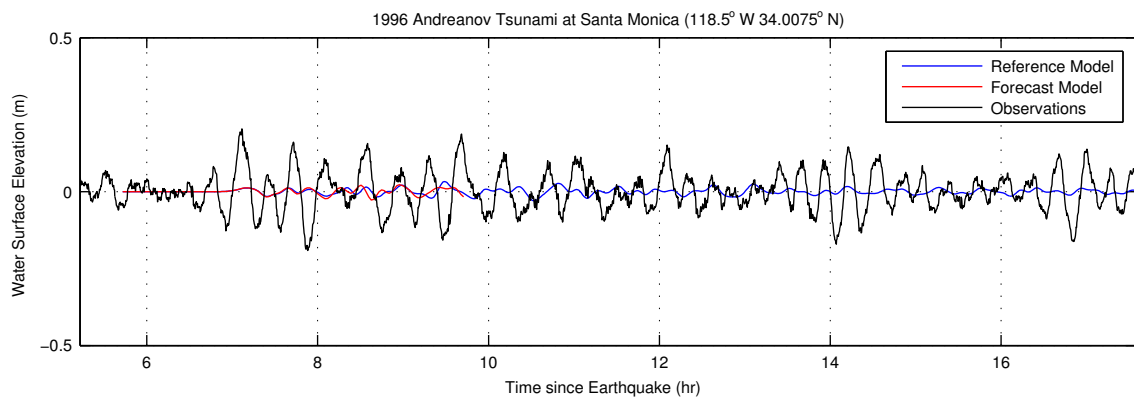
Figure 12: Comparison at the Santa Monica tide gauge of the forecast and reference models for the 1996 Andreanov Island tsunami with observed data.
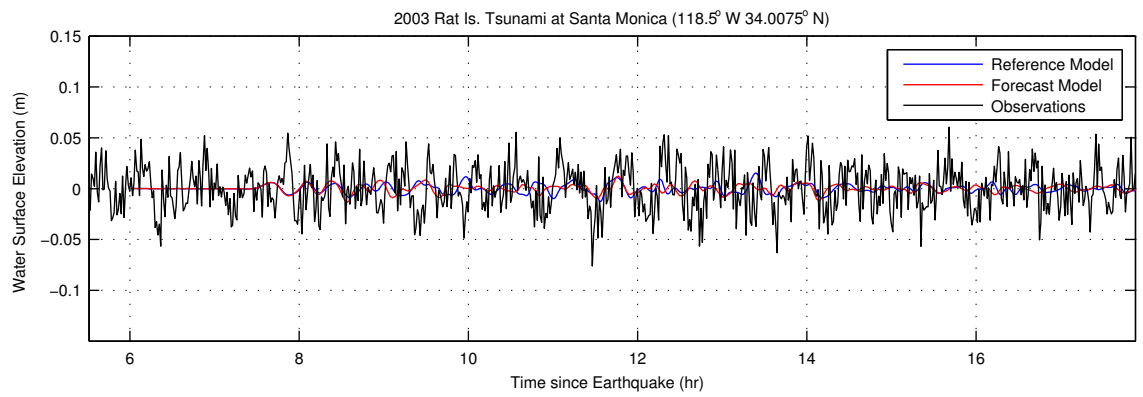
Figure 13: Comparison at the Santa Monica tide gauge of the forecast and reference models for the 2003 Rat Island tsunami with observed data.
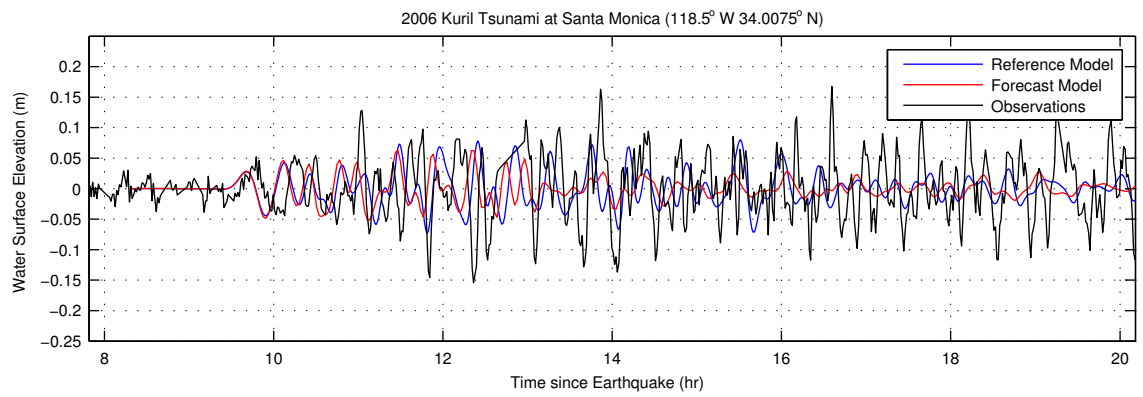
Figure 14: Comparison at the Santa Monica tide gauge of the forecast and reference models for the 2006 Kuril Islands tsunami with observed data.
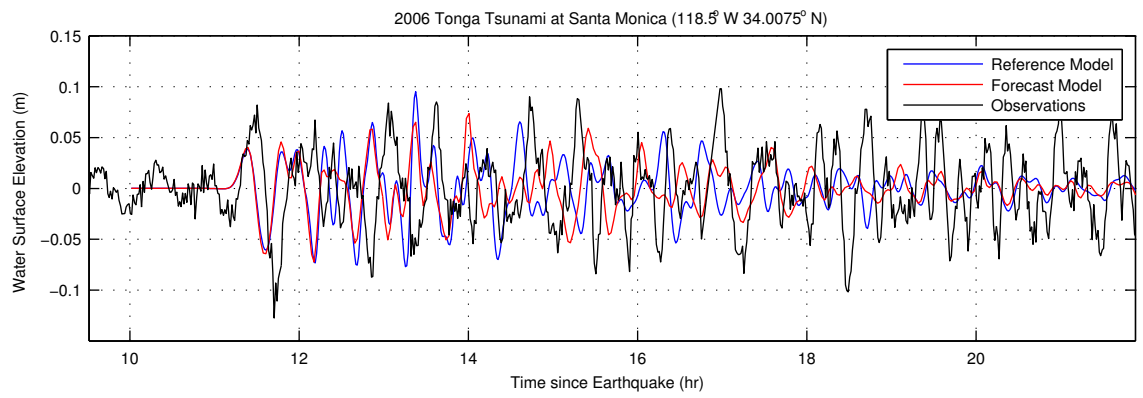
Figure 15: Comparison at the Santa Monica tide gauge of the forecast and reference models for the 2006 Tonga tsunami with observed data.
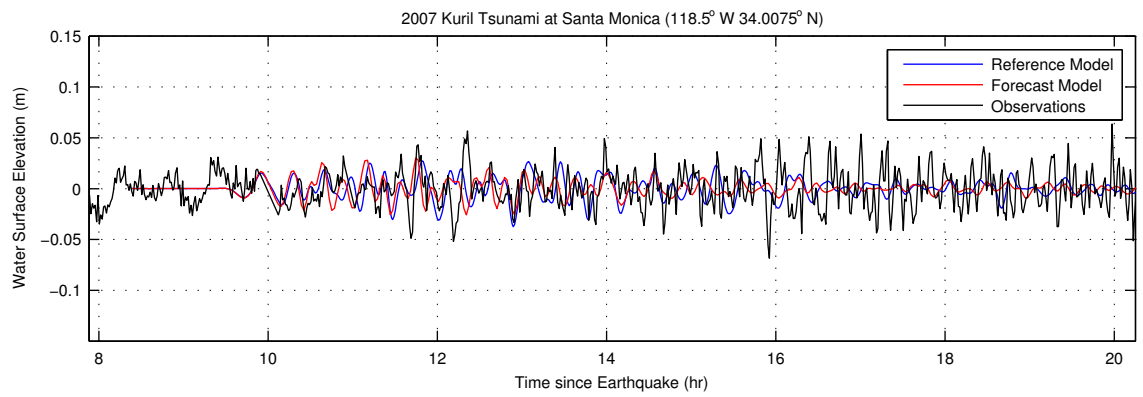
Figure 16: Comparison at the Santa Monica tide gauge of the forecast and reference models for the 2007 Kuril Islands tsunami with observed data.
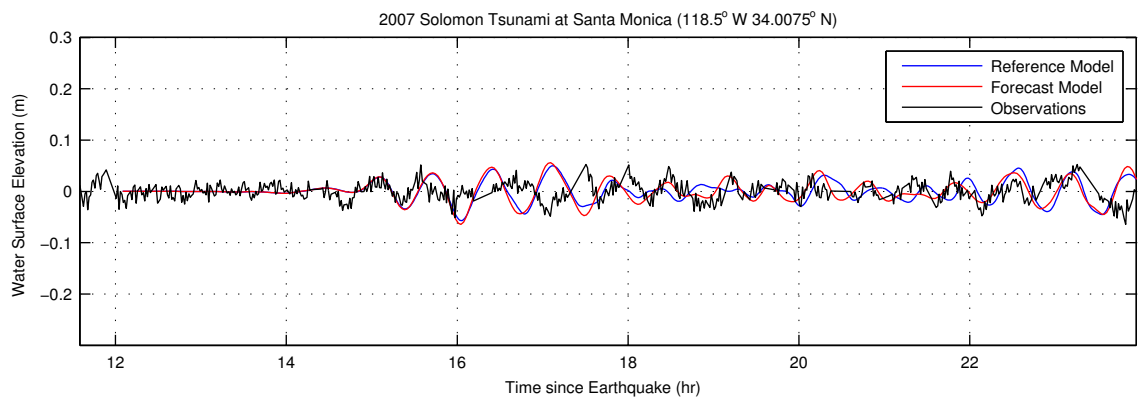
Figure 17: Comparison at the Santa Monica tide gauge of the forecast and reference models for the 2007 Solomon Islands tsunami with observed data.
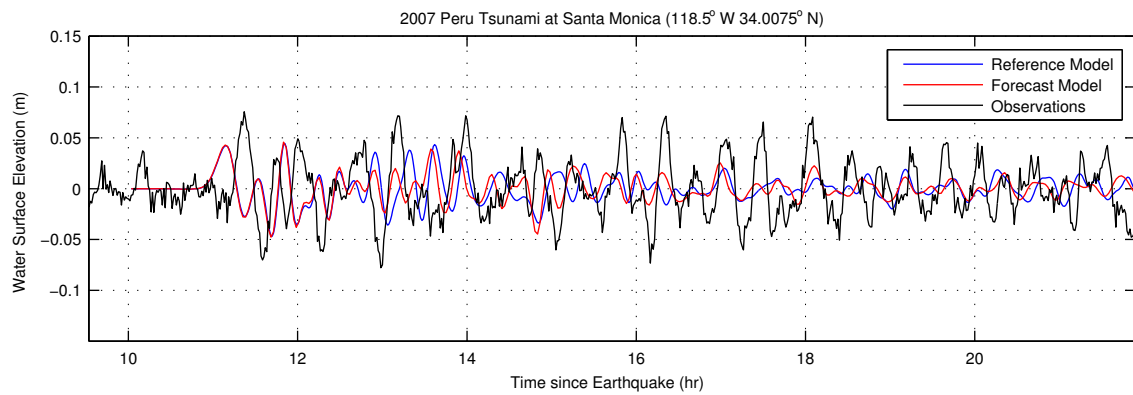
Figure 18: Comparison at the Santa Monica tide gauge of the forecast and reference models for the 2007 Peru tsunami with observed data.
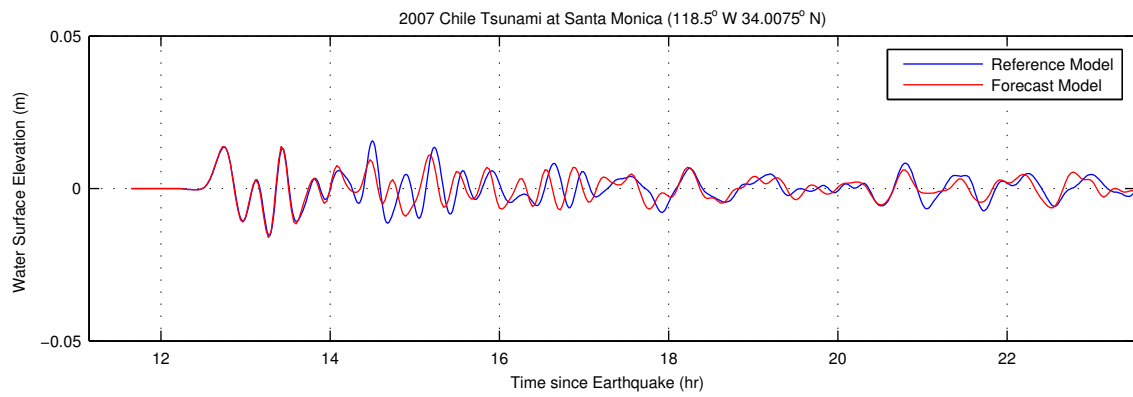
Figure 19: Comparison at the Santa Monica tide gauge of the forecast and reference models for the 2007 Chile tsunami.
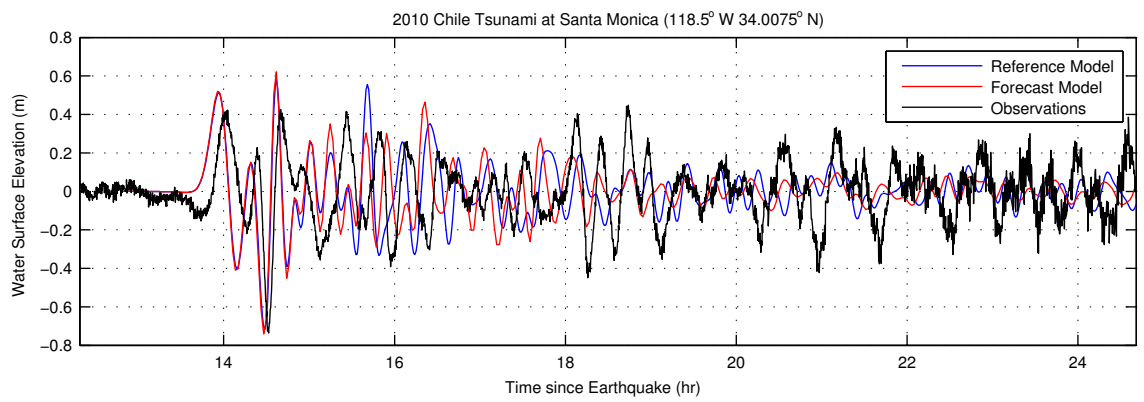
Figure 20: Comparison at the Santa Monica tide gauge of the forecast and reference models for the 2010 Chile tsunami with observed data.
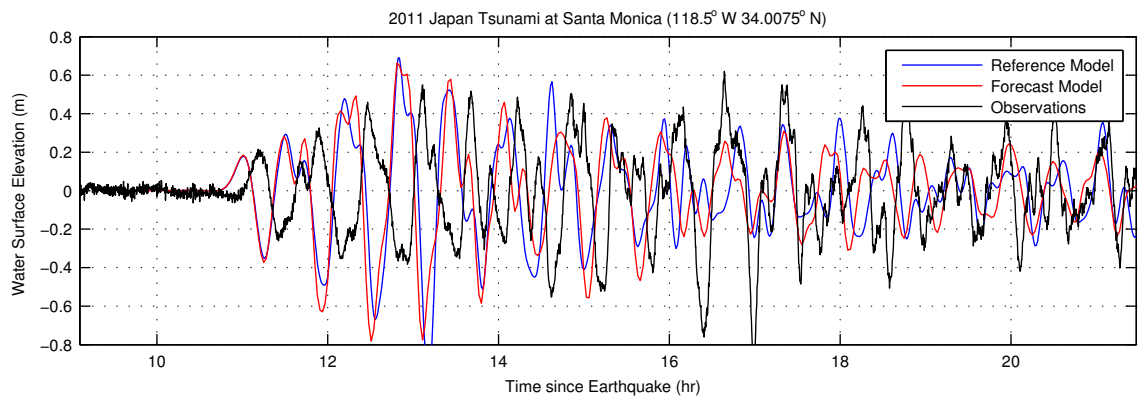
Figure 21: Comparison at the Santa Monica tide gauge of the forecast and reference models for the 2011 Japan tsunami with observed data.
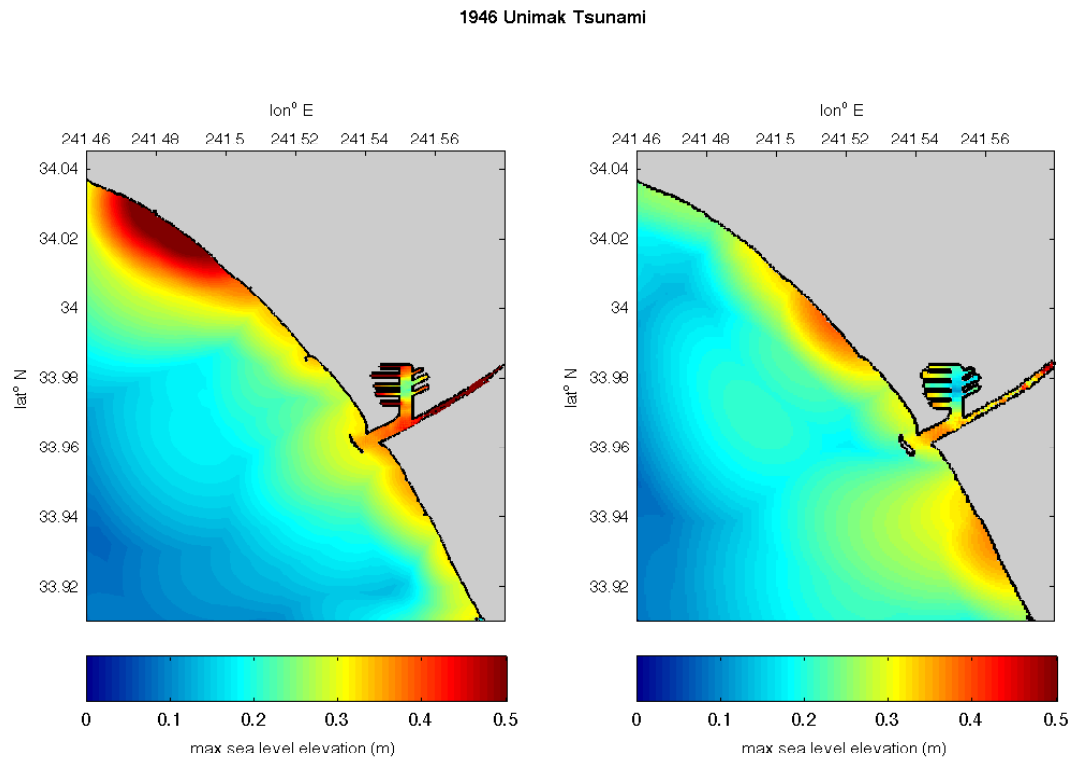
Figure 22: Maximum sea surface elevation computed with the reference (left) and forecast (right) models for the 1946 Unimak Island tsunami.
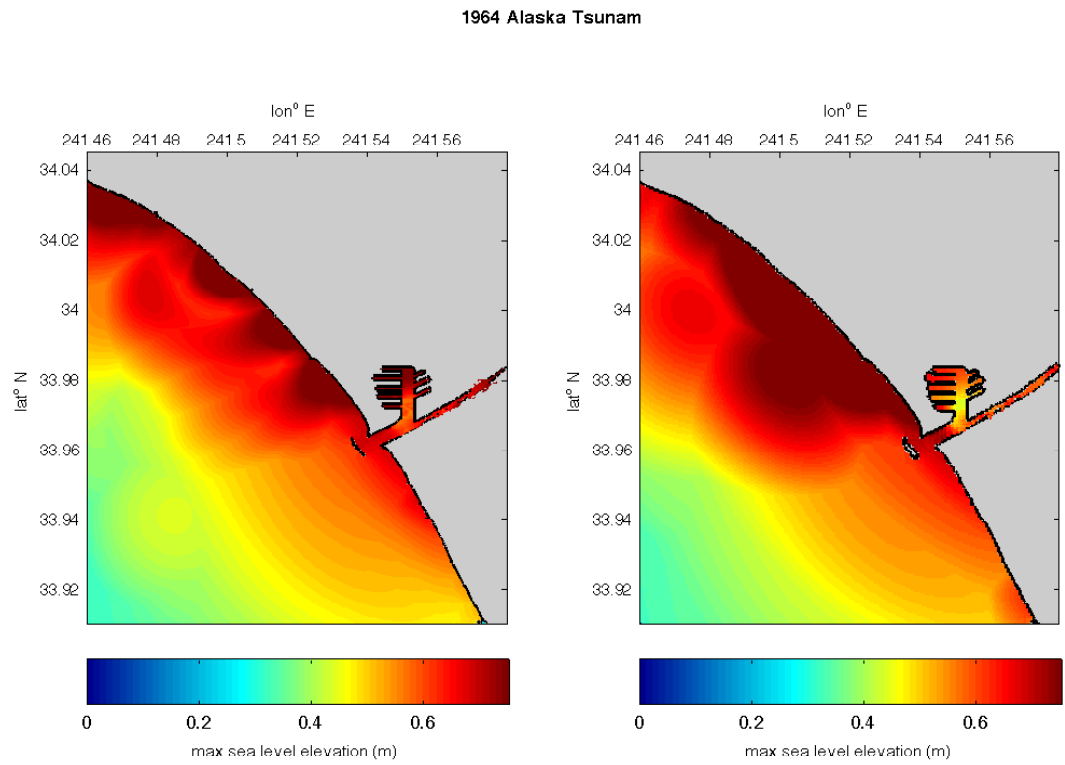
Figure 23: Maximum sea surface elevation computed with the reference (left) and forecast (right) models for the 1964 Alaska tsunami.
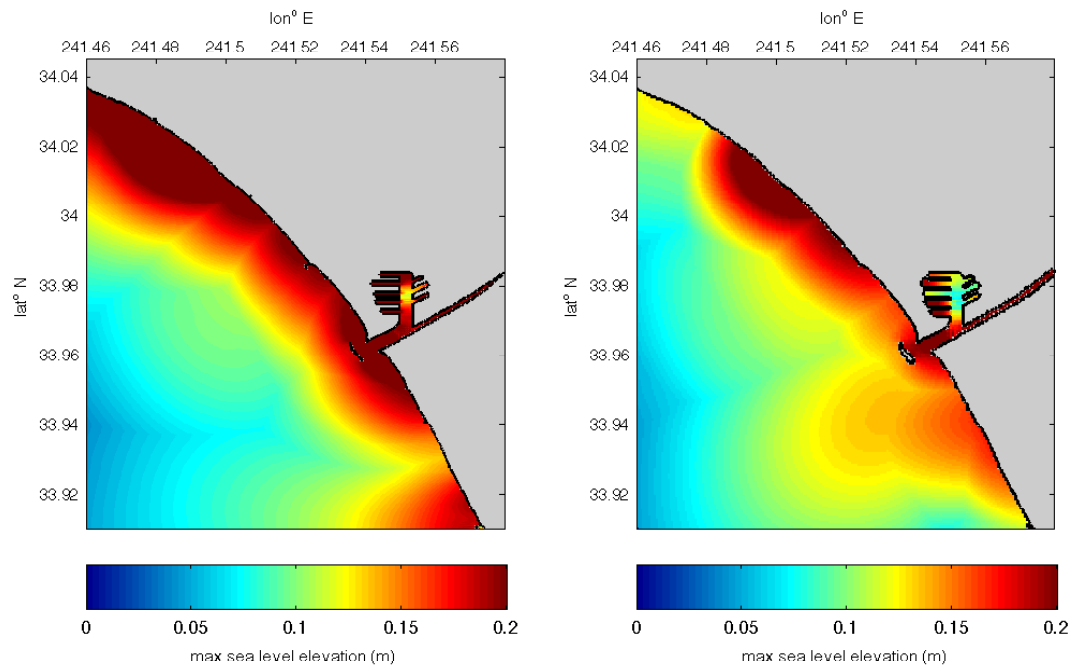
Figure 24: Maximum sea surface elevation computed with the reference (left) and forecast (right) models for the 1994 Kuril Islands tsunami.
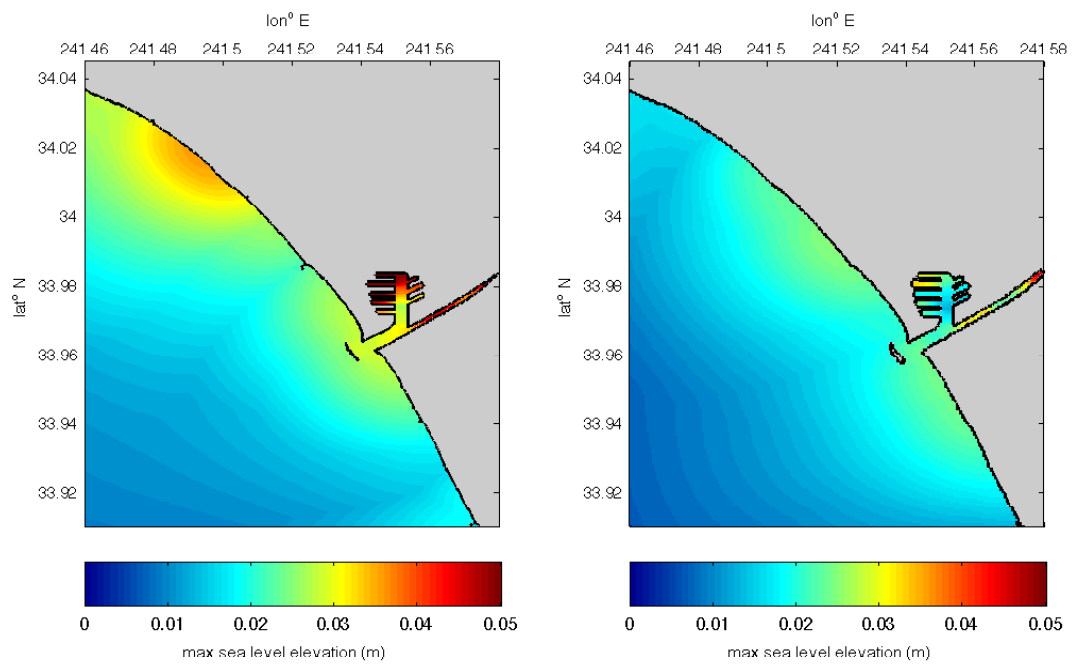
Figure 25: Maximum sea surface elevation computed with the reference (left) and forecast (right) models for the 1996 Andreanof Island tsunami.
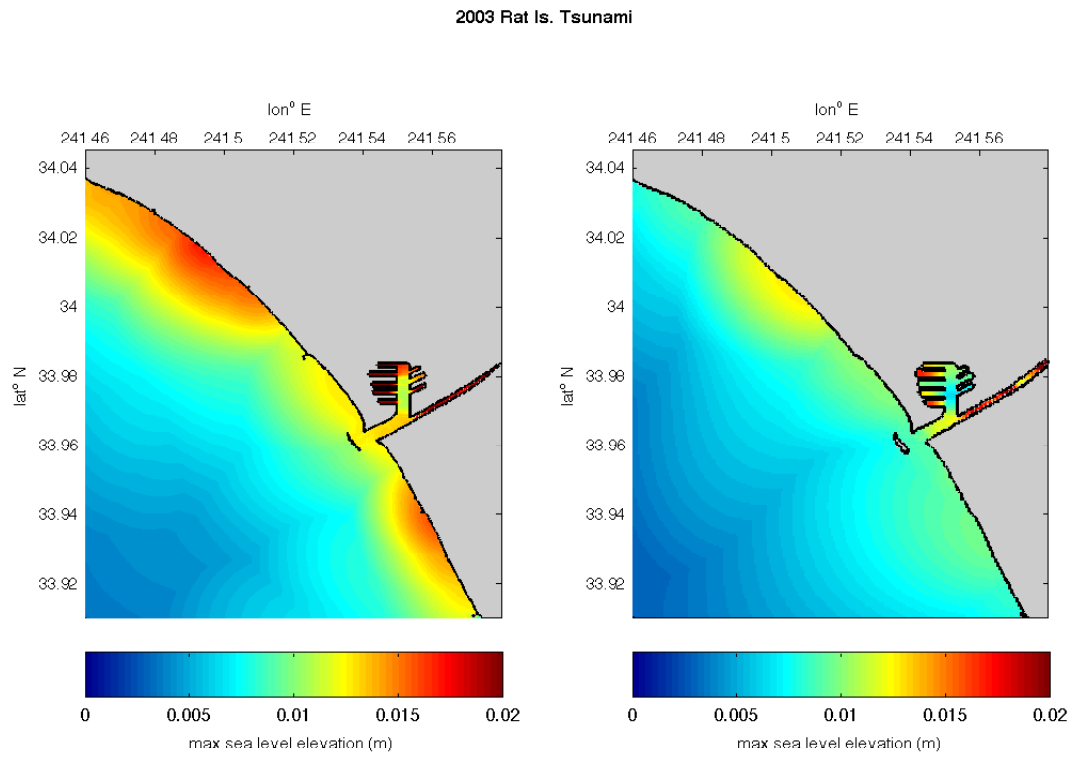
Figure 26: Maximum sea surface elevation computed with the reference (left) and forecast (right) models for the 2003 Rat Islands tsunami.
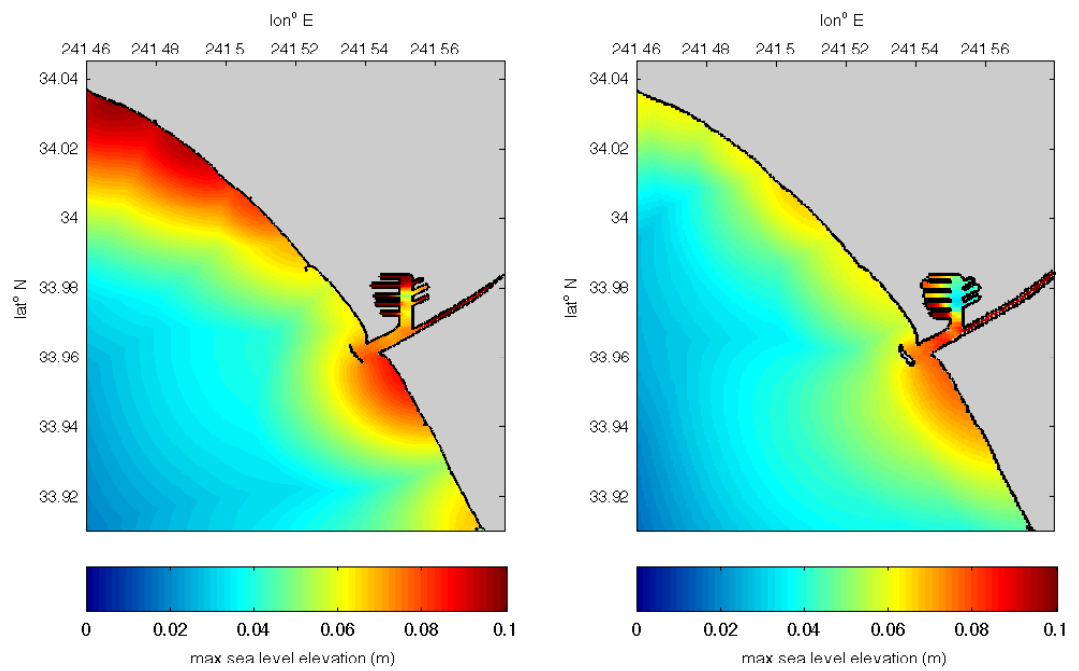
Figure 27: Maximum sea surface elevation computed with the reference (left) and forecast (right) models for the 2006 Kuril Islands tsunami.
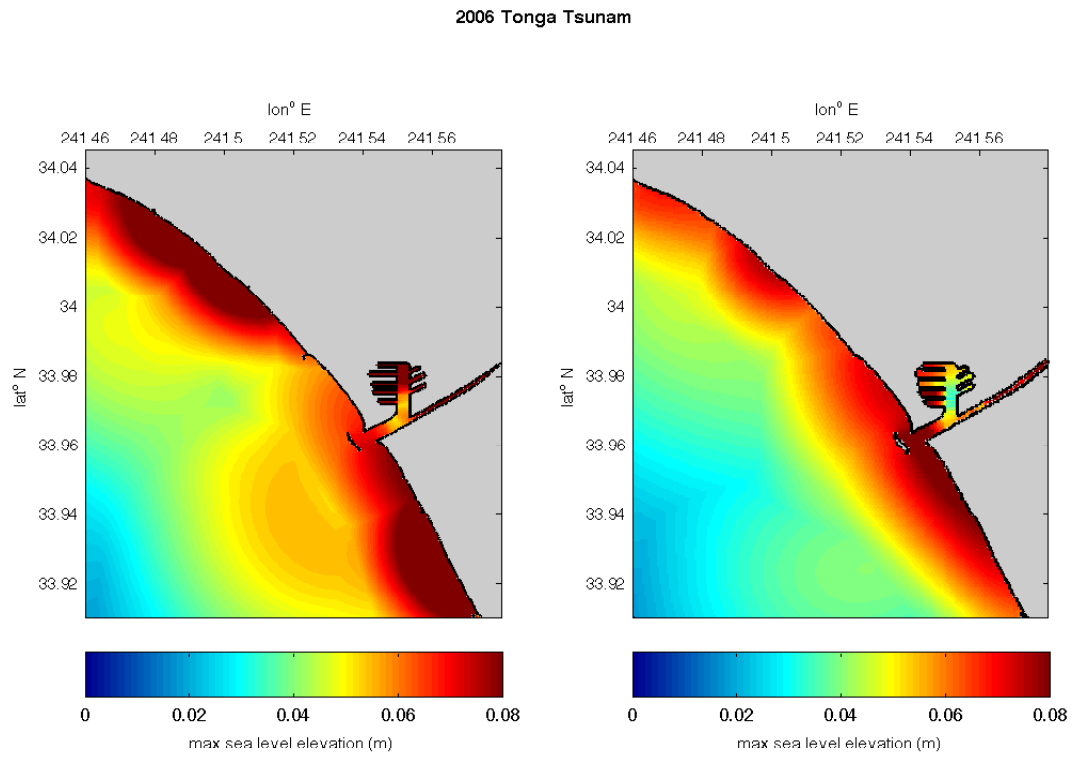
Figure 28: Maximum sea surface elevation computed with the reference (left) and forecast (right) models for the 2006 Tonga Island tsunami.
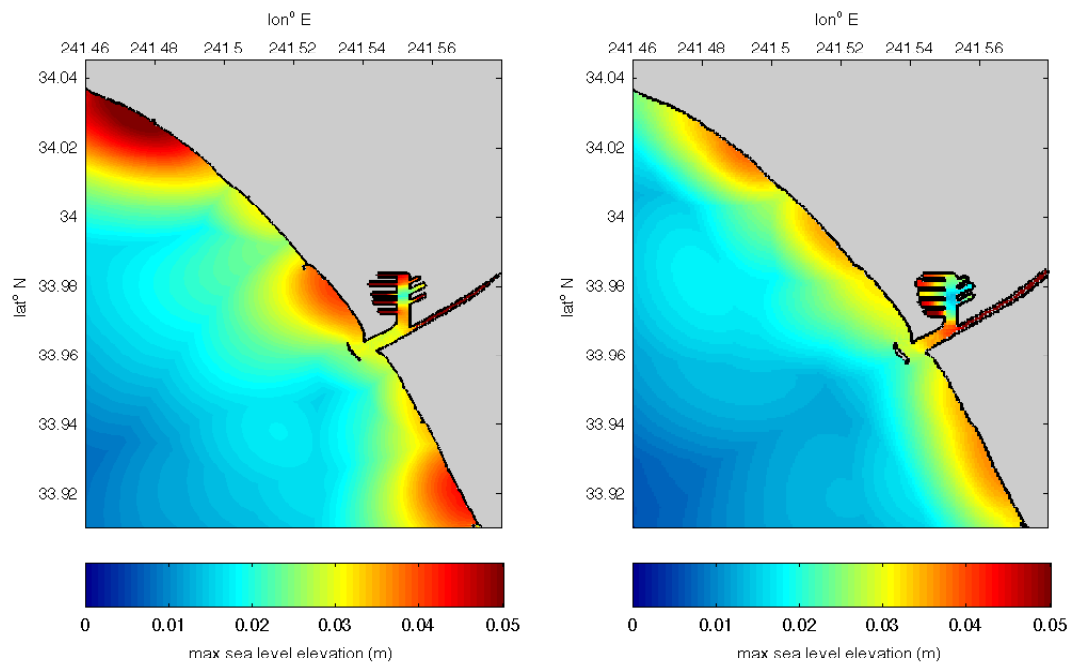
Figure 29: Maximum sea surface elevation computed with the reference (left) and forecast (right) models for the 2007 Kuril Islands tsunami.
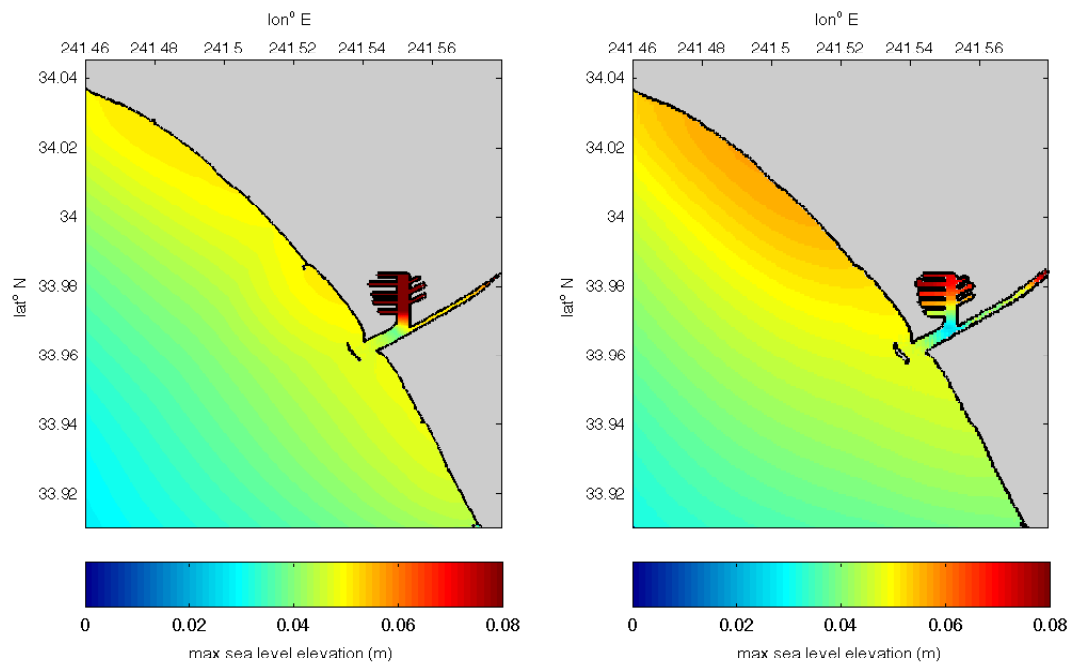
Figure 30: Maximum sea surface elevation computed with the reference (left) and forecast (right) models for the 2007 Solomon Island tsunami.
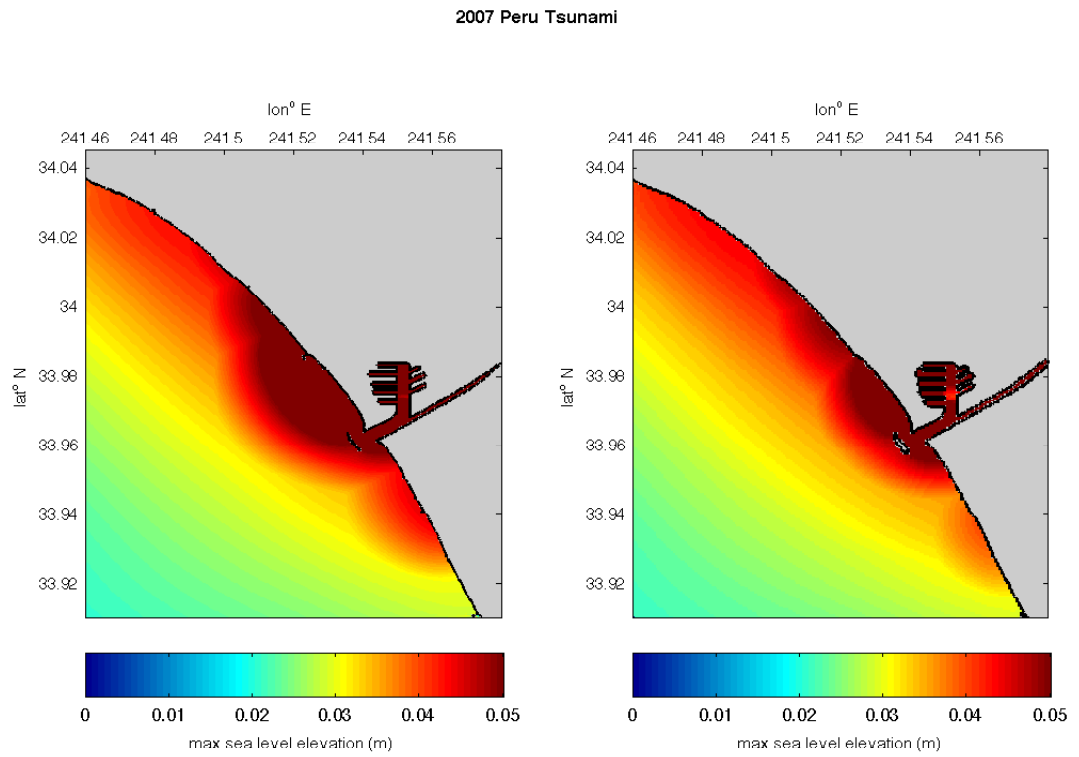
Figure 31: Maximum sea surface elevation computed with the reference (left) and forecast (right) models for the 2007 Peru tsunami.
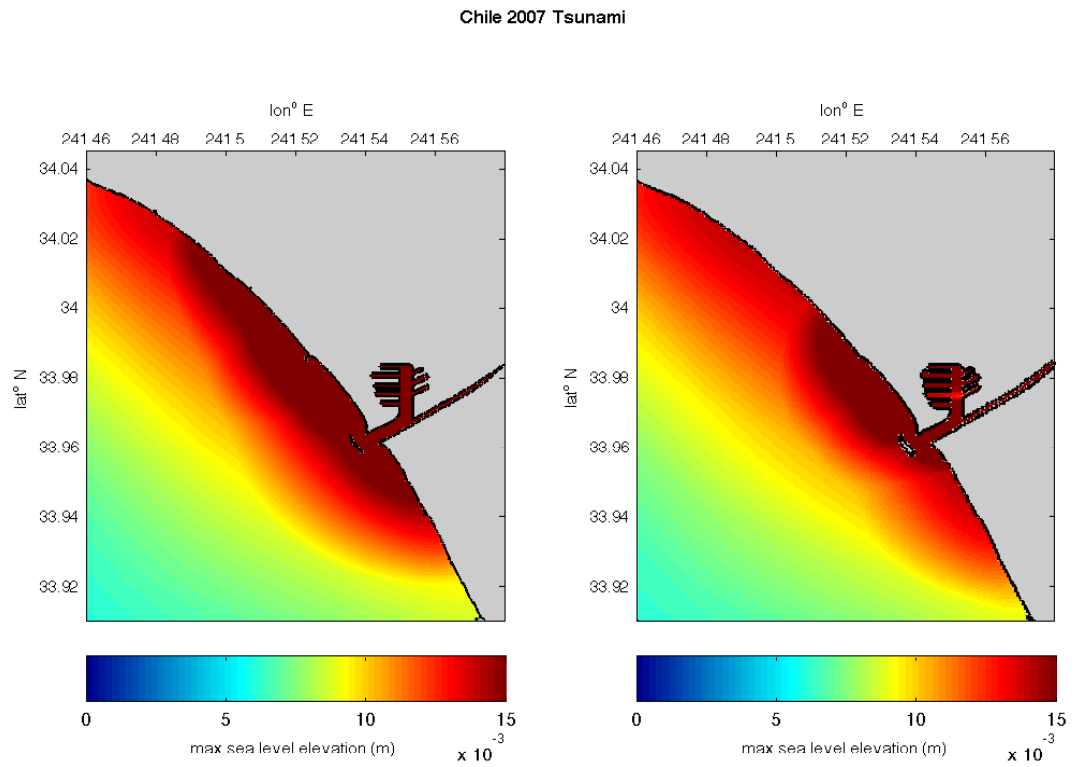
Figure 32: Maximum sea surface elevation computed with the reference (left) and forecast (right) models for the 2007 Chile tsunami.
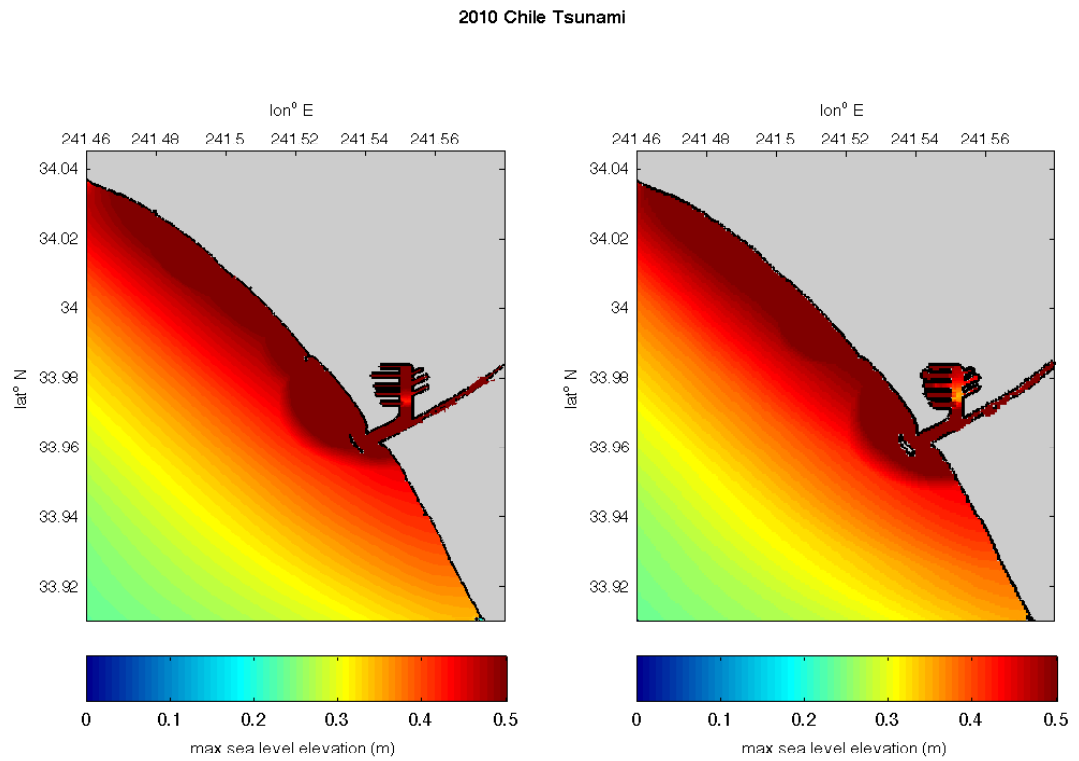
Figure 33: Maximum sea surface elevation computed with the reference (left) and forecast (right) models for the 2010 Chile tsunami.
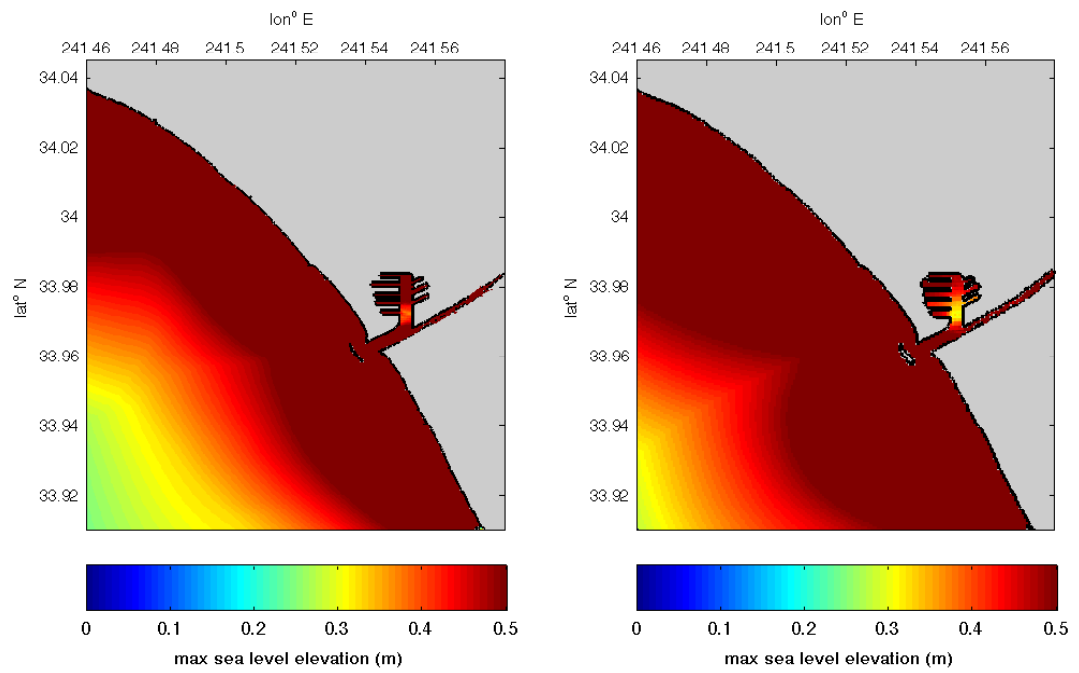
Figure 34: Maximum sea surface elevation computed with the reference (left) and forecast (right) models for the 2011 Japan tsunami.
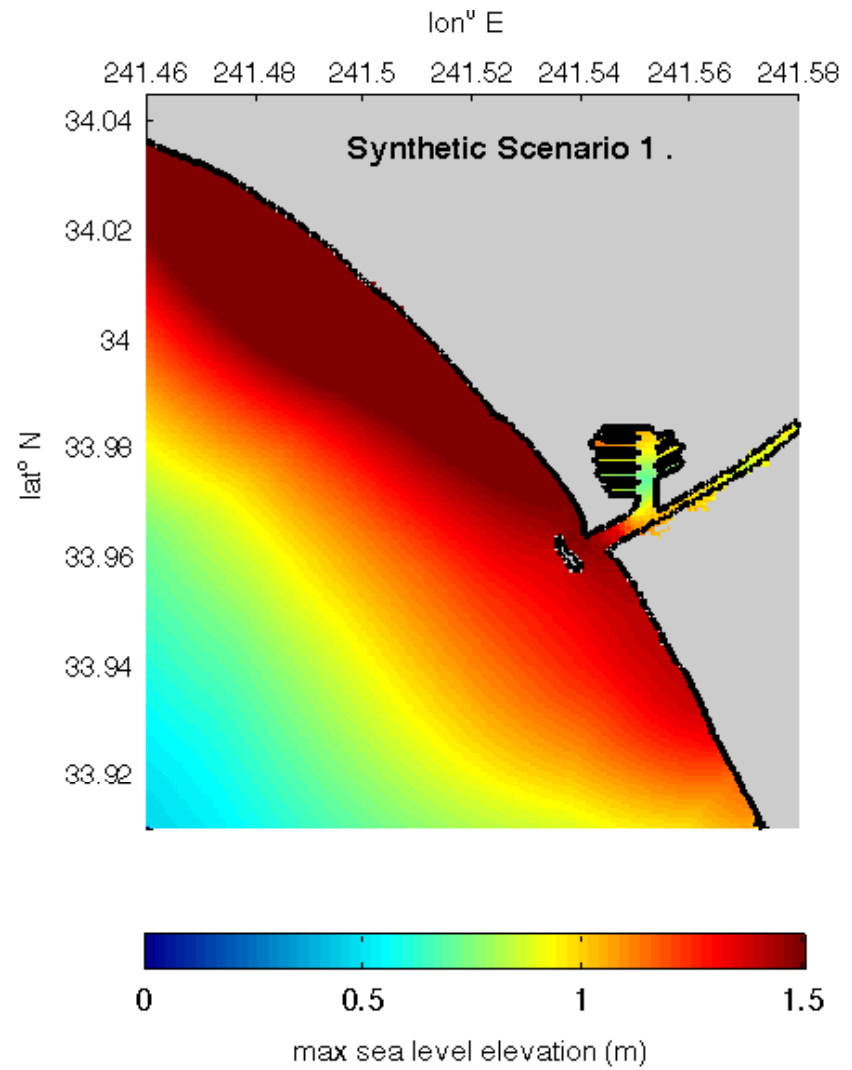
Figure 35: Maximum sea surface elevation computed with the forecast model for synthetic scenario 1 (Mw=9.3).
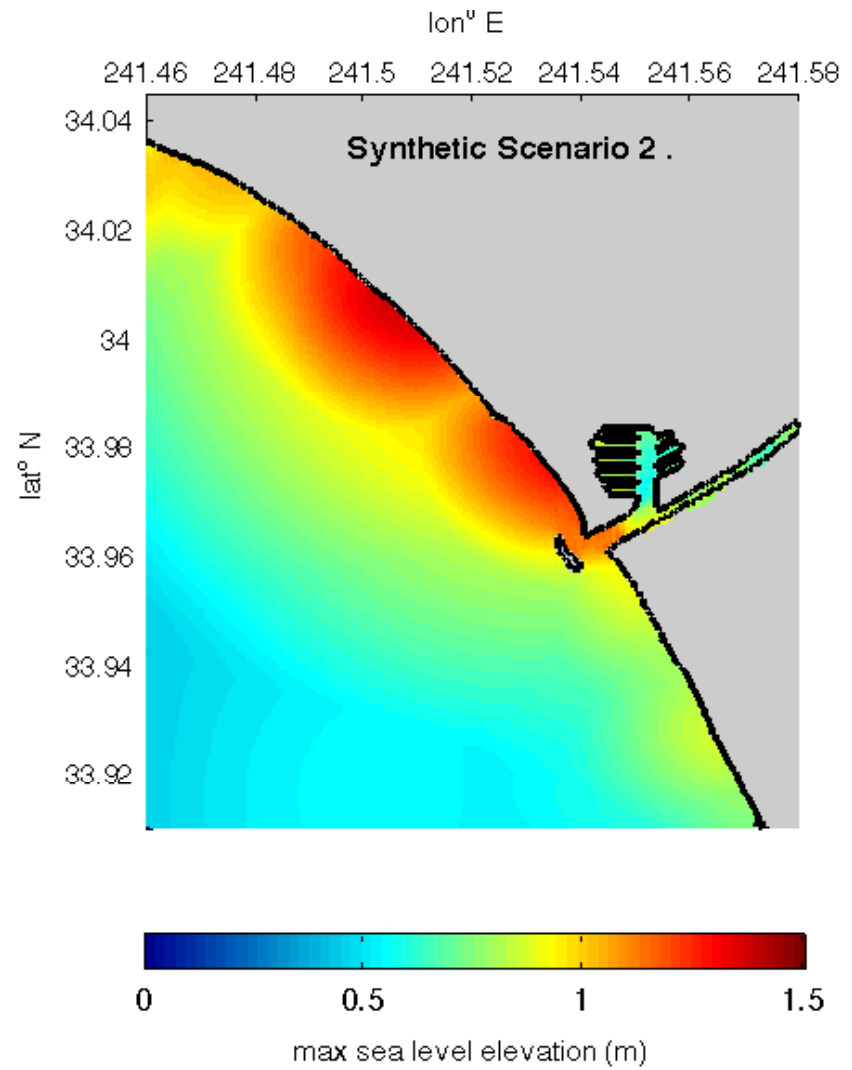
Figure 36: Maximum sea surface elevation computed with the forecast model for synthetic scenario 2 (Mw=9.3).
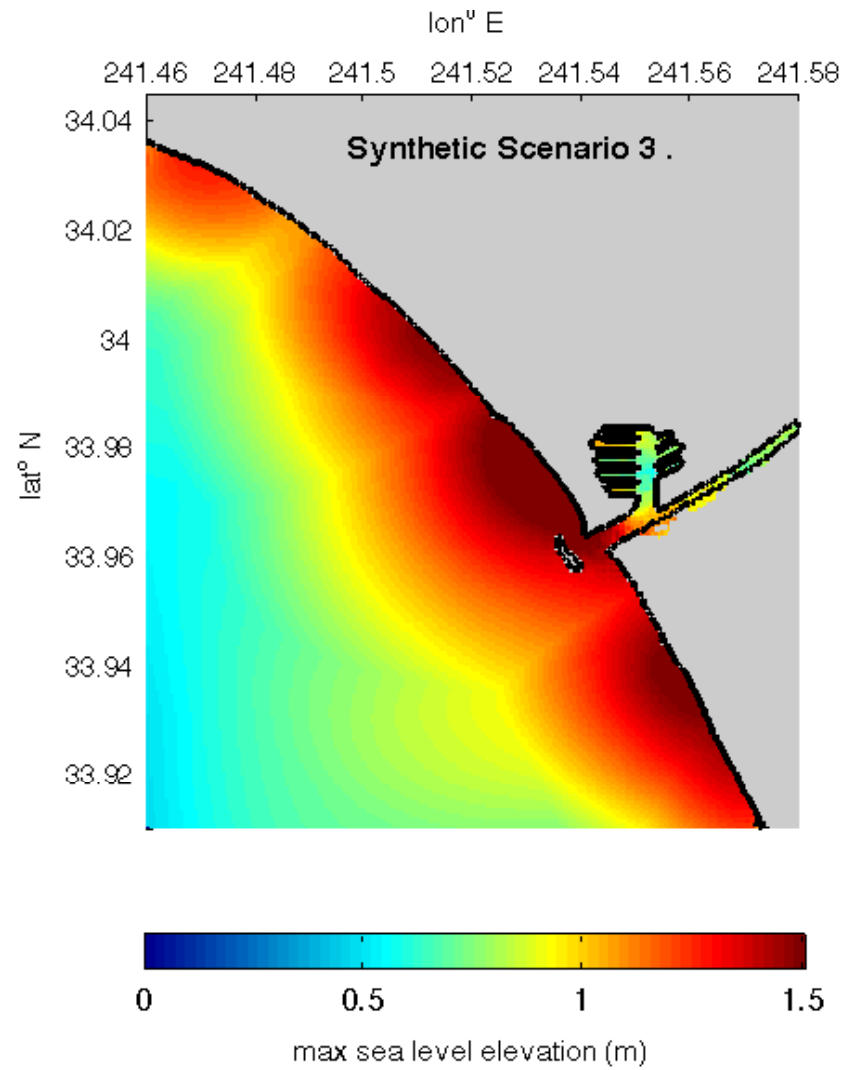
Figure 37: Maximum sea surface elevation computed with the forecast model for synthetic scenario 3 (Mw=9.3).
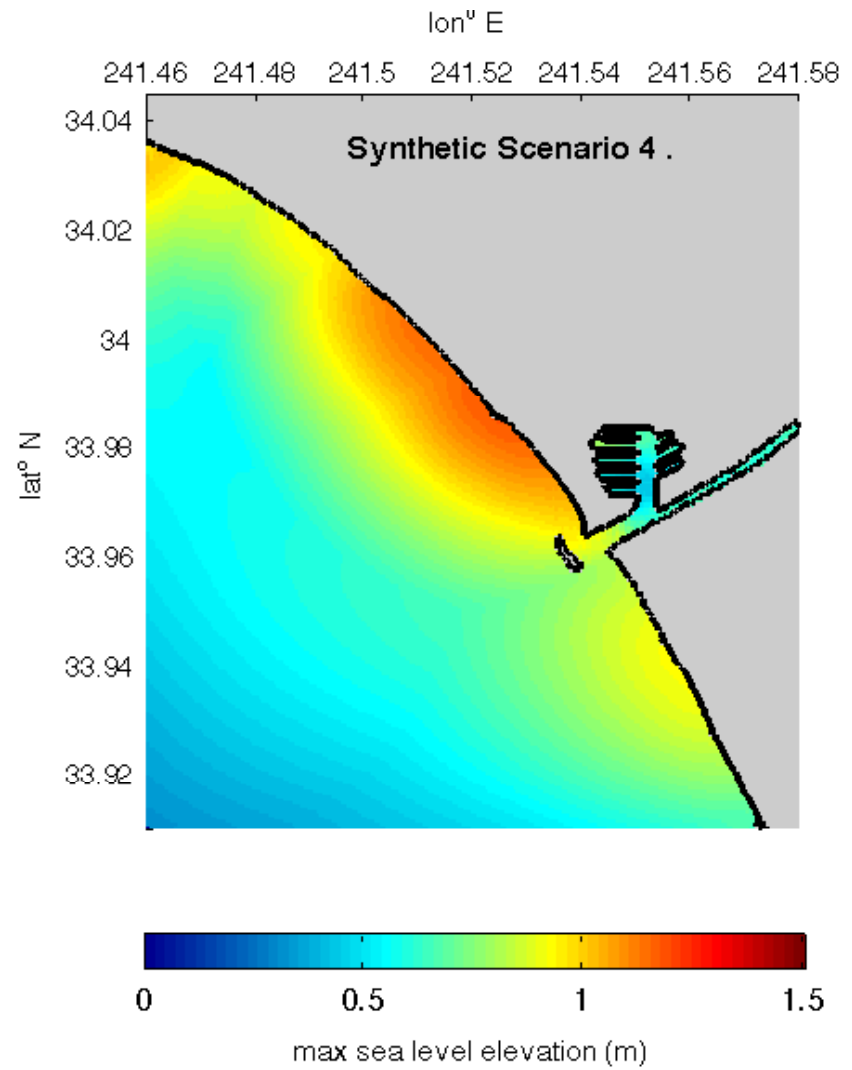
Figure 38: Maximum sea surface elevation computed with the forecast model for synthetic scenario 4 (Mw=9.3).
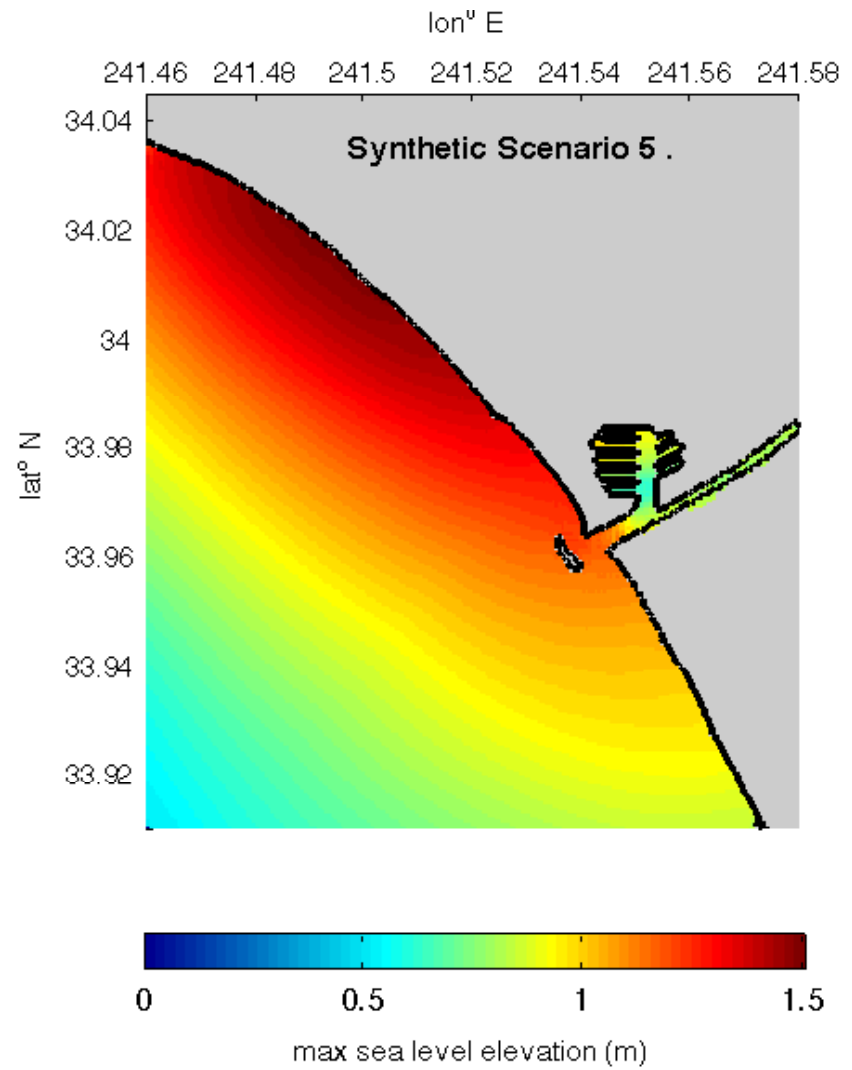
Figure 39: Maximum sea surface elevation computed with the forecast model for synthetic scenario 5 (Mw=9.3).
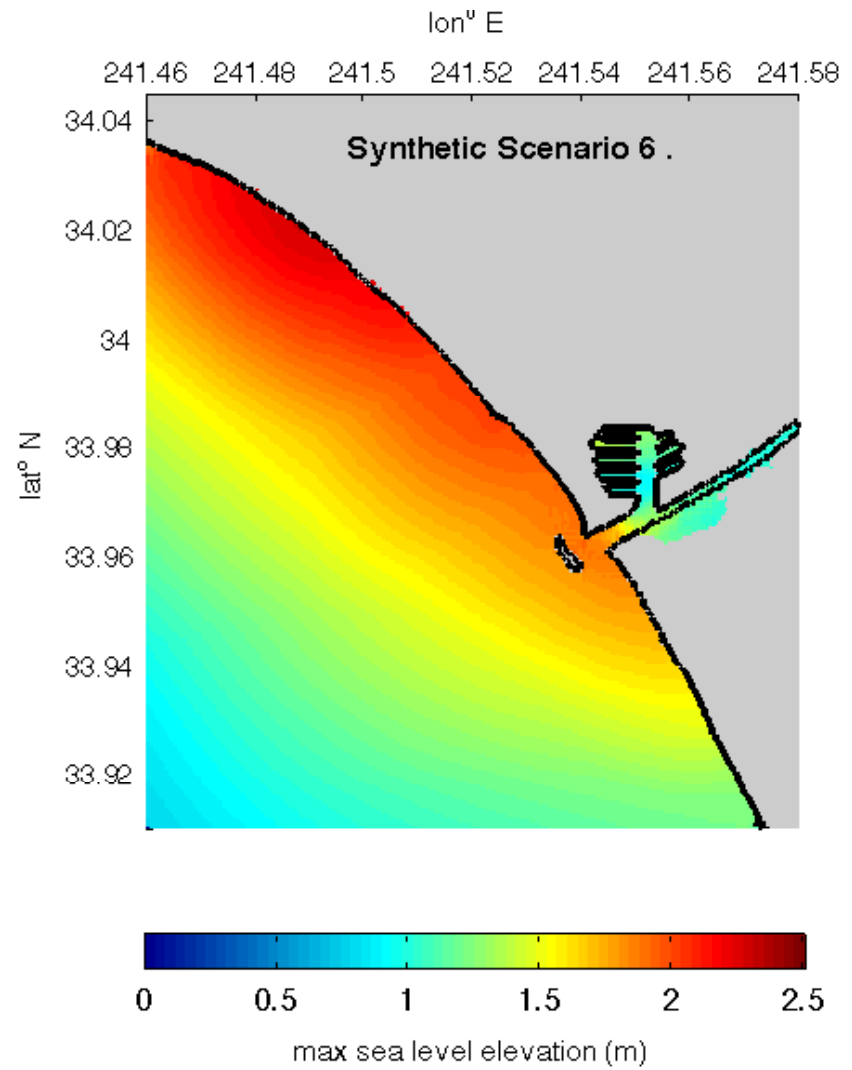
Figure 40: Maximum sea surface elevation computed with the forecast model for synthetic scenario 6 (Mw=9.3).
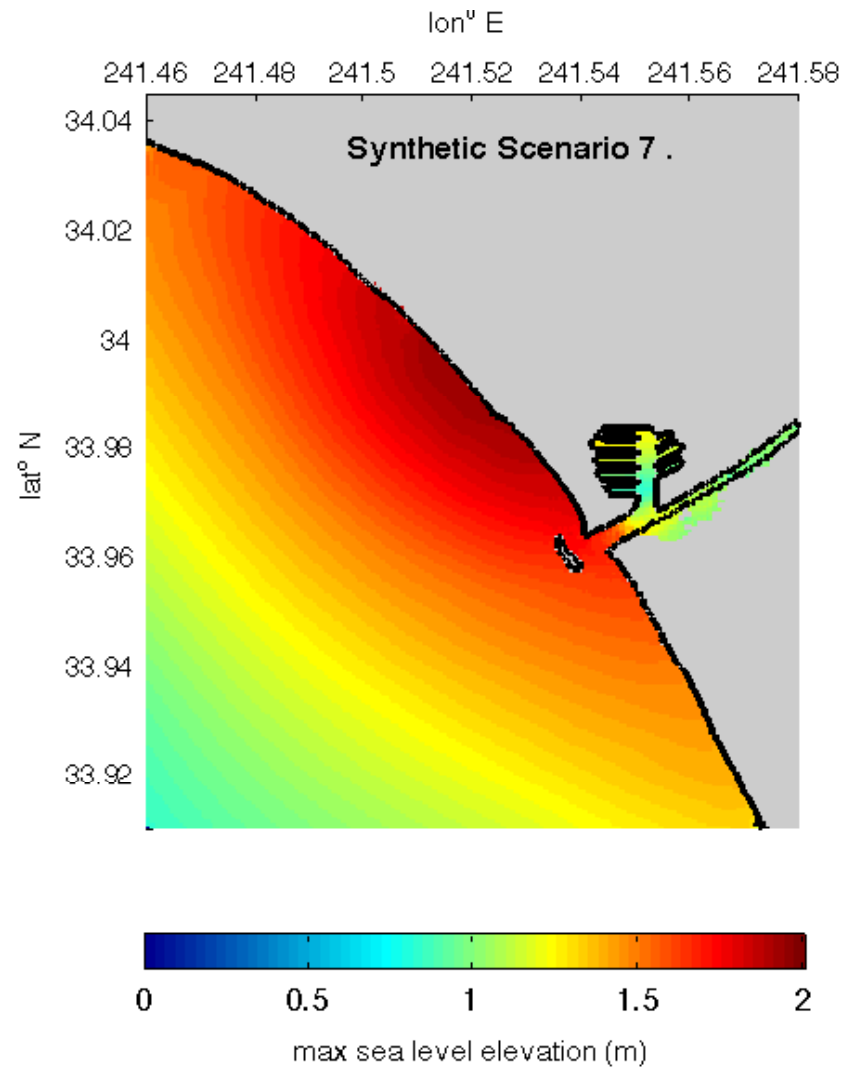
Figure 41: Maximum sea surface elevation computed with the forecast model for synthetic scenario 7 (Mw=9.3).
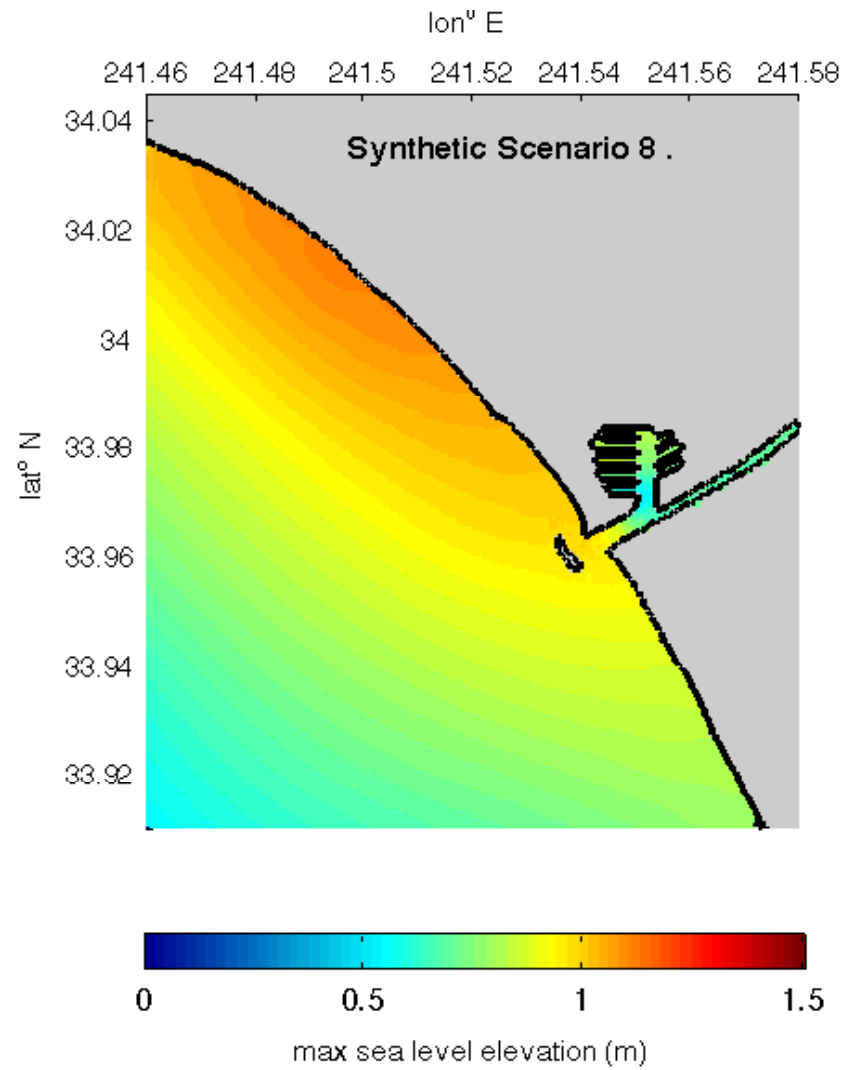
Figure 42: Maximum sea surface elevation computed with the forecast model for synthetic scenario 8 (Mw=9.3).
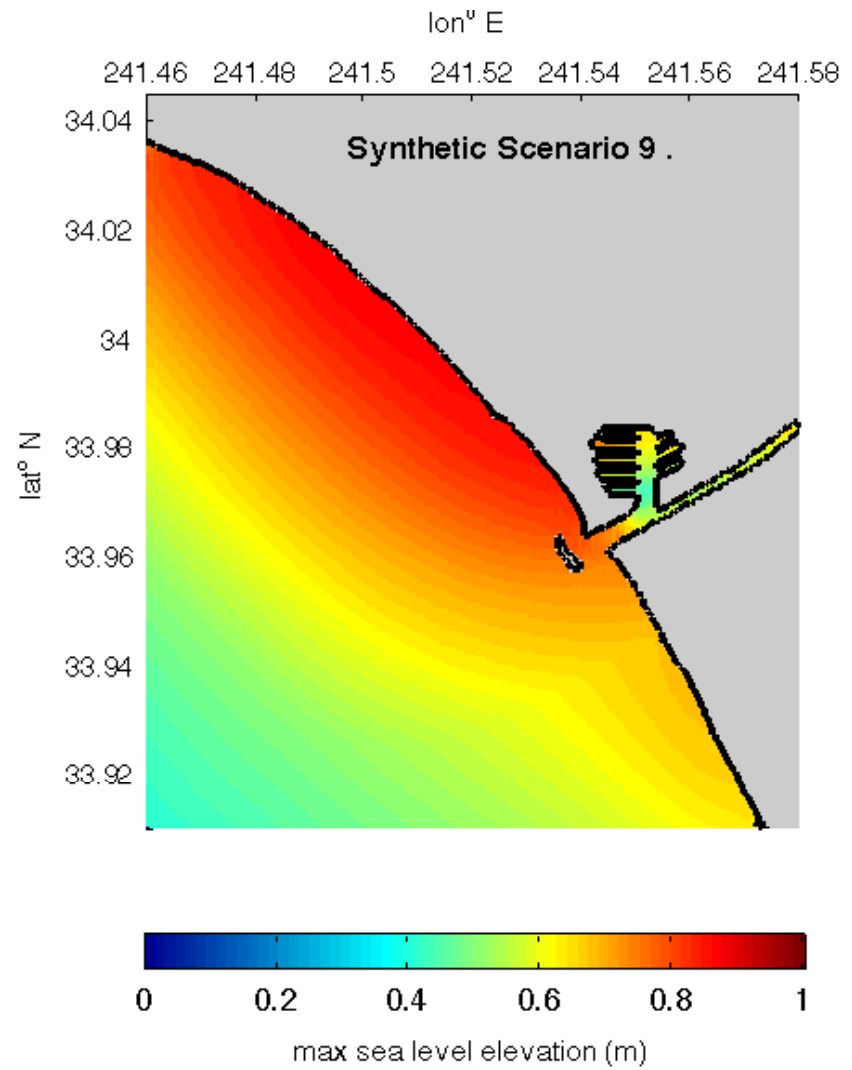
Figure 43: Maximum sea surface elevation computed with the forecast model for synthetic scenario 9 (Mw=9.3).
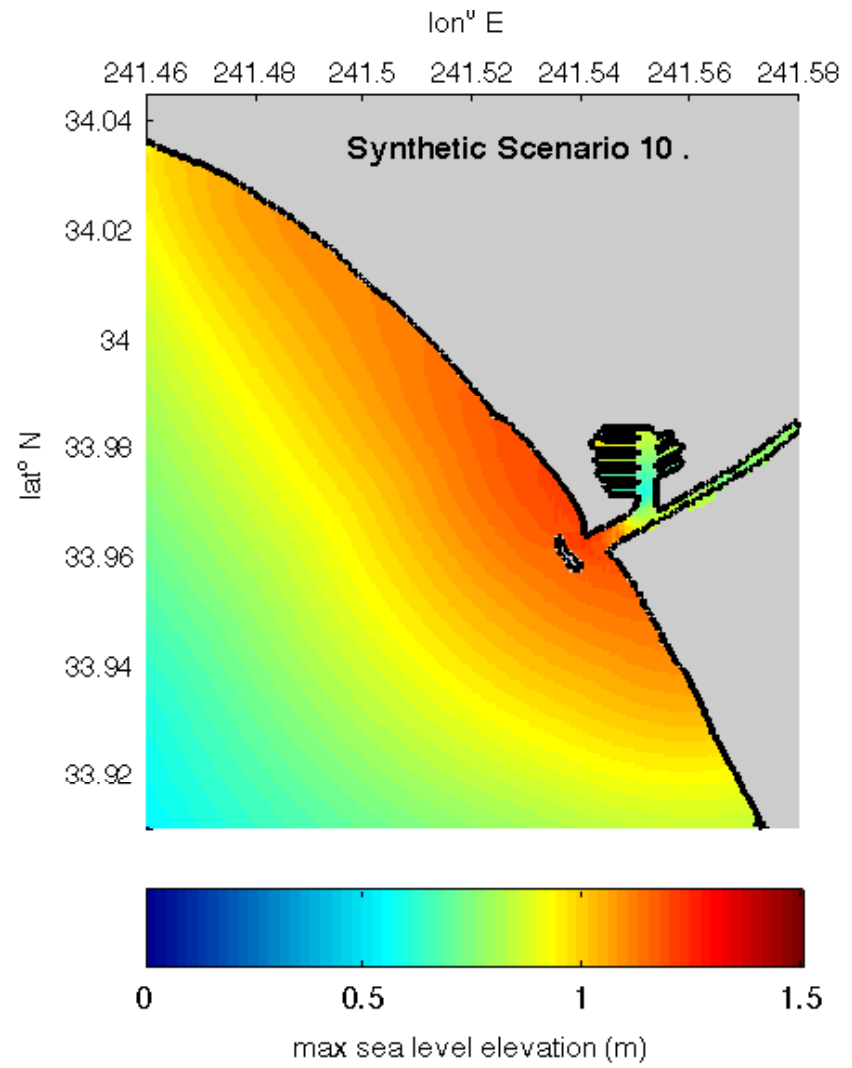
Figure 44: Maximum sea surface elevation computed with the forecast model for synthetic scenario 10 (Mw=9.3).
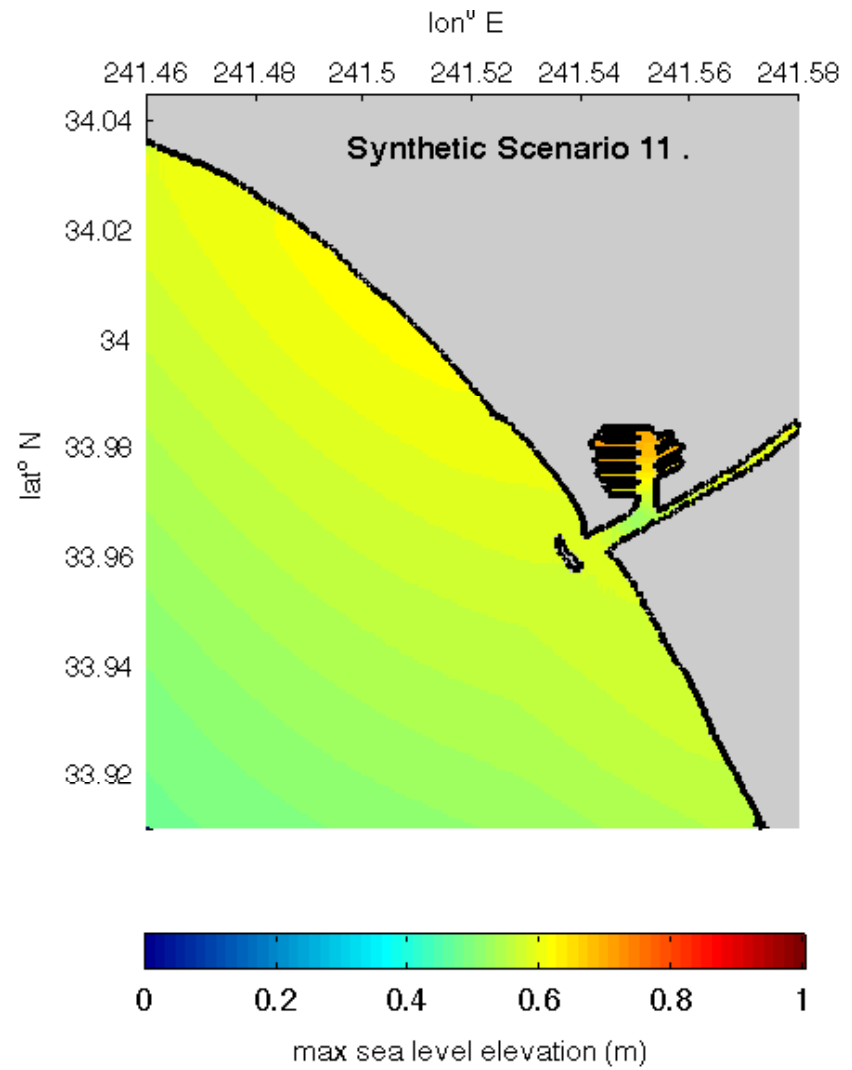
Figure 45: Maximum sea surface elevation computed with the forecast model for synthetic scenario 11 (Mw=9.3).
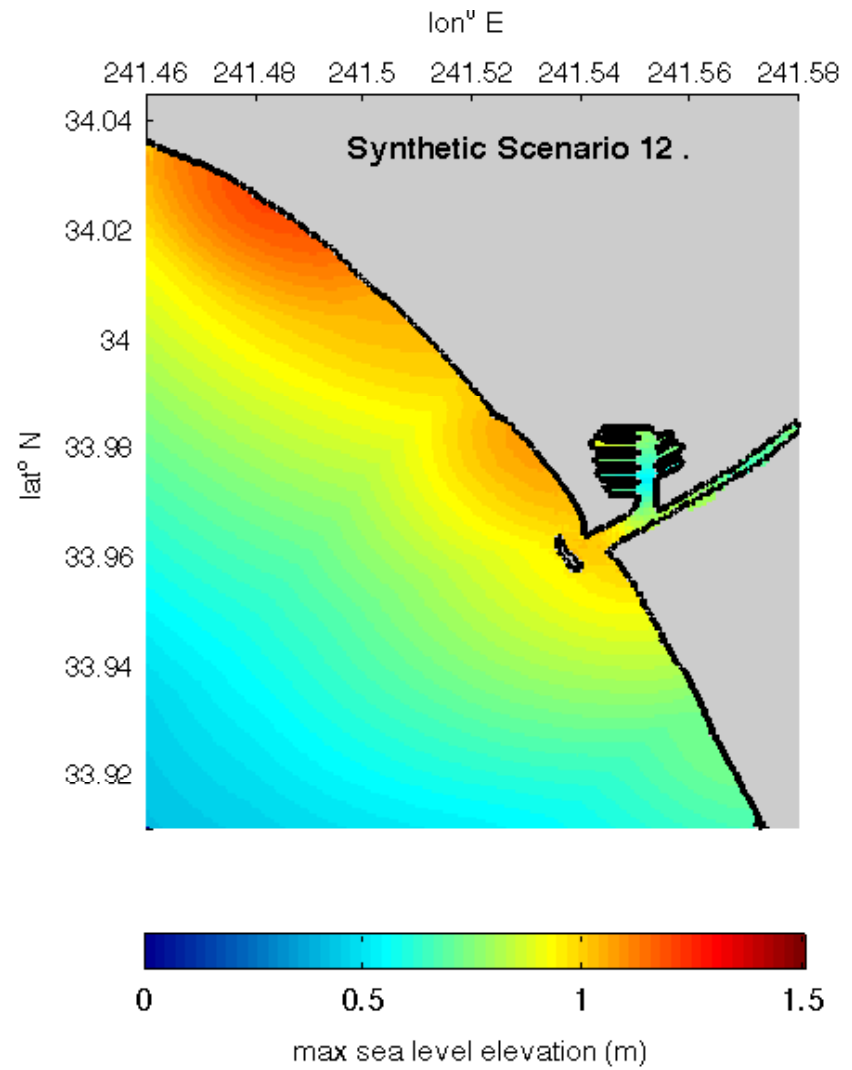
Figure 46: Maximum sea surface elevation computed with the forecast model for synthetic scenario 12 (Mw=9.3).
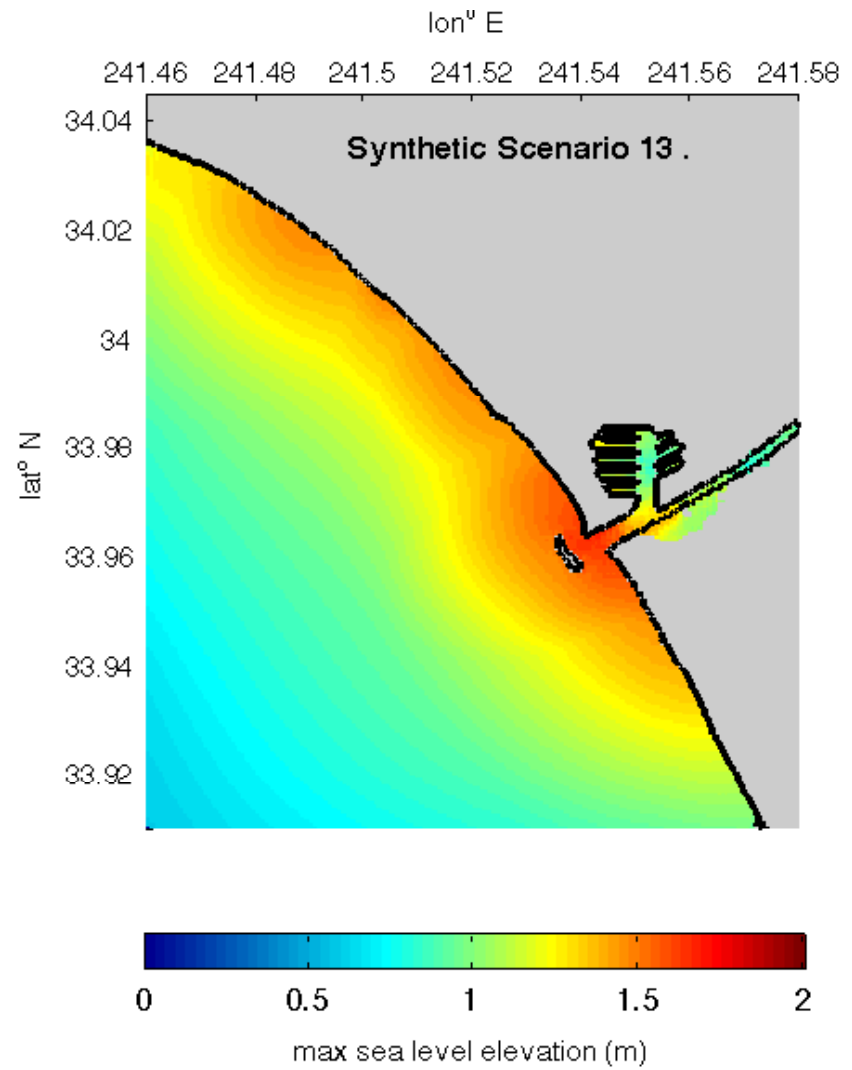
Figure 47: Maximum sea surface elevation computed with the forecast model for synthetic scenario 13 (Mw=9.3).
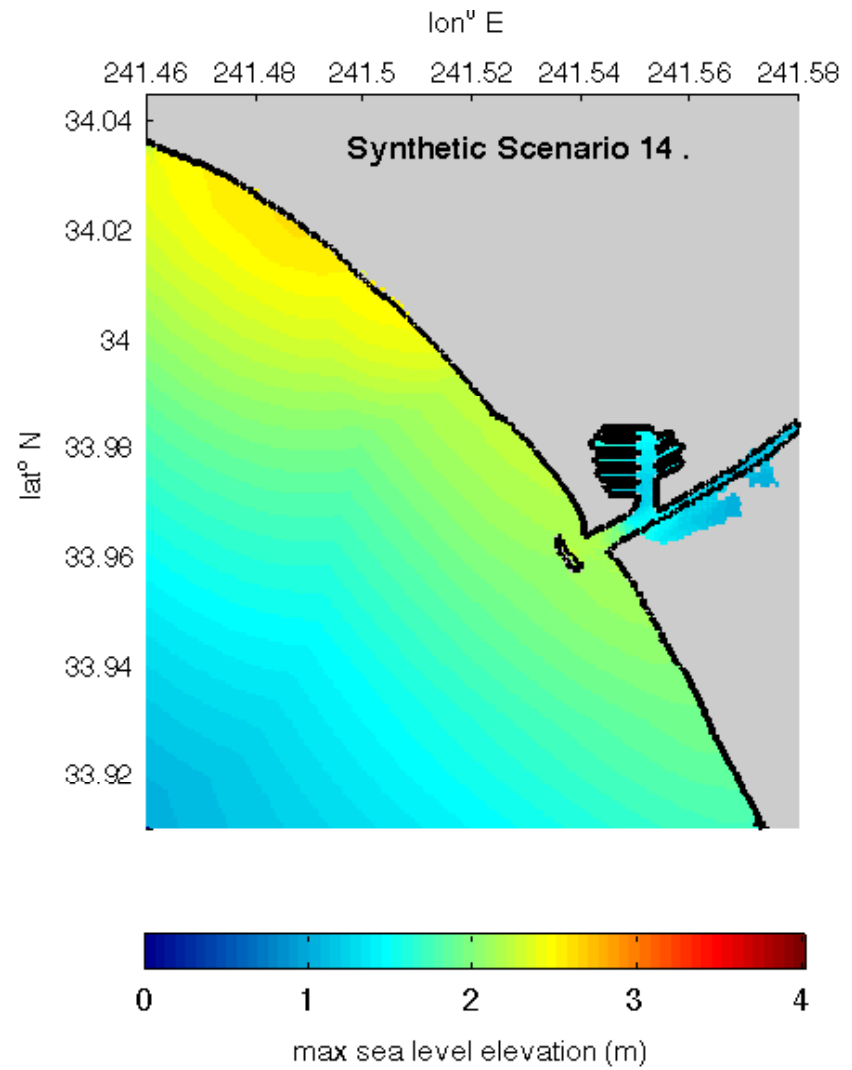
Figure 48: Maximum sea surface elevation computed with the forecast model for synthetic scenario 14 (Mw=9.3).
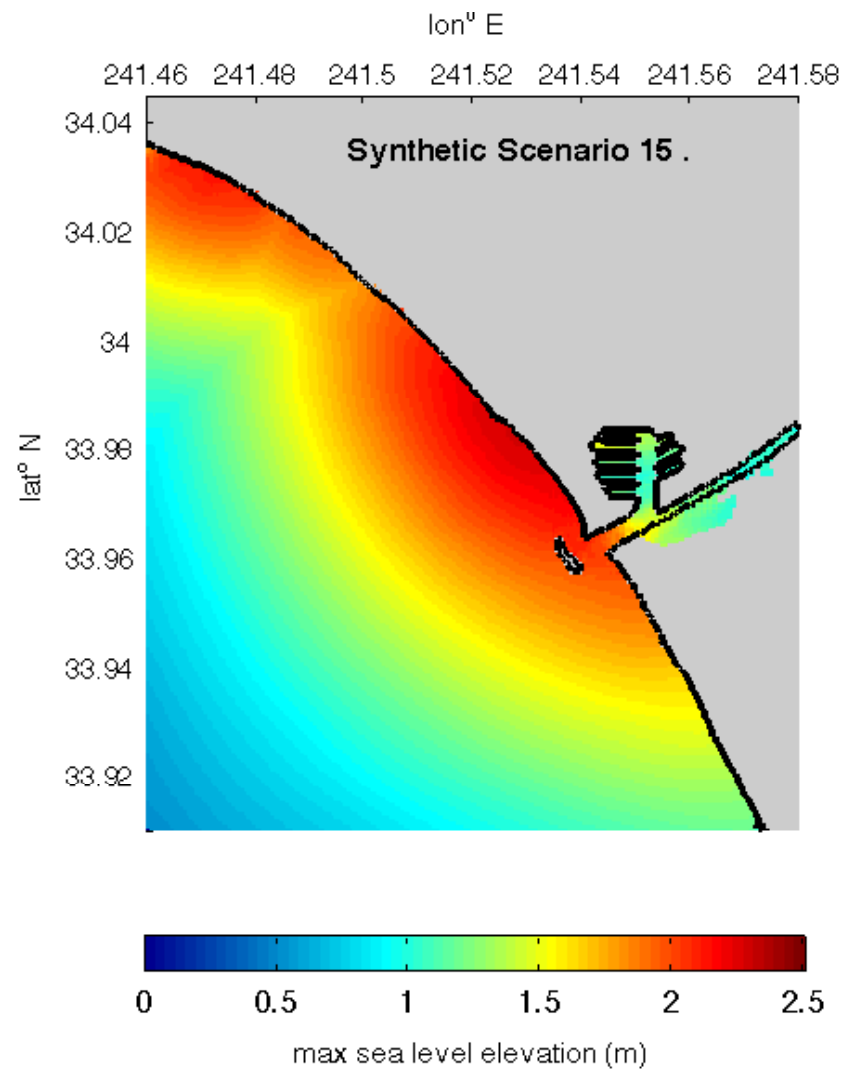
Figure 49: Maximum sea surface elevation computed with the forecast model for synthetic scenario 15 (Mw=9.3).
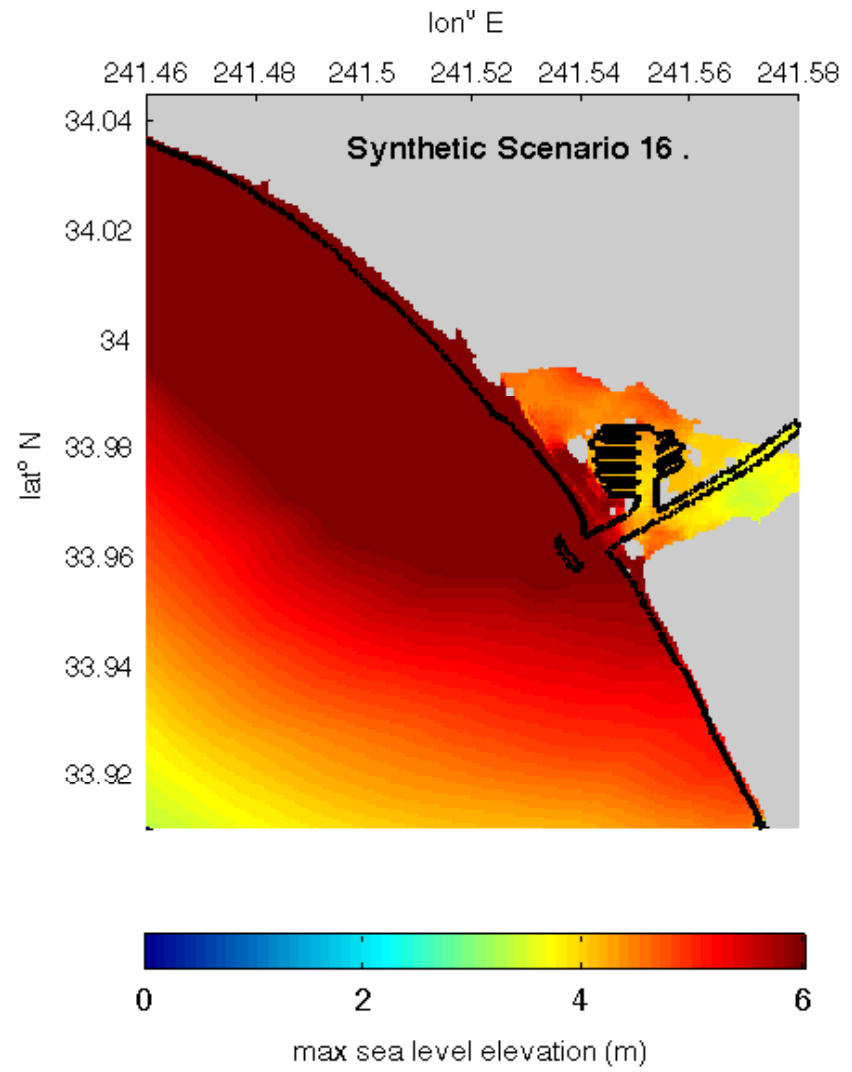
Figure 50: Maximum sea surface elevation computed with the forecast model for synthetic scenario 16 (Mw=9.3).
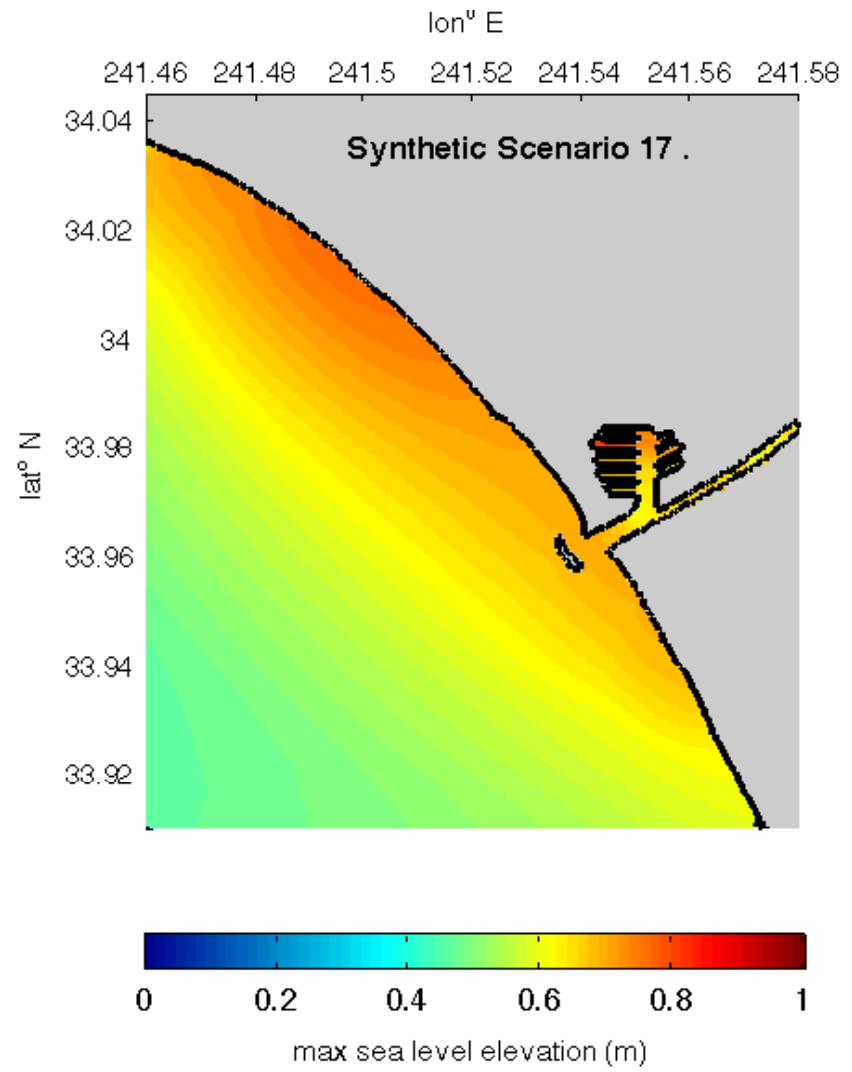
Figure 51: Maximum sea surface elevation computed with the forecast model for synthetic scenario 17 (Mw=9.3).
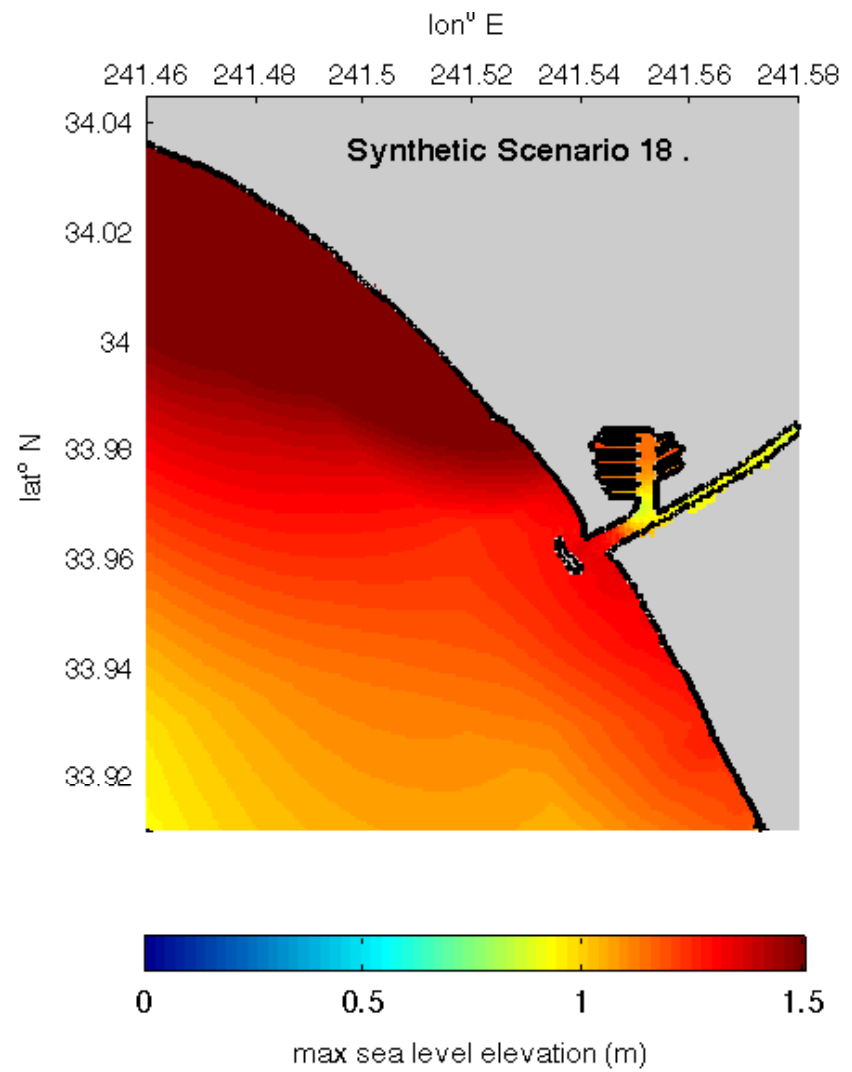
Figure 52: Maximum sea surface elevation computed with the forecast model for synthetic scenario 18 (Mw=9.3).
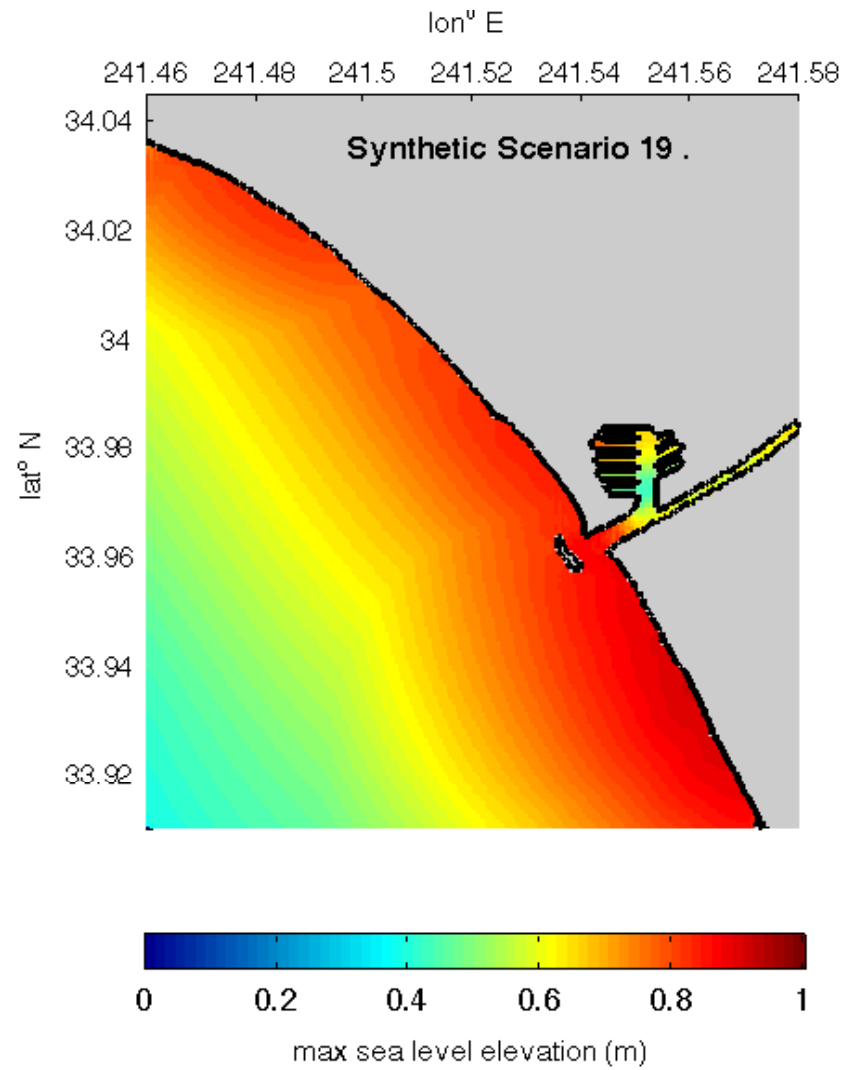
Figure 53: Maximum sea surface elevation computed with the forecast model for synthetic scenario 19 (Mw=9.3).
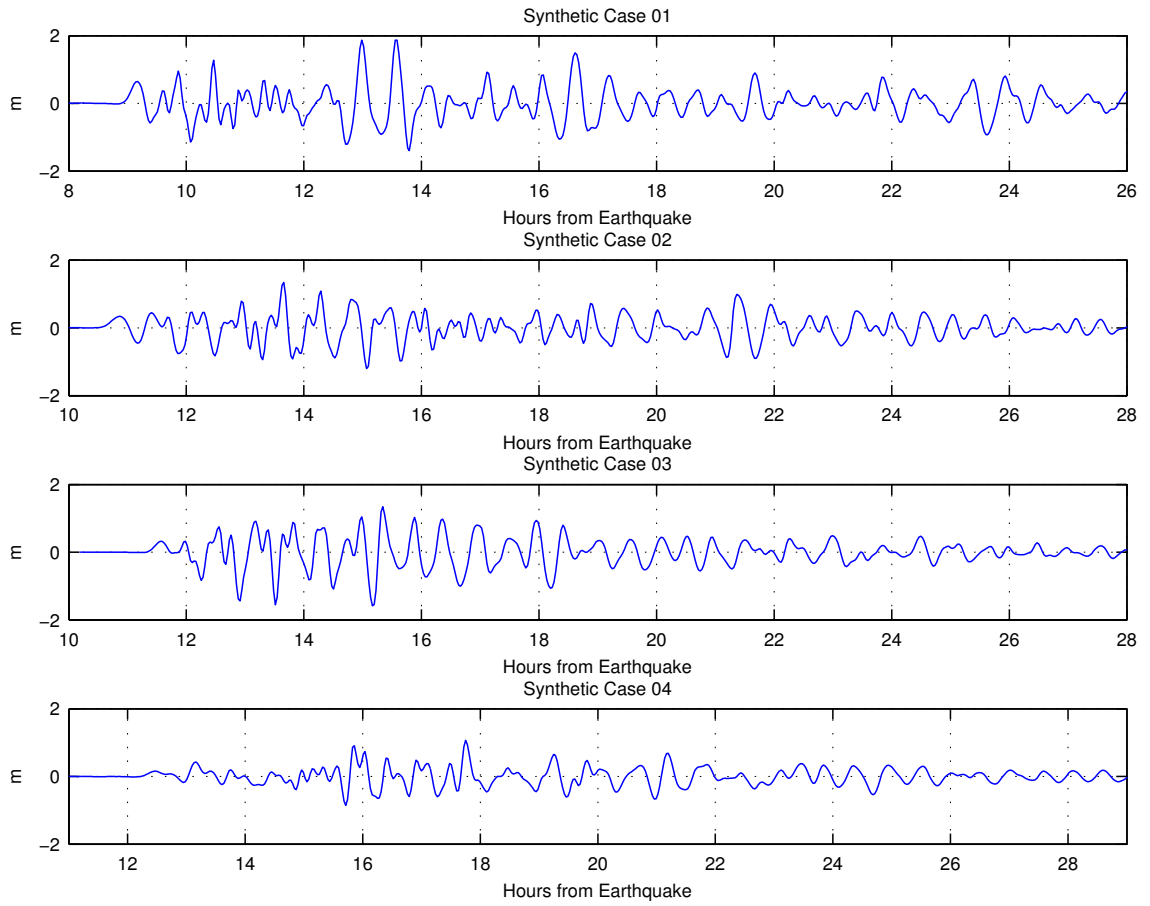
Figure 54: Predicted time-series at the Santa Monica tide gauge for synthetic scenarios 1 through 4 (from top to bottom).
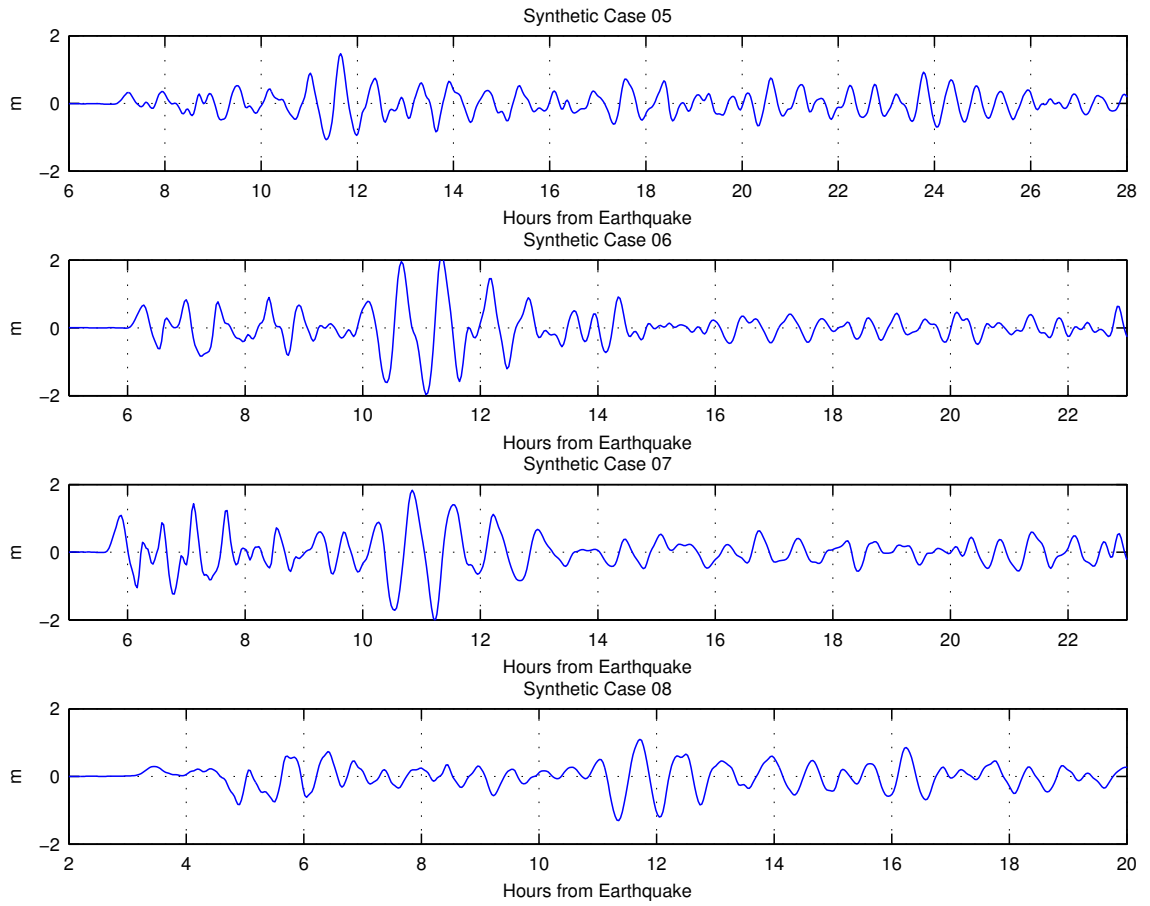
Figure 55: Predicted time-series at the Santa Monica tide gauge for synthetic scenarios 5 through 8 (from top to bottom).
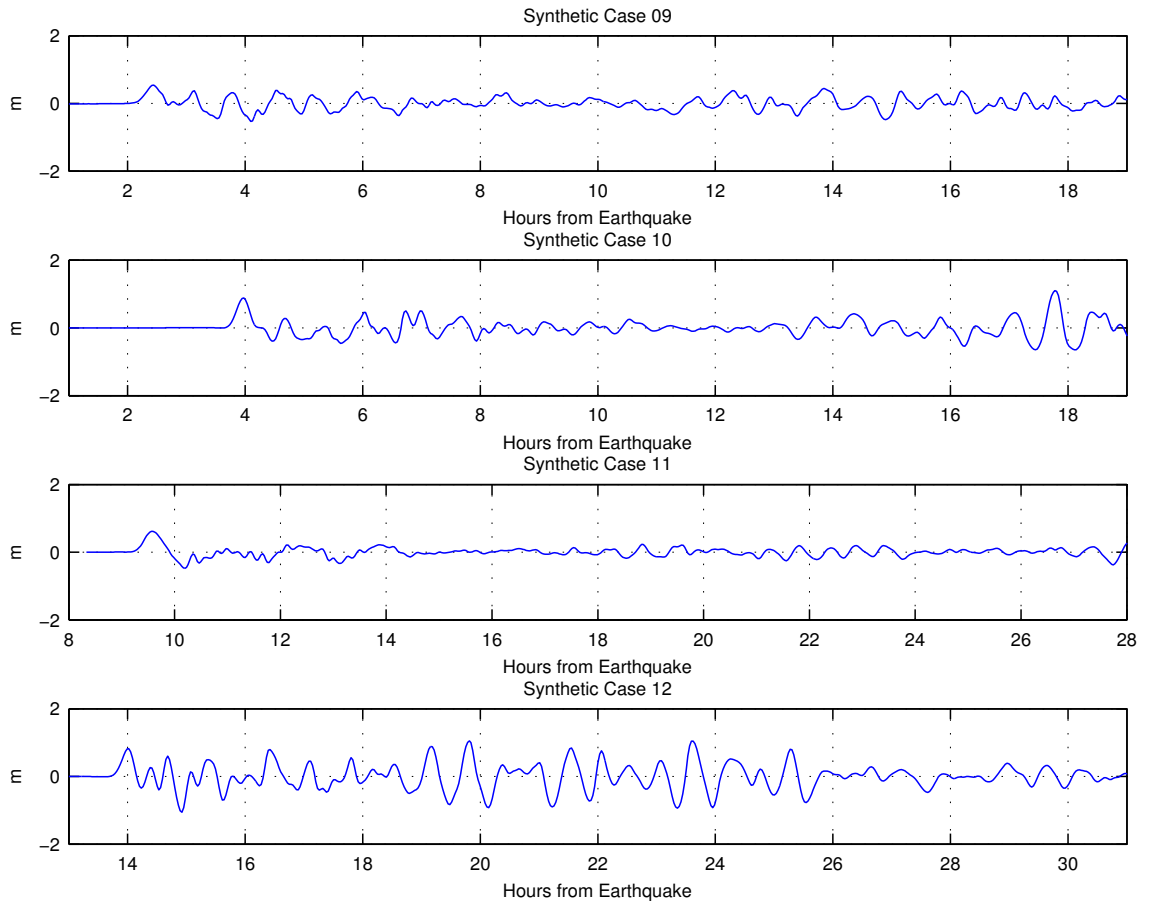
Figure 56: Predicted time-series at the Santa Monica tide gauge for synthetic scenarios 9 through 12 (from top to bottom).
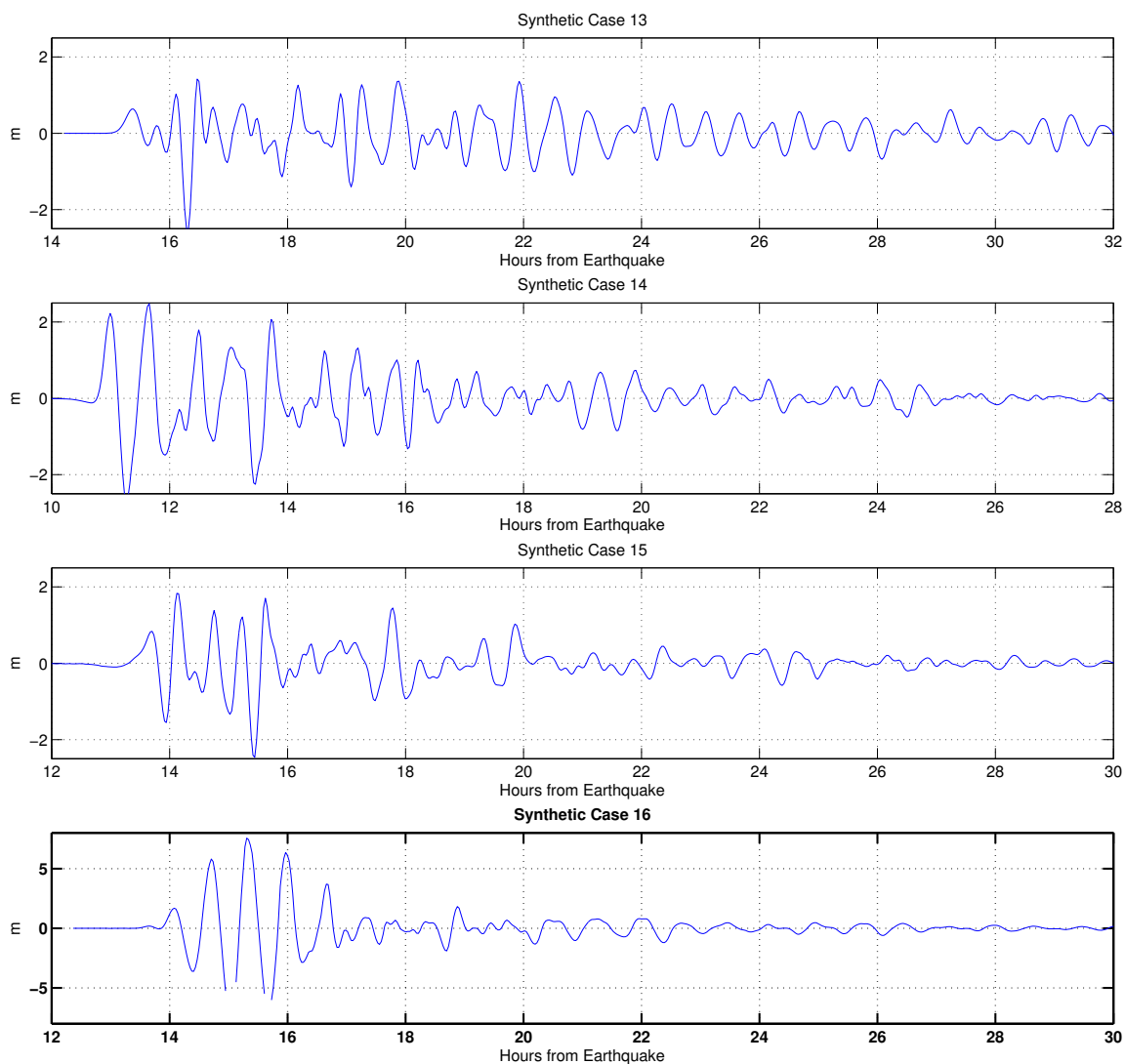
Figure 57: Predicted time-series at the Santa Monica tide gauge for synthetic scenarios 13 through 16 (from top to bottom).
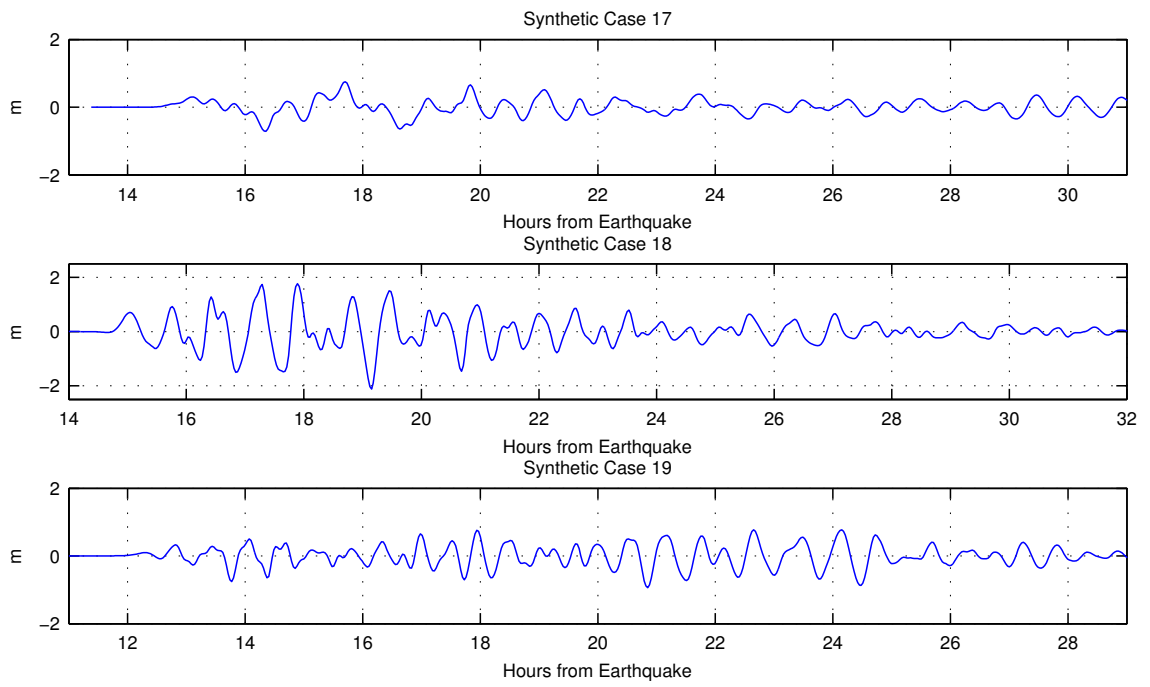
Figure 58: Predicted time-series at the Santa Monica tide gauge for synthetic scenarios 17 through 19 (from top to bottom).
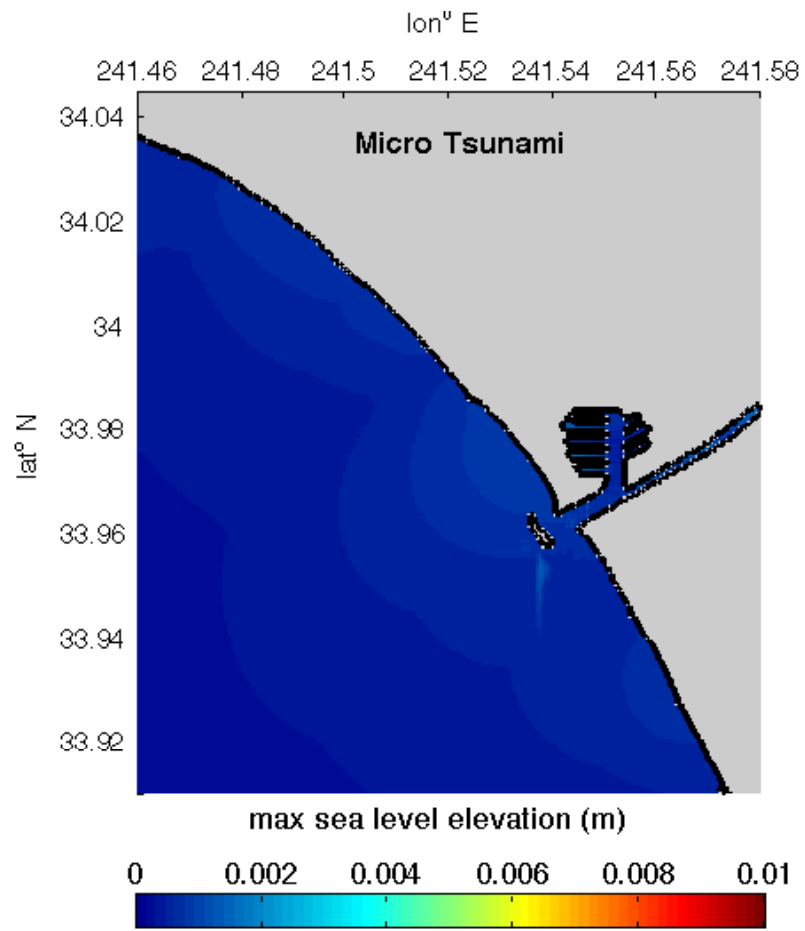
Figure 59: Maximum sea surface elevation computed with the forecast model for a micro synthetic scenario (Mw=6.2).
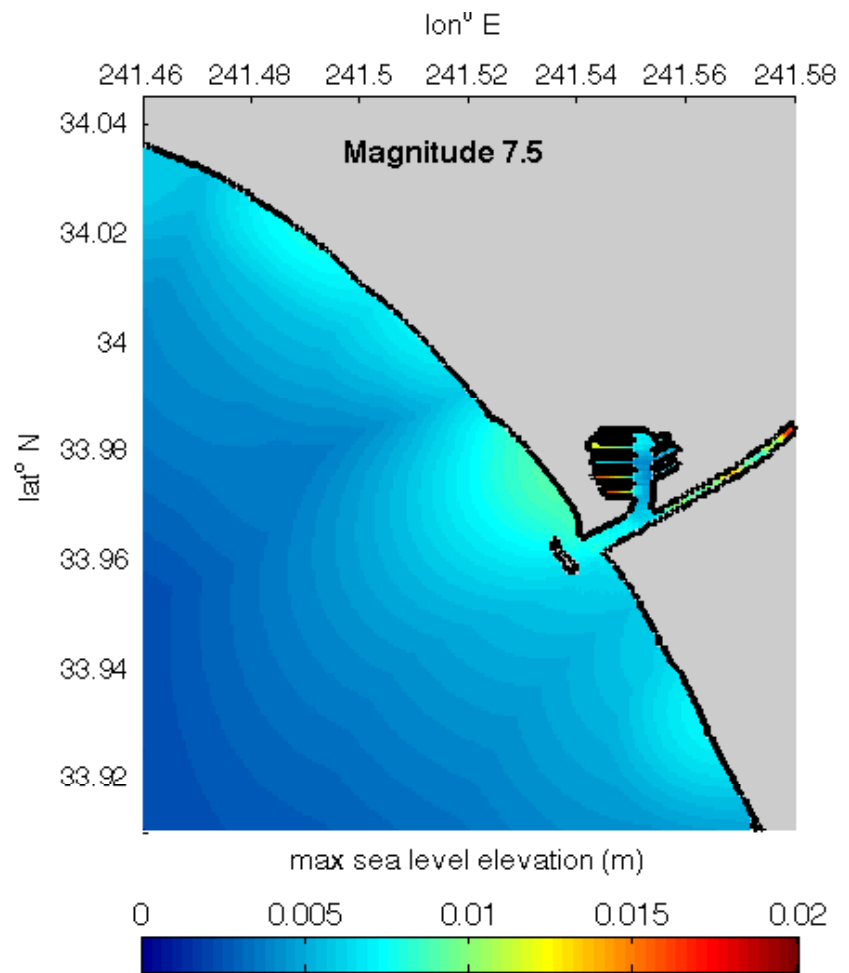
Figure 60: Maximum sea surface elevation computed with the forecast model for a mid-size synthetic scenario (Mw=7.5).

TABLES

Earthquake / Seismic				Model		
Event	**USGS Date Time (UTC) Epicenter**	**CMT Date Time (UTC) Centroid**	**Magnitude Mw**	**Tsunami Magnitude[1]**	**Subduction Zone**	**Tsunami Source**
1946 Unimak	01 Apr 12:28:56 52.75ºN 163.50ºW	01 Apr 12:28:56 53.32ºN 163.19ºW	[2]8.5	8.5	Aleutian-Alaska-Cascadia (ACSZ)	$7.5 \times b23 + 19.7 \times b24 + 3.7 \times b25$
1964 Alaska	28 Mar 03:36:00 [3]61.02ºN 147.65ºW	28 Mar 03:36:14 61.10ºN 147.50ºW	[3]9.2	9.0	Aleutian-Alaska-Cascadia (ACSZ)	$a34 \times 15.4 + a35 \times 19.4 + z34 \times 48.3 + b34 \times 18.3 + b35 \times 15.1$
1994 East Kuril	04 Oct 13:22:58 43.73ºN 147.321ºE	04 Oct 13:23:28.5 43.60ºN 147.63ºE	[5]8.3	8.1	Kamchatka-Kuril-Japan-Izu-Mariana-Yap (KISZ)	$9.0 \times a20$
1996 Andreanov	10 Jun 04:03:35 51.56ºN 175.39ºW	10 Jun 04:04:03.4 51.10ºN 177.410ºW	[5]7.9	7.8	Aleutian-Alaska-Cascadia (ACSZ)	$2.40 \times a15 + 0.80 \times b16$
2003 Rat Island	17 Nov 06:43:07 51.13ºN 178.74ºE	17 Nov 06:43:31.0 51.14ºN 177.86ºE	[5]7.7	7.8	Aleutian-Alaska-Cascadia (ACSZ)	$[6]2.81 \times b11$
2006 Tonga	03 May 15:26:39 20.13ºS 174.161ºW	03 May 15:27:03.7 20.39ºS 173.47ºW	[5]8.0	8.0	New Zealand-Kermadec-Tonga (NTSZ)	$6.6 \times b29$
2006 Kuril	15 Nov 11:14:16 46.607ºN 153.230ºE	15 Nov 11:15:08 46.71ºN 154.33ºE	[5]8.3	8.1	Kamchatka-Kuril-Japan-Izu-Mariana-Yap (KISZ)	$[6]4 \times a12 + 0.5 \times b12 + 2 \times a13 + 1.5 \times b13$
2007 Kuril	13 Jan 04:23:20 46.272ºN 154.455ºE	13 Jan 04:23:48.1 46.17ºN 154.80ºE	[5]8.1	7.9	Kamchatka-Kuril-Japan-Izu-Mariana-Yap (KISZ)	$-3.64 \times b13$
2007 Solomon	01 Apr 20:39:56 8.481ºS 156.978ºE	01 Apr 20:40:38.9 7.76ºS 156.34ºE	[3]8.1	8.2	New Britain-Solomons-Vanuatu (NVSZ)	$12.0 \times b10$
2007 Peru	15 Aug 23:40:57 13.354ºS 76.509ºW	15 Aug 23:41:57.9 13.73ºS 77.04ºW	[5]8.0	8.1	Central-South America (CSSZ)	$0.9 \times a61 + 1.25 \times b61 + 5.6 \times a62 + 6.97 \times b62 + 3.5 \times z62$
2007 Chile	14 Nov 15:40:50 22.204ºS 69.869ºW	14 Nov 15:41:11.2 22.64ºS 70.62ºW	[3]7.7	7.6	Central-South America (CSSZ)	$z73 \times 1.65$
2009 Samoa	29 Sep 17:48:10 15.509ºS 172.034ºW	29 Sep 17:48:26.8 15.13ºS 171.97ºW	[5]8.1	8.1	New Zealand-Kermadec-Tonga (NTSZ)	$[6]3.96 \times a34 + 3.96 \times b34$
2010 Chile	27 Feb 06:34:14 35.909ºS 72.733ºW	27 Feb 06:35:15.4 35.95ºS 73.15ºW	[5]8.8	8.8	Central-South America (CSSZ)	$[6]a88 \times 17.24 + a90 \times 8.82 + b88 \times 11.86 + b89 \times 18.39 + b90 \times 16.75 + z88 \times 20.78 + z90 \times 7.06$
2011 Tohoku	11 Mar 05:46:23.82 38.308ºN 142.383ºN	11 Mar 05:47:47.20 38.486ºN 142.597ºE	[5]9.0	8.9	Kamchatka-Kuril-Japan-Izu-Mariana-Yap (KISZ)	$4.66 \times b24 + 12.23 \times b25 + 26.31 \times a26 + 21.27 \times b26 + 22.75 \times a27 + 4.98 \times b27$

[1] Preliminary source – derived from source and deep-ocean observations
[2] López and Okal (2006)
[3] United States Geological Survey (USGS)

Table 1: Historical events used for model validation for Santa Monica.

Model Setup	Reference Model			Forecast Model		
	Grid A	**Grid B**	**Grid C**	**Grid A**	**Grid B**	**Grid C**
W	W123.00	W119.14	W118.54	W123.00	W119.14	W118.54
E	W117.00	W118.20	W118.42	W117.00	W118.20	W118.42
S	N32.00	N33.20	N33.909	N32.00	N33.20	N33.909
N	N35.00	N34.20	N34.045	N35.00	N34.20	N34.045
dx	30″	6″	1″	60″	12″	2″
dy	30″	6″	1″	60″	12″	2″
$nx \times ny$	721×361	565x601	433×488	361×181	283x301	252×201
dt (sec)	2.7	0.9	0.9	5.4	1.8	1.8
D_{min}	5 m			5 m		
Fric. (n^2)	0.0009			0.0009		
CPU Time	~ 55.12 min for 4-hour simulation			~ 6.68 min for 4-hour simulation		
Warning Pt.	W118.5, N34.0075					

Table 2: MOST setup parameters for reference and forecast models for Santa Monica.

SceNo.	Scenario Name	Source Zone	Tsunami Source	α (m)	Max (m)	Min (m)
Mega-tsunami scenario						
1	KISZ 1-10	Kamchatka-Yap-Mariana-Izu-Bonin	A1-A10, B1-B10	25	1.87	-1.39
2	KISZ 22-31	Kamchatka-Yap-Mariana-Izu-Bonin	A22-A31, B22-B31	25	1.33	-1.20
3	KISZ 32-41	Kamchatka-Yap-Mariana-Izu-Bonin	A32-A41, B32-B41	25	1.34	-1.58
4	KISZ 56-65	Kamchatka-Yap-Mariana-Izu-Bonin	A56-65, B56-65	25	1.06	-0.86
5	ACSZ 6-15	Aleutian-Alaska-Cascadia	A6-A15, B6-B15	25	1.47	-1.07
6	ACSZ 16-25	Aleutian-Alaska-Cascadia	A16-A25, B16-B25	25	2.17	-1.97
7	ACSZ 22-31	Aleutian-Alaska-Cascadia	A22-A31, B22-B31	25	1.83	-2.03
8	ACSZ 50-59	Aleutian-Alaska-Cascadia	A50-A59, B50-B59	25	1.10	-1.30
9	ACSZ 56-65	Aleutian-Alaska-Cascadia	A56-A65, B56-B65	25	0.87	-0.78
10	CSSZ 1-10	Central and South America	A1-A10, B1-B10	25	1.10	-0.70
11	CSSZ 37-46	Central and South America	A37-A46, B37-B46	25	0.61	-0.48
12	CSSZ 89-98	Central and South America	A89-A98, B89-B98	25	1.05	-1.06
13	CSSZ 102 – 111	Central and South America	A102-A111, B102-B111	25	1.42	-2.54
14	NTSZ 30-39	New Zealand-Kermadec-Tonga	A30-A39, B30-B39	25	2.48	-2.67
15	NVSZ 28-37	New Britain-Solomons-Vanuatu	A28-A37, B28-B37	25	1.83	-2.46
16	MOSZ 1-10	ManusOCB	A1-A10, B1-B10	25	7.56	-6.02
17	NGSZ 3-12	North New Guinea	A3-A12, B3-B12	25	0.75	-0.71
18	EPSZ 6-15	East Philippines	A6-A15, B6-B15	25	1.76	-2.12
19	RNSZ 12-21	Ryukus-Kyushu-Nankai	A12-A21, B12-B21	25	0.78	0.93
Mw 7.5 Tsunami scenario						
20	KISZ B47	Kamchatka-Yap-Mariana-Izu-Bonin	B47	1	-0.007	-0.008

Table 3: Synthetic tsunami sources used in the forecast model robustness test for Santa Monica.

Appendix A

Development of the Santa Monica, CA tsunami forecast model occurred prior to parameter changes that were made to reflect modifications to the MOST model code. As a result, the input file for running both the tsunami forecast model and the high-resolution reference inundation model in MOST have been updated accordingly. Appendix A1 and A2 provide the updated files for Santa Monica.

A.1   Reference model ⋆.in file for Santa Monica, California

0.0001 Minimum amplitude of input offshore wave (m)
5 Input minimum depth for offshore (m)
0.1 Input "dry land" depth for inundation (m)
0.0009 Input friction coefficient (n ⋆⋆2)
1 let a and b run up
100.0 max eta before blow up (m)
0.9 Input time step (sec)
47520 Input number of steps
3 Compute "A" arrays every nth time step, n=
1 Compute "B" arrays every nth time step, n=
60 Input number of steps between snapshots
1 ...Starting from
1 ...Saving grid every nth node, n=?
SMrimA.cc
SMrimB.cc
SMrimC.ext.c.ssl.mod.creek
../SRCS/santa_srcs/
./rsyn01_run2d/
1 1 1 1
1
3 145 136

A.2 Forecast model ⋆.in file for Santa Monica, California

0.0001 Minimum amplitude of input offshore wave (m)
5 Input minimum depth for offshore (m)
0.1 Input "dry land" depth for inundation (m)
0.0009 Input friction coefficient (n ⋆⋆ 2)
1 let a and b runup
100.0 max eta before blow up (m)
1.8 Input time step (sec)
47520 Input number of steps
3 Compute "A" arrays every nth time step, n=
1 Compute "B" arrays every nth time step, n=
60 Input number of steps between snapshots
1 ...Starting from
1 ...Saving grid every nth node, n=?
smonica_run2d/SMSIMA
smonica_run2d/SMSIMB smonica_run2d/SMSIMC
./
./
1 1 1 1 NetCDF output for A, B, C, SIFT
1 Timeseries locations:
3 73 68

Appendix B

Propagation Database: Pacific Ocean Unit Sources

NOAA Propagation Database presented in this section is the representation of the database as of March 2013. This database may have been updated since March 2013.
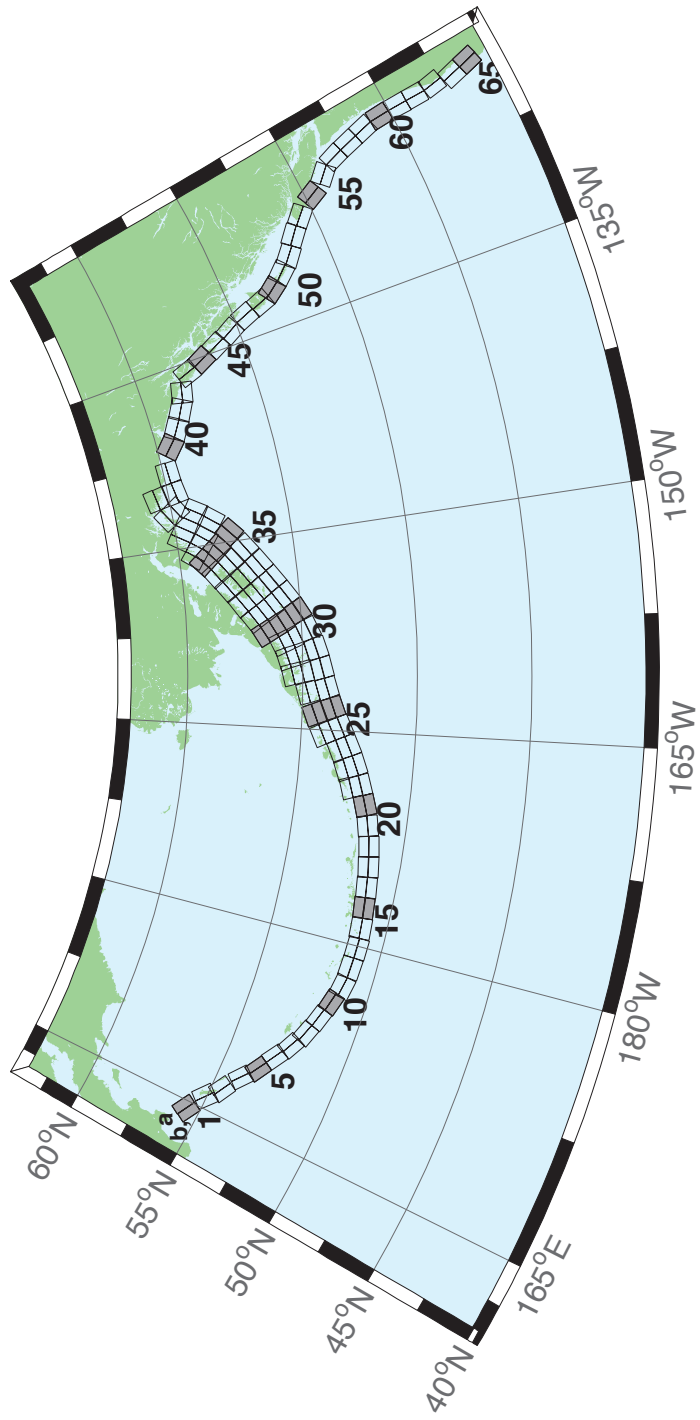
Figure B.1: Aleutian–Alaska–Cascadia Subduction Zone unit sources.

Table B.1: Earthquake parameters for Aleutian–Alaska–Cascadia Subduction Zone unit sources.

Segment	Description	Longitude(°E)	Latitude(°N)	Strike(°)	Dip(°)	Depth (km)
acsz–1a	Aleutian–Alaska–Cascadia	164.7994	55.9606	299	17	19.61
acsz–1b	Aleutian–Alaska–Cascadia	164.4310	55.5849	299	17	5
acsz–2a	Aleutian–Alaska–Cascadia	166.3418	55.4016	310.2	17	19.61
acsz–2b	Aleutian–Alaska–Cascadia	165.8578	55.0734	310.2	17	5
acsz–3a	Aleutian–Alaska–Cascadia	167.2939	54.8919	300.2	23.36	24.82
acsz–3b	Aleutian–Alaska–Cascadia	166.9362	54.5356	300.2	23.36	5
acsz–4a	Aleutian–Alaska–Cascadia	168.7131	54.2852	310.2	38.51	25.33
acsz–4b	Aleutian–Alaska–Cascadia	168.3269	54.0168	310.2	24	5
acsz–5a	Aleutian–Alaska–Cascadia	169.7447	53.7808	302.8	37.02	23.54
acsz–5b	Aleutian–Alaska–Cascadia	169.4185	53.4793	302.8	21.77	5
acsz–6a	Aleutian–Alaska–Cascadia	171.0144	53.3054	303.2	35.31	22.92
acsz–6b	Aleutian–Alaska–Cascadia	170.6813	52.9986	303.2	21	5
acsz–7a	Aleutian–Alaska–Cascadia	172.1500	52.8528	298.2	35.56	20.16
acsz–7b	Aleutian–Alaska–Cascadia	171.8665	52.5307	298.2	17.65	5
acsz–8a	Aleutian–Alaska–Cascadia	173.2726	52.4579	290.8	37.92	20.35
acsz–8b	Aleutian–Alaska–Cascadia	173.0681	52.1266	290.8	17.88	5
acsz–9a	Aleutian–Alaska–Cascadia	174.5866	52.1434	289	39.09	21.05
acsz–9b	Aleutian–Alaska–Cascadia	174.4027	51.8138	289	18.73	5
acsz–10a	Aleutian–Alaska–Cascadia	175.8784	51.8526	286.1	40.51	20.87
acsz–10b	Aleutian–Alaska–Cascadia	175.7265	51.5245	286.1	18.51	5
acsz–11a	Aleutian–Alaska–Cascadia	177.1140	51.6488	280	15	17.94
acsz–11b	Aleutian–Alaska–Cascadia	176.9937	51.2215	280	15	5
acsz–12a	Aleutian–Alaska–Cascadia	178.4500	51.5690	273	15	17.94
acsz–12b	Aleutian–Alaska–Cascadia	178.4130	51.1200	273	15	5
acsz–13a	Aleutian–Alaska–Cascadia	179.8550	51.5340	271	15	17.94
acsz–13b	Aleutian–Alaska–Cascadia	179.8420	51.0850	271	15	5
acsz–14a	Aleutian–Alaska–Cascadia	181.2340	51.5780	267	15	17.94
acsz–14b	Aleutian–Alaska–Cascadia	181.2720	51.1290	267	15	5
acsz–15a	Aleutian–Alaska–Cascadia	182.6380	51.6470	265	15	17.94
acsz–15b	Aleutian–Alaska–Cascadia	182.7000	51.2000	265	15	5
acsz–16a	Aleutian–Alaska–Cascadia	184.0550	51.7250	264	15	17.94
acsz–16b	Aleutian–Alaska–Cascadia	184.1280	51.2780	264	15	5
acsz–17a	Aleutian–Alaska–Cascadia	185.4560	51.8170	262	15	17.94
acsz–17b	Aleutian–Alaska–Cascadia	185.5560	51.3720	262	15	5
acsz–18a	Aleutian–Alaska–Cascadia	186.8680	51.9410	261	15	17.94
acsz–18b	Aleutian–Alaska–Cascadia	186.9810	51.4970	261	15	5
acsz–19a	Aleutian–Alaska–Cascadia	188.2430	52.1280	257	15	17.94
acsz–19b	Aleutian–Alaska–Cascadia	188.4060	51.6900	257	15	5
acsz–20a	Aleutian–Alaska–Cascadia	189.5810	52.3550	251	15	17.94
acsz–20b	Aleutian–Alaska–Cascadia	189.8180	51.9300	251	15	5
acsz–21a	Aleutian–Alaska–Cascadia	190.9570	52.6470	251	15	17.94
acsz–21b	Aleutian–Alaska–Cascadia	191.1960	52.2220	251	15	5
acsz–21z	Aleutian–Alaska–Cascadia	190.7399	53.0443	250.8	15	30.88
acsz–22a	Aleutian–Alaska–Cascadia	192.2940	52.9430	247	15	17.94
acsz–22b	Aleutian–Alaska–Cascadia	192.5820	52.5300	247	15	5
acsz–22z	Aleutian–Alaska–Cascadia	192.0074	53.3347	247.8	15	30.88
acsz–23a	Aleutian–Alaska–Cascadia	193.6270	53.3070	245	15	17.94
acsz–23b	Aleutian–Alaska–Cascadia	193.9410	52.9000	245	15	5
acsz–23z	Aleutian–Alaska–Cascadia	193.2991	53.6768	244.6	15	30.88
acsz–24a	Aleutian–Alaska–Cascadia	194.9740	53.6870	245	15	17.94
acsz–24b	Aleutian–Alaska–Cascadia	195.2910	53.2800	245	15	5
acsz–24y	Aleutian–Alaska–Cascadia	194.3645	54.4604	244.4	15	43.82
acsz–24z	Aleutian–Alaska–Cascadia	194.6793	54.0674	244.6	15	30.88
acsz–25a	Aleutian–Alaska–Cascadia	196.4340	54.0760	250	15	17.94
acsz–25b	Aleutian–Alaska–Cascadia	196.6930	53.6543	250	15	5
acsz–25y	Aleutian–Alaska–Cascadia	195.9009	54.8572	247.9	15	43.82
acsz–25z	Aleutian–Alaska–Cascadia	196.1761	54.4536	248.1	15	30.88
acsz–26a	Aleutian–Alaska–Cascadia	197.8970	54.3600	253	15	17.94
acsz–26b	Aleutian–Alaska–Cascadia	198.1200	53.9300	253	15	5
acsz–26y	Aleutian–Alaska–Cascadia	197.5498	55.1934	253.1	15	43.82

Segment	Description	Longitude(^{o}E)	Latitude(^{o}N)	Strike(^{o})	Dip(^{o})	Depth (km)
acsz–26z	Aleutian–Alaska–Cascadia	197.7620	54.7770	253.3	15	30.88
acsz–27a	Aleutian–Alaska–Cascadia	199.4340	54.5960	256	15	17.94
acsz–27b	Aleutian–Alaska–Cascadia	199.6200	54.1600	256	15	5
acsz–27x	Aleutian–Alaska–Cascadia	198.9736	55.8631	256.5	15	56.24
acsz–27y	Aleutian–Alaska–Cascadia	199.1454	55.4401	256.6	15	43.82
acsz–27z	Aleutian–Alaska–Cascadia	199.3135	55.0170	256.8	15	30.88
acsz–28a	Aleutian–Alaska–Cascadia	200.8820	54.8300	253	15	17.94
acsz–28b	Aleutian–Alaska–Cascadia	201.1080	54.4000	253	15	5
acsz–28x	Aleutian–Alaska–Cascadia	200.1929	56.0559	252.5	15	56.24
acsz–28y	Aleutian–Alaska–Cascadia	200.4167	55.6406	252.7	15	43.82
acsz–28z	Aleutian–Alaska–Cascadia	200.6360	55.2249	252.9	15	30.88
acsz–29a	Aleutian–Alaska–Cascadia	202.2610	55.1330	247	15	17.94
acsz–29b	Aleutian–Alaska–Cascadia	202.5650	54.7200	247	15	5
acsz–29x	Aleutian–Alaska–Cascadia	201.2606	56.2861	245.7	15	56.24
acsz–29y	Aleutian–Alaska–Cascadia	201.5733	55.8888	246	15	43.82
acsz–29z	Aleutian–Alaska–Cascadia	201.8797	55.4908	246.2	15	30.88
acsz–30a	Aleutian–Alaska–Cascadia	203.6040	55.5090	240	15	17.94
acsz–30b	Aleutian–Alaska–Cascadia	203.9970	55.1200	240	15	5
acsz–30w	Aleutian–Alaska–Cascadia	201.9901	56.9855	239.5	15	69.12
acsz–30x	Aleutian–Alaska–Cascadia	202.3851	56.6094	239.8	15	56.24
acsz–30y	Aleutian–Alaska–Cascadia	202.7724	56.2320	240.2	15	43.82
acsz–30z	Aleutian–Alaska–Cascadia	203.1521	55.8534	240.5	15	30.88
acsz–31a	Aleutian–Alaska–Cascadia	204.8950	55.9700	236	15	17.94
acsz–31b	Aleutian–Alaska–Cascadia	205.3400	55.5980	236	15	5
acsz–31w	Aleutian–Alaska–Cascadia	203.0825	57.3740	234.5	15	69.12
acsz–31x	Aleutian–Alaska–Cascadia	203.5408	57.0182	234.9	15	56.24
acsz–31y	Aleutian–Alaska–Cascadia	203.9904	56.6607	235.3	15	43.82
acsz–31z	Aleutian–Alaska–Cascadia	204.4315	56.3016	235.7	15	30.88
acsz–32a	Aleutian–Alaska–Cascadia	206.2080	56.4730	236	15	17.94
acsz–32b	Aleutian–Alaska–Cascadia	206.6580	56.1000	236	15	5
acsz–32w	Aleutian–Alaska–Cascadia	204.4129	57.8908	234.3	15	69.12
acsz–32x	Aleutian–Alaska–Cascadia	204.8802	57.5358	234.7	15	56.24
acsz–32y	Aleutian–Alaska–Cascadia	205.3385	57.1792	235.1	15	43.82
acsz–32z	Aleutian–Alaska–Cascadia	205.7880	56.8210	235.5	15	30.88
acsz–33a	Aleutian–Alaska–Cascadia	207.5370	56.9750	236	15	17.94
acsz–33b	Aleutian–Alaska–Cascadia	207.9930	56.6030	236	15	5
acsz–33w	Aleutian–Alaska–Cascadia	205.7126	58.3917	234.2	15	69.12
acsz–33x	Aleutian–Alaska–Cascadia	206.1873	58.0371	234.6	15	56.24
acsz–33y	Aleutian–Alaska–Cascadia	206.6527	57.6808	235	15	43.82
acsz–33z	Aleutian–Alaska–Cascadia	207.1091	57.3227	235.4	15	30.88
acsz–34a	Aleutian–Alaska–Cascadia	208.9371	57.5124	236	15	17.94
acsz–34b	Aleutian–Alaska–Cascadia	209.4000	57.1400	236	15	5
acsz–34w	Aleutian–Alaska–Cascadia	206.9772	58.8804	233.5	15	69.12
acsz–34x	Aleutian–Alaska–Cascadia	207.4677	58.5291	233.9	15	56.24
acsz–34y	Aleutian–Alaska–Cascadia	207.9485	58.1760	234.3	15	43.82
acsz–34z	Aleutian–Alaska–Cascadia	208.4198	57.8213	234.7	15	30.88
acsz–35a	Aleutian–Alaska–Cascadia	210.2597	58.0441	230	15	17.94
acsz–35b	Aleutian–Alaska–Cascadia	210.8000	57.7000	230	15	5
acsz–35w	Aleutian–Alaska–Cascadia	208.0204	59.3199	228.8	15	69.12
acsz–35x	Aleutian–Alaska–Cascadia	208.5715	58.9906	229.3	15	56.24
acsz–35y	Aleutian–Alaska–Cascadia	209.1122	58.6590	229.7	15	43.82
acsz–35z	Aleutian–Alaska–Cascadia	209.6425	58.3252	230.2	15	30.88
acsz–36a	Aleutian–Alaska–Cascadia	211.3249	58.6565	218	15	17.94
acsz–36b	Aleutian–Alaska–Cascadia	212.0000	58.3800	218	15	5
acsz–36w	Aleutian–Alaska–Cascadia	208.5003	59.5894	215.6	15	69.12
acsz–36x	Aleutian–Alaska–Cascadia	209.1909	59.3342	216.2	15	56.24
acsz–36y	Aleutian–Alaska–Cascadia	209.8711	59.0753	216.8	15	43.82
acsz–36z	Aleutian–Alaska–Cascadia	210.5412	58.8129	217.3	15	30.88
acsz–37a	Aleutian–Alaska–Cascadia	212.2505	59.2720	213.7	15	17.94
acsz–37b	Aleutian–Alaska–Cascadia	212.9519	59.0312	213.7	15	5
acsz–37x	Aleutian–Alaska–Cascadia	210.1726	60.0644	213	15	56.24
acsz–37y	Aleutian–Alaska–Cascadia	210.8955	59.8251	213.7	15	43.82

Segment	Description	Longitude(^{o}E)	Latitude(^{o}N)	Strike(^{o})	Dip(^{o})	Depth (km)
acsz–37z	Aleutian–Alaska–Cascadia	211.6079	59.5820	214.3	15	30.88
acsz–38a	Aleutian–Alaska–Cascadia	214.6555	60.1351	260.1	0	15
acsz–38b	Aleutian–Alaska–Cascadia	214.8088	59.6927	260.1	0	15
acsz–38y	Aleutian–Alaska–Cascadia	214.3737	60.9838	259	0	15
acsz–38z	Aleutian–Alaska–Cascadia	214.5362	60.5429	259	0	15
acsz–39a	Aleutian–Alaska–Cascadia	216.5607	60.2480	267	0	15
acsz–39b	Aleutian–Alaska–Cascadia	216.6068	59.7994	267	0	15
acsz–40a	Aleutian–Alaska–Cascadia	219.3069	59.7574	310.9	0	15
acsz–40b	Aleutian–Alaska–Cascadia	218.7288	59.4180	310.9	0	15
acsz–41a	Aleutian–Alaska–Cascadia	220.4832	59.3390	300.7	0	15
acsz–41b	Aleutian–Alaska–Cascadia	220.0382	58.9529	300.7	0	15
acsz–42a	Aleutian–Alaska–Cascadia	221.8835	58.9310	298.9	0	15
acsz–42b	Aleutian–Alaska–Cascadia	221.4671	58.5379	298.9	0	15
acsz–43a	Aleutian–Alaska–Cascadia	222.9711	58.6934	282.3	0	15
acsz–43b	Aleutian–Alaska–Cascadia	222.7887	58.2546	282.3	0	15
acsz–44a	Aleutian–Alaska–Cascadia	224.9379	57.9054	340.9	12	11.09
acsz–44b	Aleutian–Alaska–Cascadia	224.1596	57.7617	340.9	7	5
acsz–45a	Aleutian–Alaska–Cascadia	225.4994	57.1634	334.1	12	11.09
acsz–45b	Aleutian–Alaska–Cascadia	224.7740	56.9718	334.1	7	5
acsz–46a	Aleutian–Alaska–Cascadia	226.1459	56.3552	334.1	12	11.09
acsz–46b	Aleutian–Alaska–Cascadia	225.4358	56.1636	334.1	7	5
acsz–47a	Aleutian–Alaska–Cascadia	226.7731	55.5830	332.3	12	11.09
acsz–47b	Aleutian–Alaska–Cascadia	226.0887	55.3785	332.3	7	5
acsz–48a	Aleutian–Alaska–Cascadia	227.4799	54.6763	339.4	12	11.09
acsz–48b	Aleutian–Alaska–Cascadia	226.7713	54.5217	339.4	7	5
acsz–49a	Aleutian–Alaska–Cascadia	227.9482	53.8155	341.2	12	11.09
acsz–49b	Aleutian–Alaska–Cascadia	227.2462	53.6737	341.2	7	5
acsz–50a	Aleutian–Alaska–Cascadia	228.3970	53.2509	324.5	12	11.09
acsz–50b	Aleutian–Alaska–Cascadia	227.8027	52.9958	324.5	7	5
acsz–51a	Aleutian–Alaska–Cascadia	229.1844	52.6297	318.4	12	11.09
acsz–51b	Aleutian–Alaska–Cascadia	228.6470	52.3378	318.4	7	5
acsz–52a	Aleutian–Alaska–Cascadia	230.0306	52.0768	310.9	12	11.09
acsz–52b	Aleutian–Alaska–Cascadia	229.5665	51.7445	310.9	7	5
acsz–53a	Aleutian–Alaska–Cascadia	231.1735	51.5258	310.9	12	11.09
acsz–53b	Aleutian–Alaska–Cascadia	230.7150	51.1935	310.9	7	5
acsz–54a	Aleutian–Alaska–Cascadia	232.2453	50.8809	314.1	12	11.09
acsz–54b	Aleutian–Alaska–Cascadia	231.7639	50.5655	314.1	7	5
acsz–55a	Aleutian–Alaska–Cascadia	233.3066	49.9032	333.7	12	11.09
acsz–55b	Aleutian–Alaska–Cascadia	232.6975	49.7086	333.7	7	5
acsz–56a	Aleutian–Alaska–Cascadia	234.0588	49.1702	315	11	12.82
acsz–56b	Aleutian–Alaska–Cascadia	233.5849	48.8584	315	9	5
acsz–57a	Aleutian–Alaska–Cascadia	234.9041	48.2596	341	11	12.82
acsz–57b	Aleutian–Alaska–Cascadia	234.2797	48.1161	341	9	5
acsz–58a	Aleutian–Alaska–Cascadia	235.3021	47.3812	344	11	12.82
acsz–58b	Aleutian–Alaska–Cascadia	234.6776	47.2597	344	9	5
acsz–59a	Aleutian–Alaska–Cascadia	235.6432	46.5082	345	11	12.82
acsz–59b	Aleutian–Alaska–Cascadia	235.0257	46.3941	345	9	5
acsz–60a	Aleutian–Alaska–Cascadia	235.8640	45.5429	356	11	12.82
acsz–60b	Aleutian–Alaska–Cascadia	235.2363	45.5121	356	9	5
acsz–61a	Aleutian–Alaska–Cascadia	235.9106	44.6227	359	11	12.82
acsz–61b	Aleutian–Alaska–Cascadia	235.2913	44.6150	359	9	5
acsz–62a	Aleutian–Alaska–Cascadia	235.9229	43.7245	359	11	12.82
acsz–62b	Aleutian–Alaska–Cascadia	235.3130	43.7168	359	9	5
acsz–63a	Aleutian–Alaska–Cascadia	236.0220	42.9020	350	11	12.82
acsz–63b	Aleutian–Alaska–Cascadia	235.4300	42.8254	350	9	5
acsz–64a	Aleutian–Alaska–Cascadia	235.9638	41.9818	345	11	12.82
acsz–64b	Aleutian–Alaska–Cascadia	235.3919	41.8677	345	9	5
acsz–65a	Aleutian–Alaska–Cascadia	236.2643	41.1141	345	11	12.82
acsz–65b	Aleutian–Alaska–Cascadia	235.7000	41.0000	345	9	5
acsz–238a	Aleutian–Alaska–Cascadia	213.2878	59.8406	236.8	15	17.94
acsz–238y	Aleutian–Alaska–Cascadia	212.3424	60.5664	236.8	15	43.82
acsz–238z	Aleutian–Alaska–Cascadia	212.8119	60.2035	236.8	15	30.88
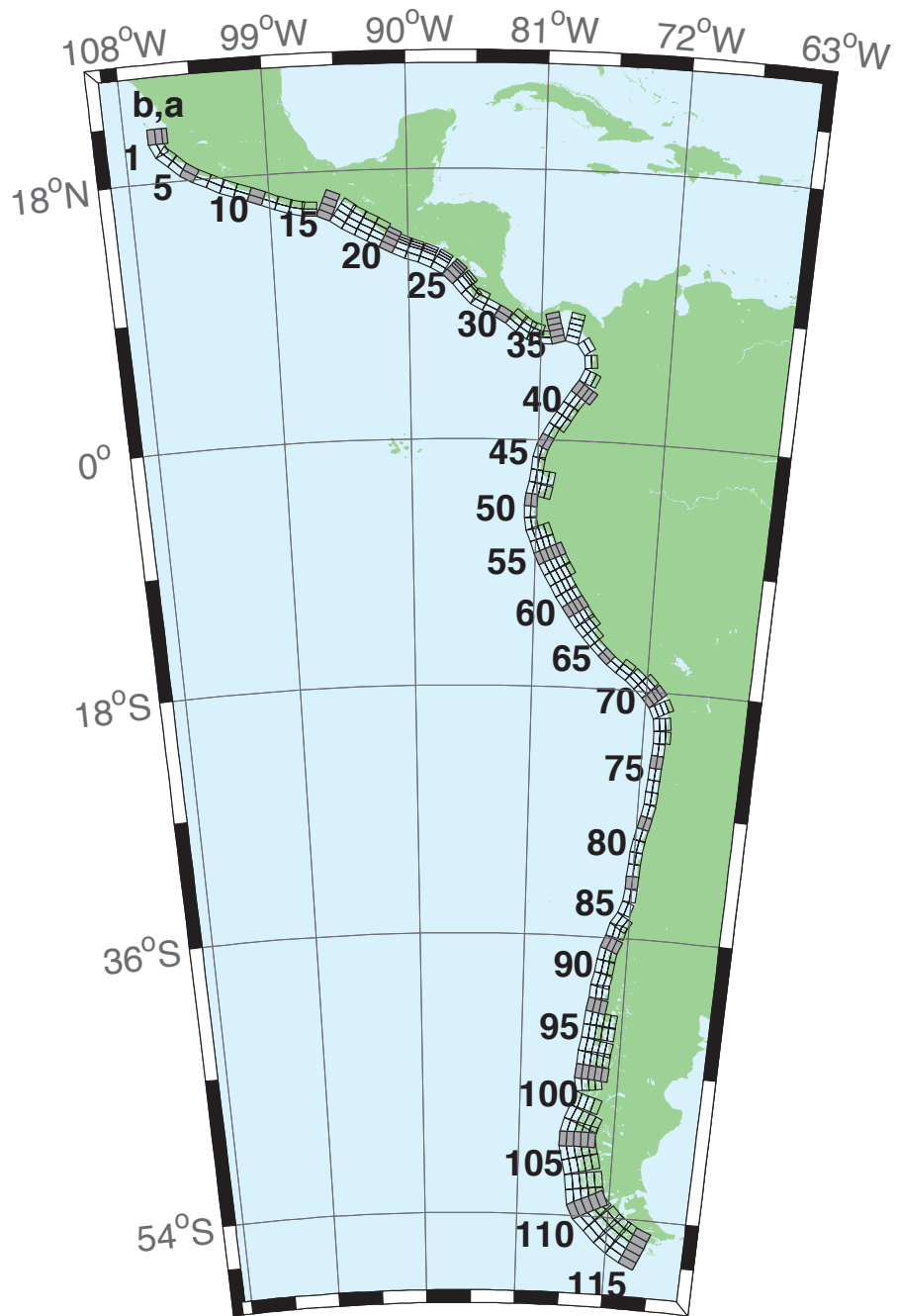
Figure B.2: Central and South America Subduction Zone unit sources.

Table B.2: Earthquake parameters for Central and South America Subduction Zone unit sources.

Segment	Description	Longitude(°E)	Latitude(°N)	Strike(°)	Dip(°)	Depth (km)
cssz–1a	Central and South America	254.4573	20.8170	359	19	15.4
cssz–1b	Central and South America	254.0035	20.8094	359	12	5
cssz–1z	Central and South America	254.7664	20.8222	359	50	31.67
cssz–2a	Central and South America	254.5765	20.2806	336.8	19	15.4
cssz–2b	Central and South America	254.1607	20.1130	336.8	12	5
cssz–3a	Central and South America	254.8789	19.8923	310.6	18.31	15.27
cssz–3b	Central and South America	254.5841	19.5685	310.6	11.85	5
cssz–4a	Central and South America	255.6167	19.2649	313.4	17.62	15.12
cssz–4b	Central and South America	255.3056	18.9537	313.4	11.68	5
cssz–5a	Central and South America	256.2240	18.8148	302.7	16.92	15
cssz–5b	Central and South America	255.9790	18.4532	302.7	11.54	5
cssz–6a	Central and South America	256.9425	18.4383	295.1	16.23	14.87
cssz–6b	Central and South America	256.7495	18.0479	295.1	11.38	5
cssz–7a	Central and South America	257.8137	18.0339	296.9	15.54	14.74
cssz–7b	Central and South America	257.6079	17.6480	296.9	11.23	5
cssz–8a	Central and South America	258.5779	17.7151	290.4	14.85	14.61
cssz–8b	Central and South America	258.4191	17.3082	290.4	11.08	5
cssz–9a	Central and South America	259.4578	17.4024	290.5	14.15	14.47
cssz–9b	Central and South America	259.2983	16.9944	290.5	10.92	5
cssz–10a	Central and South America	260.3385	17.0861	290.8	13.46	14.34
cssz–10b	Central and South America	260.1768	16.6776	290.8	10.77	5
cssz–11a	Central and South America	261.2255	16.7554	291.8	12.77	14.21
cssz–11b	Central and South America	261.0556	16.3487	291.8	10.62	5
cssz–12a	Central and South America	262.0561	16.4603	288.9	12.08	14.08
cssz–12b	Central and South America	261.9082	16.0447	288.9	10.46	5
cssz–13a	Central and South America	262.8638	16.2381	283.2	11.38	13.95
cssz–13b	Central and South America	262.7593	15.8094	283.2	10.31	5
cssz–14a	Central and South America	263.6066	16.1435	272.1	10.69	13.81
cssz–14b	Central and South America	263.5901	15.7024	272.1	10.15	5
cssz–15a	Central and South America	264.8259	15.8829	293	10	13.68
cssz–15b	Central and South America	264.6462	15.4758	293	10	5
cssz–15y	Central and South America	265.1865	16.6971	293	10	31.05
cssz–15z	Central and South America	265.0060	16.2900	293	10	22.36
cssz–16a	Central and South America	265.7928	15.3507	304.9	15	15.82
cssz–16b	Central and South America	265.5353	14.9951	304.9	12.5	5
cssz–16y	Central and South America	266.3092	16.0619	304.9	15	41.7
cssz–16z	Central and South America	266.0508	15.7063	304.9	15	28.76
cssz–17a	Central and South America	266.4947	14.9019	299.5	20	17.94
cssz–17b	Central and South America	266.2797	14.5346	299.5	15	5
cssz–17y	Central and South America	266.9259	15.6365	299.5	20	52.14
cssz–17z	Central and South America	266.7101	15.2692	299.5	20	35.04
cssz–18a	Central and South America	267.2827	14.4768	298	21.5	17.94
cssz–18b	Central and South America	267.0802	14.1078	298	15	5
cssz–18y	Central and South America	267.6888	15.2148	298	21.5	54.59
cssz–18z	Central and South America	267.4856	14.8458	298	21.5	36.27
cssz–19a	Central and South America	268.0919	14.0560	297.6	23	17.94
cssz–19b	Central and South America	267.8943	13.6897	297.6	15	5
cssz–19y	Central and South America	268.4880	14.7886	297.6	23	57.01
cssz–19z	Central and South America	268.2898	14.4223	297.6	23	37.48
cssz–20a	Central and South America	268.8929	13.6558	296.2	24	17.94
cssz–20b	Central and South America	268.7064	13.2877	296.2	15	5
cssz–20y	Central and South America	269.1796	14.2206	296.2	45.5	73.94
cssz–20z	Central and South America	269.0362	13.9382	296.2	45.5	38.28
cssz–21a	Central and South America	269.6797	13.3031	292.6	25	17.94
cssz–21b	Central and South America	269.5187	12.9274	292.6	15	5
cssz–21x	Central and South America	269.8797	13.7690	292.6	68	131.8
cssz–21y	Central and South America	269.8130	13.6137	292.6	68	85.43
cssz–21z	Central and South America	269.7463	13.4584	292.6	68	39.07
cssz–22a	Central and South America	270.4823	13.0079	288.6	25	17.94
cssz–22b	Central and South America	270.3492	12.6221	288.6	15	5

Segment	Description	Longitude(°E)	Latitude(°N)	Strike(°)	Dip(°)	Depth (km)
cssz–22x	Central and South America	270.6476	13.4864	288.6	68	131.8
cssz–22y	Central and South America	270.5925	13.3269	288.6	68	85.43
cssz–22z	Central and South America	270.5374	13.1674	288.6	68	39.07
cssz–23a	Central and South America	271.3961	12.6734	292.4	25	17.94
cssz–23b	Central and South America	271.2369	12.2972	292.4	15	5
cssz–23x	Central and South America	271.5938	13.1399	292.4	68	131.8
cssz–23y	Central and South America	271.5279	12.9844	292.4	68	85.43
cssz–23z	Central and South America	271.4620	12.8289	292.4	68	39.07
cssz–24a	Central and South America	272.3203	12.2251	300.2	25	17.94
cssz–24b	Central and South America	272.1107	11.8734	300.2	15	5
cssz–24x	Central and South America	272.5917	12.6799	300.2	67	131.1
cssz–24y	Central and South America	272.5012	12.5283	300.2	67	85.1
cssz–24z	Central and South America	272.4107	12.3767	300.2	67	39.07
cssz–25a	Central and South America	273.2075	11.5684	313.8	25	17.94
cssz–25b	Central and South America	272.9200	11.2746	313.8	15	5
cssz–25x	Central and South America	273.5950	11.9641	313.8	66	130.4
cssz–25y	Central and South America	273.4658	11.8322	313.8	66	84.75
cssz–25z	Central and South America	273.3366	11.7003	313.8	66	39.07
cssz–26a	Central and South America	273.8943	10.8402	320.4	25	17.94
cssz–26b	Central and South America	273.5750	10.5808	320.4	15	5
cssz–26x	Central and South America	274.3246	11.1894	320.4	66	130.4
cssz–26y	Central and South America	274.1811	11.0730	320.4	66	84.75
cssz–26z	Central and South America	274.0377	10.9566	320.4	66	39.07
cssz–27a	Central and South America	274.4569	10.2177	316.1	25	17.94
cssz–27b	Central and South America	274.1590	9.9354	316.1	15	5
cssz–27z	Central and South America	274.5907	10.3444	316.1	66	39.07
cssz–28a	Central and South America	274.9586	9.8695	297.1	22	14.54
cssz–28b	Central and South America	274.7661	9.4988	297.1	11	5
cssz–28z	Central and South America	275.1118	10.1643	297.1	42.5	33.27
cssz–29a	Central and South America	275.7686	9.4789	296.6	19	11.09
cssz–29b	Central and South America	275.5759	9.0992	296.6	7	5
cssz–30a	Central and South America	276.6346	8.9973	302.2	19	9.36
cssz–30b	Central and South America	276.4053	8.6381	302.2	5	5
cssz–31a	Central and South America	277.4554	8.4152	309.1	19	7.62
cssz–31b	Central and South America	277.1851	8.0854	309.1	3	5
cssz–31z	Central and South America	277.7260	8.7450	309.1	19	23.9
cssz–32a	Central and South America	278.1112	7.9425	303	18.67	8.49
cssz–32b	Central and South America	277.8775	7.5855	303	4	5
cssz–32z	Central and South America	278.3407	8.2927	303	21.67	24.49
cssz–33a	Central and South America	278.7082	7.6620	287.6	18.33	10.23
cssz–33b	Central and South America	278.5785	7.2555	287.6	6	5
cssz–33z	Central and South America	278.8328	8.0522	287.6	24.33	25.95
cssz–34a	Central and South America	279.3184	7.5592	269.5	18	17.94
cssz–34b	Central and South America	279.3223	7.1320	269.5	15	5
cssz–35a	Central and South America	280.0039	7.6543	255.9	17.67	14.54
cssz–35b	Central and South America	280.1090	7.2392	255.9	11	5
cssz–35x	Central and South America	279.7156	8.7898	255.9	29.67	79.22
cssz–35y	Central and South America	279.8118	8.4113	255.9	29.67	54.47
cssz–35z	Central and South America	279.9079	8.0328	255.9	29.67	29.72
cssz–36a	Central and South America	281.2882	7.6778	282.5	17.33	11.09
cssz–36b	Central and South America	281.1948	7.2592	282.5	7	5
cssz–36x	Central and South America	281.5368	8.7896	282.5	32.33	79.47
cssz–36y	Central and South America	281.4539	8.4190	282.5	32.33	52.73
cssz–36z	Central and South America	281.3710	8.0484	282.5	32.33	25.99
cssz–37a	Central and South America	282.5252	6.8289	326.9	17	10.23
cssz–37b	Central and South America	282.1629	6.5944	326.9	6	5
cssz–38a	Central and South America	282.9469	5.5973	355.4	17	10.23
cssz–38b	Central and South America	282.5167	5.5626	355.4	6	5
cssz–39a	Central and South America	282.7236	4.3108	24.13	17	10.23
cssz–39b	Central and South America	282.3305	4.4864	24.13	6	5
cssz–39z	Central and South America	283.0603	4.1604	24.13	35	24.85
cssz–40a	Central and South America	282.1940	3.3863	35.28	17	10.23

94

Segment	Description	Longitude(^{o}E)	Latitude(^{o}N)	Strike(^{o})	Dip(^{o})	Depth (km)
cssz–40b	Central and South America	281.8427	3.6344	35.28	6	5
cssz–40y	Central and South America	282.7956	2.9613	35.28	35	53.52
cssz–40z	Central and South America	282.4948	3.1738	35.28	35	24.85
cssz–41a	Central and South America	281.6890	2.6611	34.27	17	10.23
cssz–41b	Central and South America	281.3336	2.9030	34.27	6	5
cssz–41z	Central and South America	281.9933	2.4539	34.27	35	24.85
cssz–42a	Central and South America	281.2266	1.9444	31.29	17	10.23
cssz–42b	Central and South America	280.8593	2.1675	31.29	6	5
cssz–42z	Central and South America	281.5411	1.7533	31.29	35	24.85
cssz–43a	Central and South America	280.7297	1.1593	33.3	17	10.23
cssz–43b	Central and South America	280.3706	1.3951	33.3	6	5
cssz–43z	Central and South America	281.0373	0.9573	33.3	35	24.85
cssz–44a	Central and South America	280.3018	0.4491	28.8	17	10.23
cssz–44b	Central and South America	279.9254	0.6560	28.8	6	5
cssz–45a	Central and South America	279.9083	-0.3259	26.91	10	8.49
cssz–45b	Central and South America	279.5139	-0.1257	26.91	4	5
cssz–46a	Central and South America	279.6461	-0.9975	15.76	10	8.49
cssz–46b	Central and South America	279.2203	-0.8774	15.76	4	5
cssz–47a	Central and South America	279.4972	-1.7407	6.9	10	8.49
cssz–47b	Central and South America	279.0579	-1.6876	6.9	4	5
cssz–48a	Central and South America	279.3695	-2.6622	8.96	10	8.49
cssz–48b	Central and South America	278.9321	-2.5933	8.96	4	5
cssz–48y	Central and South America	280.2444	-2.8000	8.96	10	25.85
cssz–48z	Central and South America	279.8070	-2.7311	8.96	10	17.17
cssz–49a	Central and South America	279.1852	-3.6070	13.15	10	8.49
cssz–49b	Central and South America	278.7536	-3.5064	13.15	4	5
cssz–49y	Central and South America	280.0486	-3.8082	13.15	10	25.85
cssz–49z	Central and South America	279.6169	-3.7076	13.15	10	17.17
cssz–50a	Central and South America	279.0652	-4.3635	4.78	10.33	9.64
cssz–50b	Central and South America	278.6235	-4.3267	4.78	5.33	5
cssz–51a	Central and South America	279.0349	-5.1773	359.4	10.67	10.81
cssz–51b	Central and South America	278.5915	-5.1817	359.4	6.67	5
cssz–52a	Central and South America	279.1047	-5.9196	349.8	11	11.96
cssz–52b	Central and South America	278.6685	-5.9981	349.8	8	5
cssz–53a	Central and South America	279.3044	-6.6242	339.2	10.25	11.74
cssz–53b	Central and South America	278.8884	-6.7811	339.2	7.75	5
cssz–53y	Central and South America	280.1024	-6.3232	339.2	19.25	37.12
cssz–53z	Central and South America	279.7035	-6.4737	339.2	19.25	20.64
cssz–54a	Central and South America	279.6256	-7.4907	340.8	9.5	11.53
cssz–54b	Central and South America	279.2036	-7.6365	340.8	7.5	5
cssz–54y	Central and South America	280.4267	-7.2137	340.8	20.5	37.29
cssz–54z	Central and South America	280.0262	-7.3522	340.8	20.5	19.78
cssz–55a	Central and South America	279.9348	-8.2452	335.4	8.75	11.74
cssz–55b	Central and South America	279.5269	-8.4301	335.4	7.75	5
cssz–55x	Central and South America	281.0837	-7.7238	335.4	21.75	56.4
cssz–55y	Central and South America	280.7009	-7.8976	335.4	21.75	37.88
cssz–55z	Central and South America	280.3180	-8.0714	335.4	21.75	19.35
cssz–56a	Central and South America	280.3172	-8.9958	331.6	8	11.09
cssz–56b	Central and South America	279.9209	-9.2072	331.6	7	5
cssz–56x	Central and South America	281.4212	-8.4063	331.6	23	57.13
cssz–56y	Central and South America	281.0534	-8.6028	331.6	23	37.59
cssz–56z	Central and South America	280.6854	-8.7993	331.6	23	18.05
cssz–57a	Central and South America	280.7492	-9.7356	328.7	8.6	10.75
cssz–57b	Central and South America	280.3640	-9.9663	328.7	6.6	5
cssz–57x	Central and South America	281.8205	-9.0933	328.7	23.4	57.94
cssz–57y	Central and South America	281.4636	-9.3074	328.7	23.4	38.08
cssz–57z	Central and South America	281.1065	-9.5215	328.7	23.4	18.22
cssz–58a	Central and South America	281.2275	-10.5350	330.5	9.2	10.4
cssz–58b	Central and South America	280.8458	-10.7532	330.5	6.2	5
cssz–58y	Central and South America	281.9548	-10.1306	330.5	23.8	38.57
cssz–58z	Central and South America	281.5913	-10.3328	330.5	23.8	18.39
cssz–59a	Central and South America	281.6735	-11.2430	326.2	9.8	10.05

Table B.2 – continued

Segment	Description	Longitude(^{o}E)	Latitude(^{o}N)	Strike(^{o})	Dip(^{o})	Depth (km)
cssz–59b	Central and South America	281.2982	-11.4890	326.2	5.8	5
cssz–59y	Central and South America	282.3675	-10.7876	326.2	24.2	39.06
cssz–59z	Central and South America	282.0206	-11.0153	326.2	24.2	18.56
cssz–60a	Central and South America	282.1864	-11.9946	326.5	10.4	9.71
cssz–60b	Central and South America	281.8096	-12.2384	326.5	5.4	5
cssz–60y	Central and South America	282.8821	-11.5438	326.5	24.6	39.55
cssz–60z	Central and South America	282.5344	-11.7692	326.5	24.6	18.73
cssz–61a	Central and South America	282.6944	-12.7263	325.5	11	9.36
cssz–61b	Central and South America	282.3218	-12.9762	325.5	5	5
cssz–61y	Central and South America	283.3814	-12.2649	325.5	25	40.03
cssz–61z	Central and South America	283.0381	-12.4956	325.5	25	18.9
cssz–62a	Central and South America	283.1980	-13.3556	319	11	9.79
cssz–62b	Central and South America	282.8560	-13.6451	319	5.5	5
cssz–62y	Central and South America	283.8178	-12.8300	319	27	42.03
cssz–62z	Central and South America	283.5081	-13.0928	319	27	19.33
cssz–63a	Central and South America	283.8032	-14.0147	317.9	11	10.23
cssz–63b	Central and South America	283.4661	-14.3106	317.9	6	5
cssz–63z	Central and South America	284.1032	-13.7511	317.9	29	19.77
cssz–64a	Central and South America	284.4144	-14.6482	315.7	13	11.96
cssz–64b	Central and South America	284.0905	-14.9540	315.7	8	5
cssz–65a	Central and South America	285.0493	-15.2554	313.2	15	13.68
cssz–65b	Central and South America	284.7411	-15.5715	313.2	10	5
cssz–66a	Central and South America	285.6954	-15.7816	307.7	14.5	13.68
cssz–66b	Central and South America	285.4190	-16.1258	307.7	10	5
cssz–67a	Central and South America	286.4127	-16.2781	304.3	14	13.68
cssz–67b	Central and South America	286.1566	-16.6381	304.3	10	5
cssz–67z	Central and South America	286.6552	-15.9365	304.3	23	25.78
cssz–68a	Central and South America	287.2481	-16.9016	311.8	14	13.68
cssz–68b	Central and South America	286.9442	-17.2264	311.8	10	5
cssz–68z	Central and South America	287.5291	-16.6007	311.8	26	25.78
cssz–69a	Central and South America	287.9724	-17.5502	314.9	14	13.68
cssz–69b	Central and South America	287.6496	-17.8590	314.9	10	5
cssz–69y	Central and South America	288.5530	-16.9934	314.9	29	50.02
cssz–69z	Central and South America	288.2629	-17.2718	314.9	29	25.78
cssz–70a	Central and South America	288.6731	-18.2747	320.4	14	13.25
cssz–70b	Central and South America	288.3193	-18.5527	320.4	9.5	5
cssz–70y	Central and South America	289.3032	-17.7785	320.4	30	50.35
cssz–70z	Central and South America	288.9884	-18.0266	320.4	30	25.35
cssz–71a	Central and South America	289.3089	-19.1854	333.2	14	12.82
cssz–71b	Central and South America	288.8968	-19.3820	333.2	9	5
cssz–71y	Central and South America	290.0357	-18.8382	333.2	31	50.67
cssz–71z	Central and South America	289.6725	-19.0118	333.2	31	24.92
cssz–72a	Central and South America	289.6857	-20.3117	352.4	14	12.54
cssz–72b	Central and South America	289.2250	-20.3694	352.4	8.67	5
cssz–72z	Central and South America	290.0882	-20.2613	352.4	32	24.63
cssz–73a	Central and South America	289.7731	-21.3061	358.9	14	12.24
cssz–73b	Central and South America	289.3053	-21.3142	358.9	8.33	5
cssz–73z	Central and South America	290.1768	-21.2991	358.9	33	24.34
cssz–74a	Central and South America	289.7610	-22.2671	3.06	14	11.96
cssz–74b	Central and South America	289.2909	-22.2438	3.06	8	5
cssz–75a	Central and South America	289.6982	-23.1903	4.83	14.09	11.96
cssz–75b	Central and South America	289.2261	-23.1536	4.83	8	5
cssz–76a	Central and South America	289.6237	-24.0831	4.67	14.18	11.96
cssz–76b	Central and South America	289.1484	-24.0476	4.67	8	5
cssz–77a	Central and South America	289.5538	-24.9729	4.3	14.27	11.96
cssz–77b	Central and South America	289.0750	-24.9403	4.3	8	5
cssz–78a	Central and South America	289.4904	-25.8621	3.86	14.36	11.96
cssz–78b	Central and South America	289.0081	-25.8328	3.86	8	5
cssz–79a	Central and South America	289.3491	-26.8644	11.34	14.45	11.96
cssz–79b	Central and South America	288.8712	-26.7789	11.34	8	5
cssz–80a	Central and South America	289.1231	-27.7826	14.16	14.54	11.96
cssz–80b	Central and South America	288.6469	-27.6762	14.16	8	5

Segment	Description	Longitude(^{o}E)	Latitude(^{o}N)	Strike(^{o})	Dip(^{o})	Depth (km)
cssz–81a	Central and South America	288.8943	-28.6409	13.19	14.63	11.96
cssz–81b	Central and South America	288.4124	-28.5417	13.19	8	5
cssz–82a	Central and South America	288.7113	-29.4680	9.68	14.72	11.96
cssz–82b	Central and South America	288.2196	-29.3950	9.68	8	5
cssz–83a	Central and South America	288.5944	-30.2923	5.36	14.81	11.96
cssz–83b	Central and South America	288.0938	-30.2517	5.36	8	5
cssz–84a	Central and South America	288.5223	-31.1639	3.8	14.9	11.96
cssz–84b	Central and South America	288.0163	-31.1351	3.8	8	5
cssz–85a	Central and South America	288.4748	-32.0416	2.55	15	11.96
cssz–85b	Central and South America	287.9635	-32.0223	2.55	8	5
cssz–86a	Central and South America	288.3901	-33.0041	7.01	15	11.96
cssz–86b	Central and South America	287.8768	-32.9512	7.01	8	5
cssz–87a	Central and South America	288.1050	-34.0583	19.4	15	11.96
cssz–87b	Central and South America	287.6115	-33.9142	19.4	8	5
cssz–88a	Central and South America	287.5309	-35.0437	32.81	15	11.96
cssz–88b	Central and South America	287.0862	-34.8086	32.81	8	5
cssz–88z	Central and South America	287.9308	-35.2545	32.81	30	24.9
cssz–89a	Central and South America	287.2380	-35.5993	14.52	16.67	11.96
cssz–89b	Central and South America	286.7261	-35.4914	14.52	8	5
cssz–89z	Central and South America	287.7014	-35.6968	14.52	30	26.3
cssz–90a	Central and South America	286.8442	-36.5645	22.64	18.33	11.96
cssz–90b	Central and South America	286.3548	-36.4004	22.64	8	5
cssz–90z	Central and South America	287.2916	-36.7142	22.64	30	27.68
cssz–91a	Central and South America	286.5925	-37.2488	10.9	20	11.96
cssz–91b	Central and South America	286.0721	-37.1690	10.9	8	5
cssz–91z	Central and South America	287.0726	-37.3224	10.9	30	29.06
cssz–92a	Central and South America	286.4254	-38.0945	8.23	20	11.96
cssz–92b	Central and South America	285.8948	-38.0341	8.23	8	5
cssz–92z	Central and South America	286.9303	-38.1520	8.23	26.67	29.06
cssz–93a	Central and South America	286.2047	-39.0535	13.46	20	11.96
cssz–93b	Central and South America	285.6765	-38.9553	13.46	8	5
cssz–93z	Central and South America	286.7216	-39.1495	13.46	23.33	29.06
cssz–94a	Central and South America	286.0772	-39.7883	3.4	20	11.96
cssz–94b	Central and South America	285.5290	-39.7633	3.4	8	5
cssz–94z	Central and South America	286.6255	-39.8133	3.4	20	29.06
cssz–95a	Central and South America	285.9426	-40.7760	9.84	20	11.96
cssz–95b	Central and South America	285.3937	-40.7039	9.84	8	5
cssz–95z	Central and South America	286.4921	-40.8481	9.84	20	29.06
cssz–96a	Central and South America	285.7839	-41.6303	7.6	20	11.96
cssz–96b	Central and South America	285.2245	-41.5745	7.6	8	5
cssz–96x	Central and South America	287.4652	-41.7977	7.6	20	63.26
cssz–96y	Central and South America	286.9043	-41.7419	7.6	20	46.16
cssz–96z	Central and South America	286.3439	-41.6861	7.6	20	29.06
cssz–97a	Central and South America	285.6695	-42.4882	5.3	20	11.96
cssz–97b	Central and South America	285.0998	-42.4492	5.3	8	5
cssz–97x	Central and South America	287.3809	-42.6052	5.3	20	63.26
cssz–97y	Central and South America	286.8101	-42.5662	5.3	20	46.16
cssz–97z	Central and South America	286.2396	-42.5272	5.3	20	29.06
cssz–98a	Central and South America	285.5035	-43.4553	10.53	20	11.96
cssz–98b	Central and South America	284.9322	-43.3782	10.53	8	5
cssz–98x	Central and South America	287.2218	-43.6866	10.53	20	63.26
cssz–98y	Central and South America	286.6483	-43.6095	10.53	20	46.16
cssz–98z	Central and South America	286.0755	-43.5324	10.53	20	29.06
cssz–99a	Central and South America	285.3700	-44.2595	4.86	20	11.96
cssz–99b	Central and South America	284.7830	-44.2237	4.86	8	5
cssz–99x	Central and South America	287.1332	-44.3669	4.86	20	63.26
cssz–99y	Central and South America	286.5451	-44.3311	4.86	20	46.16
cssz–99z	Central and South America	285.9574	-44.2953	4.86	20	29.06
cssz–100a	Central and South America	285.2713	-45.1664	5.68	20	11.96
cssz–100b	Central and South America	284.6758	-45.1246	5.68	8	5
cssz–100x	Central and South America	287.0603	-45.2918	5.68	20	63.26
cssz–100y	Central and South America	286.4635	-45.2500	5.68	20	46.16

Segment	Description	Longitude(°E)	Latitude(°N)	Strike(°)	Dip(°)	Depth (km)
cssz–100z	Central and South America	285.8672	-45.2082	5.68	20	29.06
cssz–101a	Central and South America	285.3080	-45.8607	352.6	20	9.36
cssz–101b	Central and South America	284.7067	-45.9152	352.6	5	5
cssz–101y	Central and South America	286.5089	-45.7517	352.6	20	43.56
cssz–101z	Central and South America	285.9088	-45.8062	352.6	20	26.46
cssz–102a	Central and South America	285.2028	-47.1185	17.72	5	9.36
cssz–102b	Central and South America	284.5772	-46.9823	17.72	5	5
cssz–102y	Central and South America	286.4588	-47.3909	17.72	5	18.07
cssz–102z	Central and South America	285.8300	-47.2547	17.72	5	13.72
cssz–103a	Central and South America	284.7075	-48.0396	23.37	7.5	11.53
cssz–103b	Central and South America	284.0972	-47.8630	23.37	7.5	5
cssz–103x	Central and South America	286.5511	-48.5694	23.37	7.5	31.11
cssz–103y	Central and South America	285.9344	-48.3928	23.37	7.5	24.58
cssz–103z	Central and South America	285.3199	-48.2162	23.37	7.5	18.05
cssz–104a	Central and South America	284.3440	-48.7597	14.87	10	13.68
cssz–104b	Central and South America	283.6962	-48.6462	14.87	10	5
cssz–104x	Central and South America	286.2962	-49.1002	14.87	10	39.73
cssz–104y	Central and South America	285.6440	-48.9867	14.87	10	31.05
cssz–104z	Central and South America	284.9933	-48.8732	14.87	10	22.36
cssz–105a	Central and South America	284.2312	-49.4198	0.25	9.67	13.4
cssz–105b	Central and South America	283.5518	-49.4179	0.25	9.67	5
cssz–105x	Central and South America	286.2718	-49.4255	0.25	9.67	38.59
cssz–105y	Central and South America	285.5908	-49.4236	0.25	9.67	30.2
cssz–105z	Central and South America	284.9114	-49.4217	0.25	9.67	21.8
cssz–106a	Central and South America	284.3730	-50.1117	347.5	9.25	13.04
cssz–106b	Central and South America	283.6974	-50.2077	347.5	9.25	5
cssz–106x	Central and South America	286.3916	-49.8238	347.5	9.25	37.15
cssz–106y	Central and South America	285.7201	-49.9198	347.5	9.25	29.11
cssz–106z	Central and South America	285.0472	-50.0157	347.5	9.25	21.07
cssz–107a	Central and South America	284.7130	-50.9714	346.5	9	12.82
cssz–107b	Central and South America	284.0273	-51.0751	346.5	9	5
cssz–107x	Central and South America	286.7611	-50.6603	346.5	9	36.29
cssz–107y	Central and South America	286.0799	-50.7640	346.5	9	28.47
cssz–107z	Central and South America	285.3972	-50.8677	346.5	9	20.64
cssz–108a	Central and South America	285.0378	-51.9370	352	8.67	12.54
cssz–108b	Central and South America	284.3241	-51.9987	352	8.67	5
cssz–108x	Central and South America	287.1729	-51.7519	352	8.67	35.15
cssz–108y	Central and South America	286.4622	-51.8136	352	8.67	27.61
cssz–108z	Central and South America	285.7505	-51.8753	352	8.67	20.07
cssz–109a	Central and South America	285.2635	-52.8439	353.1	8.33	12.24
cssz–109b	Central and South America	284.5326	-52.8974	353.1	8.33	5
cssz–109x	Central and South America	287.4508	-52.6834	353.1	8.33	33.97
cssz–109y	Central and South America	286.7226	-52.7369	353.1	8.33	26.73
cssz–109z	Central and South America	285.9935	-52.7904	353.1	8.33	19.49
cssz–110a	Central and South America	285.5705	-53.4139	334.2	8	11.96
cssz–110b	Central and South America	284.8972	-53.6076	334.2	8	5
cssz–110x	Central and South America	287.5724	-52.8328	334.2	8	32.83
cssz–110y	Central and South America	286.9081	-53.0265	334.2	8	25.88
cssz–110z	Central and South America	286.2408	-53.2202	334.2	8	18.92
cssz–111a	Central and South America	286.1627	-53.8749	313.8	8	11.96
cssz–111b	Central and South America	285.6382	-54.1958	313.8	8	5
cssz–111x	Central and South America	287.7124	-52.9122	313.8	8	32.83
cssz–111y	Central and South America	287.1997	-53.2331	313.8	8	25.88
cssz–111z	Central and South America	286.6832	-53.5540	313.8	8	18.92
cssz–112a	Central and South America	287.3287	-54.5394	316.4	8	11.96
cssz–112b	Central and South America	286.7715	-54.8462	316.4	8	5
cssz–112x	Central and South America	288.9756	-53.6190	316.4	8	32.83
cssz–112y	Central and South America	288.4307	-53.9258	316.4	8	25.88
cssz–112z	Central and South America	287.8817	-54.2326	316.4	8	18.92
cssz–113a	Central and South America	288.3409	-55.0480	307.6	8	11.96
cssz–113b	Central and South America	287.8647	-55.4002	307.6	8	5
cssz–113x	Central and South America	289.7450	-53.9914	307.6	8	32.83
cssz–113y	Central and South America	289.2810	-54.3436	307.6	8	25.88
cssz–113z	Central and South America	288.8130	-54.6958	307.6	8	18.92
cssz–114a	Central and South America	289.5342	-55.5026	301.5	8	11.96

Table B.2 – continued

Segment	Description	Longitude(^{o}E)	Latitude(^{o}N)	Strike(^{o})	Dip(^{o})	Depth (km)
cssz–114b	Central and South America	289.1221	-55.8819	301.5	8	5
cssz–114x	Central and South America	290.7472	-54.3647	301.5	8	32.83
cssz–114y	Central and South America	290.3467	-54.7440	301.5	8	25.88
cssz–114z	Central and South America	289.9424	-55.1233	301.5	8	18.92
cssz–115a	Central and South America	290.7682	-55.8485	292.7	8	11.96
cssz–115b	Central and South America	290.4608	-56.2588	292.7	8	5
cssz–115x	Central and South America	291.6714	-54.6176	292.7	8	32.83
cssz–115y	Central and South America	291.3734	-55.0279	292.7	8	25.88
cssz–115z	Central and South America	291.0724	-55.4382	292.7	8	18.92
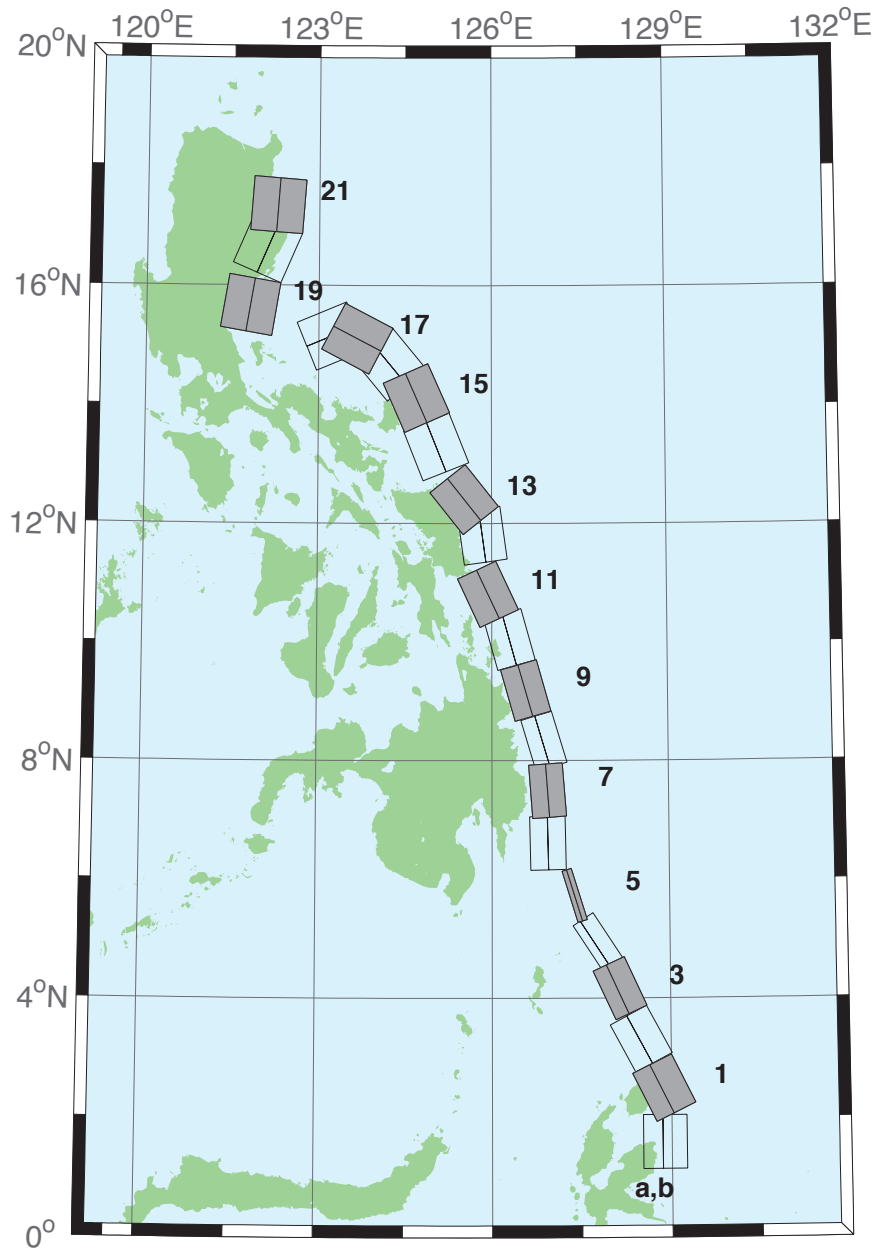
Figure B.3: Eastern Philippines Subduction Zone unit sources.

Table B.3: Earthquake parameters for Eastern Philippines Subduction Zone unit sources.

Segment	Description	Longitude(^{o}E)	Latitude(^{o}N)	Strike(^{o})	Dip(^{o})	Depth (km)
epsz–0a	Eastern Philippines	128.5264	1.5930	180	44	26.92
epsz–0b	Eastern Philippines	128.8496	1.5930	180	26	5
epsz–1a	Eastern Philippines	128.5521	2.3289	153.6	44.2	27.62
epsz–1b	Eastern Philippines	128.8408	2.4720	153.6	26.9	5
epsz–2a	Eastern Philippines	128.1943	3.1508	151.9	45.9	32.44
epsz–2b	Eastern Philippines	128.4706	3.2979	151.9	32.8	5.35
epsz–3a	Eastern Philippines	127.8899	4.0428	155.2	57.3	40.22
epsz–3b	Eastern Philippines	128.1108	4.1445	155.2	42.7	6.31
epsz–4a	Eastern Philippines	127.6120	4.8371	146.8	71.4	48.25
epsz–4b	Eastern Philippines	127.7324	4.9155	146.8	54.8	7.39
epsz–5a	Eastern Philippines	127.3173	5.7040	162.9	79.9	57.4
epsz–5b	Eastern Philippines	127.3930	5.7272	162.9	79.4	8.25
epsz–6a	Eastern Philippines	126.6488	6.6027	178.9	48.6	45.09
epsz–6b	Eastern Philippines	126.9478	6.6085	178.9	48.6	7.58
epsz–7a	Eastern Philippines	126.6578	7.4711	175.8	50.7	45.52
epsz–7b	Eastern Philippines	126.9439	7.4921	175.8	50.7	6.83
epsz–8a	Eastern Philippines	126.6227	8.2456	163.3	56.7	45.6
epsz–8b	Eastern Philippines	126.8614	8.3164	163.3	48.9	7.92
epsz–9a	Eastern Philippines	126.2751	9.0961	164.1	47	43.59
epsz–9b	Eastern Philippines	126.5735	9.1801	164.1	44.9	8.3
epsz–10a	Eastern Philippines	125.9798	9.9559	164.5	43.1	42.25
epsz–10b	Eastern Philippines	126.3007	10.0438	164.5	43.1	8.09
epsz–11a	Eastern Philippines	125.6079	10.6557	155	37.8	38.29
epsz–11b	Eastern Philippines	125.9353	10.8059	155	37.8	7.64
epsz–12a	Eastern Philippines	125.4697	11.7452	172.1	36	37.01
epsz–12b	Eastern Philippines	125.8374	11.7949	172.1	36	7.62
epsz–13a	Eastern Philippines	125.2238	12.1670	141.5	32.4	33.87
epsz–13b	Eastern Philippines	125.5278	12.4029	141.5	32.4	7.08
epsz–14a	Eastern Philippines	124.6476	13.1365	158.2	23	25.92
epsz–14b	Eastern Philippines	125.0421	13.2898	158.2	23	6.38
epsz–15a	Eastern Philippines	124.3107	13.9453	156.1	24.1	26.51
epsz–15b	Eastern Philippines	124.6973	14.1113	156.1	24.1	6.09
epsz–16a	Eastern Philippines	123.8998	14.4025	140.3	19.5	21.69
epsz–16b	Eastern Philippines	124.2366	14.6728	140.3	19.5	5
epsz–17a	Eastern Philippines	123.4604	14.7222	117.6	15.3	18.19
epsz–17b	Eastern Philippines	123.6682	15.1062	117.6	15.3	5
epsz–18a	Eastern Philippines	123.3946	14.7462	67.4	15	17.94
epsz–18b	Eastern Philippines	123.2219	15.1467	67.4	15	5
epsz–19a	Eastern Philippines	121.3638	15.7400	189.6	15	17.94
epsz–19b	Eastern Philippines	121.8082	15.6674	189.6	15	5
epsz–20a	Eastern Philippines	121.6833	16.7930	203.3	15	17.94
epsz–20b	Eastern Philippines	122.0994	16.6216	203.3	15	5
epsz–21a	Eastern Philippines	121.8279	17.3742	184.2	15	17.94
epsz–21b	Eastern Philippines	122.2814	17.3425	184.2	15	5
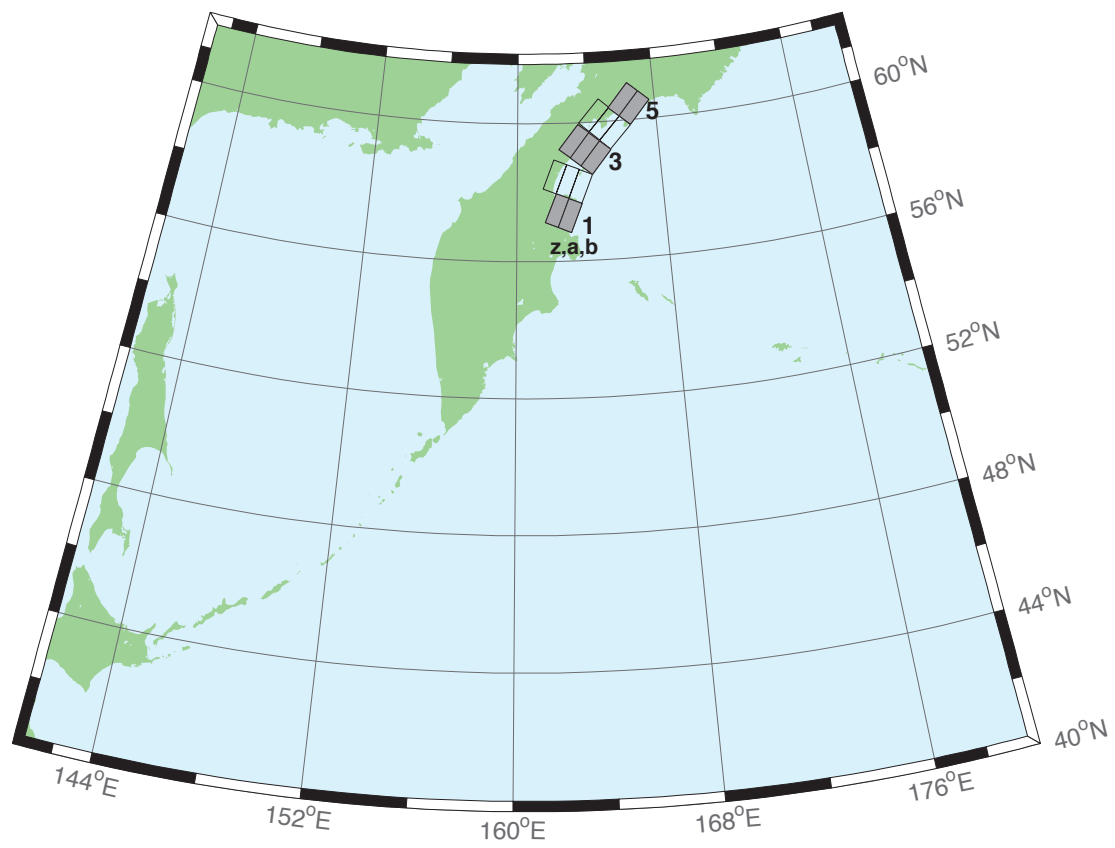
Figure B.4: Kamchatka-Bering Subduction Zone unit sources.

Table B.4: Earthquake parameters for Kamchatka-Bering Subduction Zone unit sources.

Segment	Description	Longitude(^{o}E)	Latitude(^{o}N)	Strike(^{o})	Dip(^{o})	Depth (km)
kbsz–1a	Kamchatka-Bering	161.8374	57.5485	201.5	29	26.13
kbsz–1b	Kamchatka-Bering	162.5162	57.4030	202.1	25	5
kbsz–2a	Kamchatka-Bering	162.4410	58.3816	201.7	29	26.13
kbsz–2b	Kamchatka-Bering	163.1344	58.2343	202.3	25	5
kbsz–2z	Kamchatka-Bering	161.7418	58.5249	201.1	29	50.37
kbsz–3a	Kamchatka-Bering	163.5174	59.3493	218.9	29	26.13
kbsz–3b	Kamchatka-Bering	164.1109	59.1001	219.4	25	5
kbsz–3z	Kamchatka-Bering	162.9150	59.5958	218.4	29	50.37
kbsz–4a	Kamchatka-Bering	164.7070	60.0632	222.2	29	26.13
kbsz–4b	Kamchatka-Bering	165.2833	59.7968	222.7	25	5
kbsz–4z	Kamchatka-Bering	164.1212	60.3270	221.7	29	50.37
kbsz–5a	Kamchatka-Bering	165.8652	60.7261	220.5	29	26.13
kbsz–5b	Kamchatka-Bering	166.4692	60.4683	221	25	5
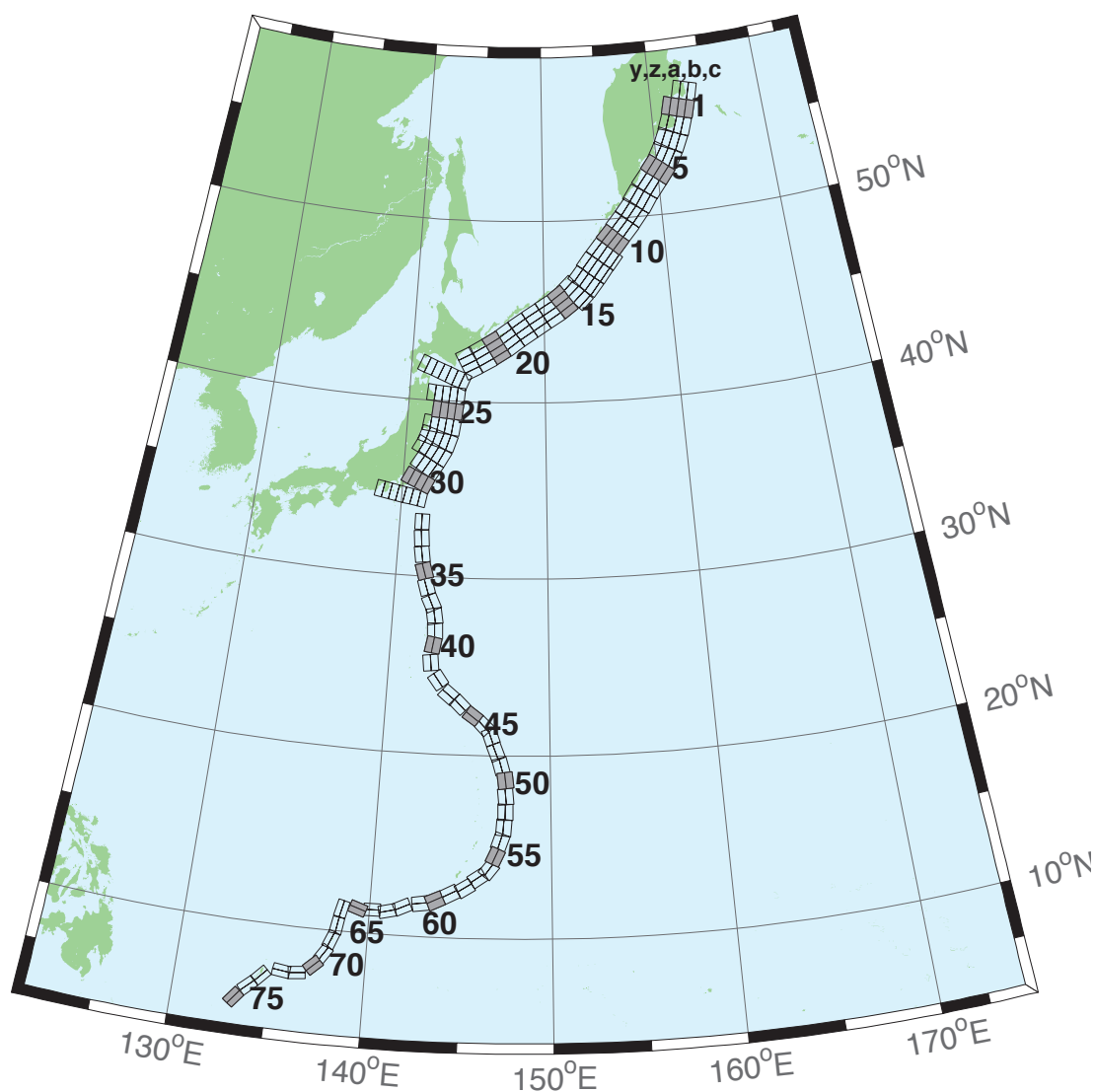
Figure B.5: Kamchatka-Kuril-Japan-Izu-Mariana-Yap Subduction Zone unit sources.

Table B.5: Earthquake parameters for Kamchatka-Kuril-Japan-Izu-Mariana-Yap Sub-duction Zone unit sources.

Segment	Description	Longitude(°E)	Latitude(°N)	Strike(°)	Dip(°)	Depth (km)
kisz–0a	Kamchatka-Kuril-Japan-Izu-Mariana-Yap	162.8200	56.3667	194.4	29	26.13
kisz–0b	Kamchatka-Kuril-Japan-Izu-Mariana-Yap	163.5057	56.2677	195	25	5
kisz–0z	Kamchatka-Kuril-Japan-Izu-Mariana-Yap	162.1309	56.4618	193.8	29	50.37
kisz–1a	Kamchatka-Kuril-Japan-Izu-Mariana-Yap	162.4318	55.5017	195	29	26.13
kisz–1b	Kamchatka-Kuril-Japan-Izu-Mariana-Yap	163.1000	55.4000	195	25	5
kisz–1y	Kamchatka-Kuril-Japan-Izu-Mariana-Yap	161.0884	55.7050	195	29	74.61
kisz–1z	Kamchatka-Kuril-Japan-Izu-Mariana-Yap	161.7610	55.6033	195	29	50.37
kisz–2a	Kamchatka-Kuril-Japan-Izu-Mariana-Yap	161.9883	54.6784	200	29	26.13
kisz–2b	Kamchatka-Kuril-Japan-Izu-Mariana-Yap	162.6247	54.5440	200	25	5
kisz–2y	Kamchatka-Kuril-Japan-Izu-Mariana-Yap	160.7072	54.9471	200	29	74.61
kisz–2z	Kamchatka-Kuril-Japan-Izu-Mariana-Yap	161.3488	54.8127	200	29	50.37
kisz–3a	Kamchatka-Kuril-Japan-Izu-Mariana-Yap	161.4385	53.8714	204	29	26.13
kisz–3b	Kamchatka-Kuril-Japan-Izu-Mariana-Yap	162.0449	53.7116	204	25	5
kisz–3y	Kamchatka-Kuril-Japan-Izu-Mariana-Yap	160.2164	54.1910	204	29	74.61
kisz–3z	Kamchatka-Kuril-Japan-Izu-Mariana-Yap	160.8286	54.0312	204	29	50.37
kisz–4a	Kamchatka-Kuril-Japan-Izu-Mariana-Yap	160.7926	53.1087	210	29	26.13
kisz–4b	Kamchatka-Kuril-Japan-Izu-Mariana-Yap	161.3568	52.9123	210	25	5
kisz–4y	Kamchatka-Kuril-Japan-Izu-Mariana-Yap	159.6539	53.5015	210	29	74.61
kisz–4z	Kamchatka-Kuril-Japan-Izu-Mariana-Yap	160.2246	53.3051	210	29	50.37
kisz–5a	Kamchatka-Kuril-Japan-Izu-Mariana-Yap	160.0211	52.4113	218	29	26.13
kisz–5b	Kamchatka-Kuril-Japan-Izu-Mariana-Yap	160.5258	52.1694	218	25	5
kisz–5y	Kamchatka-Kuril-Japan-Izu-Mariana-Yap	159.0005	52.8950	218	29	74.61
kisz–5z	Kamchatka-Kuril-Japan-Izu-Mariana-Yap	159.5122	52.6531	218	29	50.37
kisz–6a	Kamchatka-Kuril-Japan-Izu-Mariana-Yap	159.1272	51.7034	218	29	26.13
kisz–6b	Kamchatka-Kuril-Japan-Izu-Mariana-Yap	159.6241	51.4615	218	25	5
kisz–6y	Kamchatka-Kuril-Japan-Izu-Mariana-Yap	158.1228	52.1871	218	29	74.61
kisz–6z	Kamchatka-Kuril-Japan-Izu-Mariana-Yap	158.6263	51.9452	218	29	50.37
kisz–7a	Kamchatka-Kuril-Japan-Izu-Mariana-Yap	158.2625	50.9549	214	29	26.13
kisz–7b	Kamchatka-Kuril-Japan-Izu-Mariana-Yap	158.7771	50.7352	214	25	5
kisz–7y	Kamchatka-Kuril-Japan-Izu-Mariana-Yap	157.2236	51.3942	214	29	74.61
kisz–7z	Kamchatka-Kuril-Japan-Izu-Mariana-Yap	157.7443	51.1745	214	29	50.37
kisz–8a	Kamchatka-Kuril-Japan-Izu-Mariana-Yap	157.4712	50.2459	218	31	27.7
kisz–8b	Kamchatka-Kuril-Japan-Izu-Mariana-Yap	157.9433	50.0089	218	27	5
kisz–8y	Kamchatka-Kuril-Japan-Izu-Mariana-Yap	156.5176	50.7199	218	31	79.2
kisz–8z	Kamchatka-Kuril-Japan-Izu-Mariana-Yap	156.9956	50.4829	218	31	53.45
kisz–9a	Kamchatka-Kuril-Japan-Izu-Mariana-Yap	156.6114	49.5583	220	31	27.7
kisz–9b	Kamchatka-Kuril-Japan-Izu-Mariana-Yap	157.0638	49.3109	220	27	5
kisz–9y	Kamchatka-Kuril-Japan-Izu-Mariana-Yap	155.6974	50.0533	220	31	79.2
kisz–9z	Kamchatka-Kuril-Japan-Izu-Mariana-Yap	156.1556	49.8058	220	31	53.45
kisz–10a	Kamchatka-Kuril-Japan-Izu-Mariana-Yap	155.7294	48.8804	221	31	27.7
kisz–10b	Kamchatka-Kuril-Japan-Izu-Mariana-Yap	156.1690	48.6278	221	27	5
kisz–10y	Kamchatka-Kuril-Japan-Izu-Mariana-Yap	154.8413	49.3856	221	31	79.2
kisz–10z	Kamchatka-Kuril-Japan-Izu-Mariana-Yap	155.2865	49.1330	221	31	53.45
kisz–11a	Kamchatka-Kuril-Japan-Izu-Mariana-Yap	154.8489	48.1821	219	31	27.7
kisz–11b	Kamchatka-Kuril-Japan-Izu-Mariana-Yap	155.2955	47.9398	219	27	5
kisz–11y	Kamchatka-Kuril-Japan-Izu-Mariana-Yap	153.9472	48.6667	219	31	79.2
kisz–11z	Kamchatka-Kuril-Japan-Izu-Mariana-Yap	154.3991	48.4244	219	31	53.45
kisz–11c	Kamchatka-Kuril-Japan-Izu-Mariana-Yap	156.0358	47.5374	39	57.89	4.602
kisz–12a	Kamchatka-Kuril-Japan-Izu-Mariana-Yap	153.9994	47.4729	217	31	27.7
kisz–12b	Kamchatka-Kuril-Japan-Izu-Mariana-Yap	154.4701	47.2320	217	27	5
kisz–12y	Kamchatka-Kuril-Japan-Izu-Mariana-Yap	153.0856	47.9363	217	31	79.2
kisz–12z	Kamchatka-Kuril-Japan-Izu-Mariana-Yap	153.5435	47.7046	217	31	53.45
kisz–12c	Kamchatka-Kuril-Japan-Izu-Mariana-Yap	155.2208	46.8473	37	57.89	4.602
kisz–13a	Kamchatka-Kuril-Japan-Izu-Mariana-Yap	153.2239	46.7564	218	31	27.7
kisz–13b	Kamchatka-Kuril-Japan-Izu-Mariana-Yap	153.6648	46.5194	218	27	5
kisz–13y	Kamchatka-Kuril-Japan-Izu-Mariana-Yap	152.3343	47.2304	218	31	79.2
kisz–13z	Kamchatka-Kuril-Japan-Izu-Mariana-Yap	152.7801	46.9934	218	31	53.45
kisz–13c	Kamchatka-Kuril-Japan-Izu-Mariana-Yap	154.3957	46.1257	38	57.89	4.602
kisz–14a	Kamchatka-Kuril-Japan-Izu-Mariana-Yap	152.3657	46.1514	225	23	24.54
kisz–14b	Kamchatka-Kuril-Japan-Izu-Mariana-Yap	152.7855	45.8591	225	23	5

Continued on next page

105

Segment	Description	Longitude(^{o}E)	Latitude(^{o}N)	Strike(^{o})	Dip(^{o})	Depth (km)
kisz–14y	Kamchatka-Kuril-Japan-Izu-Mariana-Yap	151.5172	46.7362	225	23	63.62
kisz–14z	Kamchatka-Kuril-Japan-Izu-Mariana-Yap	151.9426	46.4438	225	23	44.08
kisz–14c	Kamchatka-Kuril-Japan-Izu-Mariana-Yap	153.4468	45.3976	45	57.89	4.602
kisz–15a	Kamchatka-Kuril-Japan-Izu-Mariana-Yap	151.4663	45.5963	233	25	23.73
kisz–15b	Kamchatka-Kuril-Japan-Izu-Mariana-Yap	151.8144	45.2712	233	22	5
kisz–15y	Kamchatka-Kuril-Japan-Izu-Mariana-Yap	150.7619	46.2465	233	25	65.99
kisz–15z	Kamchatka-Kuril-Japan-Izu-Mariana-Yap	151.1151	45.9214	233	25	44.86
kisz–16a	Kamchatka-Kuril-Japan-Izu-Mariana-Yap	150.4572	45.0977	237	25	23.73
kisz–16b	Kamchatka-Kuril-Japan-Izu-Mariana-Yap	150.7694	44.7563	237	22	5
kisz–16y	Kamchatka-Kuril-Japan-Izu-Mariana-Yap	149.8253	45.7804	237	25	65.99
kisz–16z	Kamchatka-Kuril-Japan-Izu-Mariana-Yap	150.1422	45.4390	237	25	44.86
kisz–17a	Kamchatka-Kuril-Japan-Izu-Mariana-Yap	149.3989	44.6084	237	25	23.73
kisz–17b	Kamchatka-Kuril-Japan-Izu-Mariana-Yap	149.7085	44.2670	237	22	5
kisz–17y	Kamchatka-Kuril-Japan-Izu-Mariana-Yap	148.7723	45.2912	237	25	65.99
kisz–17z	Kamchatka-Kuril-Japan-Izu-Mariana-Yap	149.0865	44.9498	237	25	44.86
kisz–18a	Kamchatka-Kuril-Japan-Izu-Mariana-Yap	148.3454	44.0982	235	25	23.73
kisz–18b	Kamchatka-Kuril-Japan-Izu-Mariana-Yap	148.6687	43.7647	235	22	5
kisz–18y	Kamchatka-Kuril-Japan-Izu-Mariana-Yap	147.6915	44.7651	235	25	65.99
kisz–18z	Kamchatka-Kuril-Japan-Izu-Mariana-Yap	148.0194	44.4316	235	25	44.86
kisz–19a	Kamchatka-Kuril-Japan-Izu-Mariana-Yap	147.3262	43.5619	233	25	23.73
kisz–19b	Kamchatka-Kuril-Japan-Izu-Mariana-Yap	147.6625	43.2368	233	22	5
kisz–19y	Kamchatka-Kuril-Japan-Izu-Mariana-Yap	146.6463	44.2121	233	25	65.99
kisz–19z	Kamchatka-Kuril-Japan-Izu-Mariana-Yap	146.9872	43.8870	233	25	44.86
kisz–20a	Kamchatka-Kuril-Japan-Izu-Mariana-Yap	146.3513	43.0633	237	25	23.73
kisz–20b	Kamchatka-Kuril-Japan-Izu-Mariana-Yap	146.6531	42.7219	237	22	5
kisz–20y	Kamchatka-Kuril-Japan-Izu-Mariana-Yap	145.7410	43.7461	237	25	65.99
kisz–20z	Kamchatka-Kuril-Japan-Izu-Mariana-Yap	146.0470	43.4047	237	25	44.86
kisz–21a	Kamchatka-Kuril-Japan-Izu-Mariana-Yap	145.3331	42.5948	239	25	23.73
kisz–21b	Kamchatka-Kuril-Japan-Izu-Mariana-Yap	145.6163	42.2459	239	22	5
kisz–21y	Kamchatka-Kuril-Japan-Izu-Mariana-Yap	144.7603	43.2927	239	25	65.99
kisz–21z	Kamchatka-Kuril-Japan-Izu-Mariana-Yap	145.0475	42.9438	239	25	44.86
kisz–22a	Kamchatka-Kuril-Japan-Izu-Mariana-Yap	144.3041	42.1631	242	25	23.73
kisz–22b	Kamchatka-Kuril-Japan-Izu-Mariana-Yap	144.5605	41.8037	242	22	5
kisz–22y	Kamchatka-Kuril-Japan-Izu-Mariana-Yap	143.7854	42.8819	242	25	65.99
kisz–22z	Kamchatka-Kuril-Japan-Izu-Mariana-Yap	144.0455	42.5225	242	25	44.86
kisz–23a	Kamchatka-Kuril-Japan-Izu-Mariana-Yap	143.2863	41.3335	202	21	21.28
kisz–23b	Kamchatka-Kuril-Japan-Izu-Mariana-Yap	143.8028	41.1764	202	19	5
kisz–23v	Kamchatka-Kuril-Japan-Izu-Mariana-Yap	140.6816	42.1189	202	21	110.9
kisz–23w	Kamchatka-Kuril-Japan-Izu-Mariana-Yap	141.2050	41.9618	202	21	92.95
kisz–23x	Kamchatka-Kuril-Japan-Izu-Mariana-Yap	141.7273	41.8047	202	21	75.04
kisz–23y	Kamchatka-Kuril-Japan-Izu-Mariana-Yap	142.2482	41.6476	202	21	57.12
kisz–23z	Kamchatka-Kuril-Japan-Izu-Mariana-Yap	142.7679	41.4905	202	21	39.2
kisz–24a	Kamchatka-Kuril-Japan-Izu-Mariana-Yap	142.9795	40.3490	185	21	21.28
kisz–24b	Kamchatka-Kuril-Japan-Izu-Mariana-Yap	143.5273	40.3125	185	19	5
kisz–24x	Kamchatka-Kuril-Japan-Izu-Mariana-Yap	141.3339	40.4587	185	21	75.04
kisz–24y	Kamchatka-Kuril-Japan-Izu-Mariana-Yap	141.8827	40.4221	185	21	57.12
kisz–24z	Kamchatka-Kuril-Japan-Izu-Mariana-Yap	142.4312	40.3856	185	21	39.2
kisz–25a	Kamchatka-Kuril-Japan-Izu-Mariana-Yap	142.8839	39.4541	185	21	21.28
kisz–25b	Kamchatka-Kuril-Japan-Izu-Mariana-Yap	143.4246	39.4176	185	19	5
kisz–25y	Kamchatka-Kuril-Japan-Izu-Mariana-Yap	141.8012	39.5272	185	21	57.12
kisz–25z	Kamchatka-Kuril-Japan-Izu-Mariana-Yap	142.3426	39.4907	185	21	39.2
kisz–26a	Kamchatka-Kuril-Japan-Izu-Mariana-Yap	142.7622	38.5837	188	21	21.28
kisz–26b	Kamchatka-Kuril-Japan-Izu-Mariana-Yap	143.2930	38.5254	188	19	5
kisz–26x	Kamchatka-Kuril-Japan-Izu-Mariana-Yap	141.1667	38.7588	188	21	75.04
kisz–26y	Kamchatka-Kuril-Japan-Izu-Mariana-Yap	141.6990	38.7004	188	21	57.12
kisz–26z	Kamchatka-Kuril-Japan-Izu-Mariana-Yap	142.2308	38.6421	188	21	39.2
kisz–27a	Kamchatka-Kuril-Japan-Izu-Mariana-Yap	142.5320	37.7830	198	21	21.28
kisz–27b	Kamchatka-Kuril-Japan-Izu-Mariana-Yap	143.0357	37.6534	198	19	5
kisz–27x	Kamchatka-Kuril-Japan-Izu-Mariana-Yap	141.0142	38.1717	198	21	75.04
kisz–27y	Kamchatka-Kuril-Japan-Izu-Mariana-Yap	141.5210	38.0421	198	21	57.12
kisz–27z	Kamchatka-Kuril-Japan-Izu-Mariana-Yap	142.0269	37.9126	198	21	39.2
kisz–28a	Kamchatka-Kuril-Japan-Izu-Mariana-Yap	142.1315	37.0265	208	21	21.28

Continued on next page

Segment	Description	Longitude(^{o}E)	Latitude(^{o}N)	Strike(^{o})	Dip(^{o})	Depth (km)
kisz–28b	Kamchatka-Kuril-Japan-Izu-Mariana-Yap	142.5941	36.8297	208	19	5
kisz–28x	Kamchatka-Kuril-Japan-Izu-Mariana-Yap	140.7348	37.6171	208	21	75.04
kisz–28y	Kamchatka-Kuril-Japan-Izu-Mariana-Yap	141.2016	37.4202	208	21	57.12
kisz–28z	Kamchatka-Kuril-Japan-Izu-Mariana-Yap	141.6671	37.2234	208	21	39.2
kisz–29a	Kamchatka-Kuril-Japan-Izu-Mariana-Yap	141.5970	36.2640	211	21	21.28
kisz–29b	Kamchatka-Kuril-Japan-Izu-Mariana-Yap	142.0416	36.0481	211	19	5
kisz–29y	Kamchatka-Kuril-Japan-Izu-Mariana-Yap	140.7029	36.6960	211	21	57.12
kisz–29z	Kamchatka-Kuril-Japan-Izu-Mariana-Yap	141.1506	36.4800	211	21	39.2
kisz–30a	Kamchatka-Kuril-Japan-Izu-Mariana-Yap	141.0553	35.4332	205	21	21.28
kisz–30b	Kamchatka-Kuril-Japan-Izu-Mariana-Yap	141.5207	35.2560	205	19	5
kisz–30y	Kamchatka-Kuril-Japan-Izu-Mariana-Yap	140.1204	35.7876	205	21	57.12
kisz–30z	Kamchatka-Kuril-Japan-Izu-Mariana-Yap	140.5883	35.6104	205	21	39.2
kisz–31a	Kamchatka-Kuril-Japan-Izu-Mariana-Yap	140.6956	34.4789	190	22	22.1
kisz–31b	Kamchatka-Kuril-Japan-Izu-Mariana-Yap	141.1927	34.4066	190	20	5
kisz–31v	Kamchatka-Kuril-Japan-Izu-Mariana-Yap	138.2025	34.8405	190	22	115.8
kisz–31w	Kamchatka-Kuril-Japan-Izu-Mariana-Yap	138.7021	34.7682	190	22	97.02
kisz–31x	Kamchatka-Kuril-Japan-Izu-Mariana-Yap	139.2012	34.6958	190	22	78.29
kisz–31y	Kamchatka-Kuril-Japan-Izu-Mariana-Yap	139.6997	34.6235	190	22	59.56
kisz–31z	Kamchatka-Kuril-Japan-Izu-Mariana-Yap	140.1979	34.5512	190	22	40.83
kisz–32a	Kamchatka-Kuril-Japan-Izu-Mariana-Yap	141.0551	33.0921	180	32	23.48
kisz–32b	Kamchatka-Kuril-Japan-Izu-Mariana-Yap	141.5098	33.0921	180	21.69	5
kisz–33a	Kamchatka-Kuril-Japan-Izu-Mariana-Yap	141.0924	32.1047	173.8	27.65	20.67
kisz–33b	Kamchatka-Kuril-Japan-Izu-Mariana-Yap	141.5596	32.1473	173.8	18.27	5
kisz–34a	Kamchatka-Kuril-Japan-Izu-Mariana-Yap	141.1869	31.1851	172.1	25	18.26
kisz–34b	Kamchatka-Kuril-Japan-Izu-Mariana-Yap	141.6585	31.2408	172.1	15.38	5
kisz–35a	Kamchatka-Kuril-Japan-Izu-Mariana-Yap	141.4154	30.1707	163	25	17.12
kisz–35b	Kamchatka-Kuril-Japan-Izu-Mariana-Yap	141.8662	30.2899	163	14.03	5
kisz–36a	Kamchatka-Kuril-Japan-Izu-Mariana-Yap	141.6261	29.2740	161.7	25.73	18.71
kisz–36b	Kamchatka-Kuril-Japan-Izu-Mariana-Yap	142.0670	29.4012	161.7	15.91	5
kisz–37a	Kamchatka-Kuril-Japan-Izu-Mariana-Yap	142.0120	28.3322	154.7	20	14.54
kisz–37b	Kamchatka-Kuril-Japan-Izu-Mariana-Yap	142.4463	28.5124	154.7	11	5
kisz–38a	Kamchatka-Kuril-Japan-Izu-Mariana-Yap	142.2254	27.6946	170.3	20	14.54
kisz–38b	Kamchatka-Kuril-Japan-Izu-Mariana-Yap	142.6955	27.7659	170.3	11	5
kisz–39a	Kamchatka-Kuril-Japan-Izu-Mariana-Yap	142.3085	26.9127	177.2	24.23	17.42
kisz–39b	Kamchatka-Kuril-Japan-Izu-Mariana-Yap	142.7674	26.9325	177.2	14.38	5
kisz–40a	Kamchatka-Kuril-Japan-Izu-Mariana-Yap	142.2673	26.1923	189.4	26.49	22.26
kisz–40b	Kamchatka-Kuril-Japan-Izu-Mariana-Yap	142.7090	26.1264	189.4	20.2	5
kisz–41a	Kamchatka-Kuril-Japan-Izu-Mariana-Yap	142.1595	25.0729	173.7	22.07	19.08
kisz–41b	Kamchatka-Kuril-Japan-Izu-Mariana-Yap	142.6165	25.1184	173.7	16.36	5
kisz–42a	Kamchatka-Kuril-Japan-Izu-Mariana-Yap	142.7641	23.8947	143.5	21.54	18.4
kisz–42b	Kamchatka-Kuril-Japan-Izu-Mariana-Yap	143.1321	24.1432	143.5	15.54	5
kisz–43a	Kamchatka-Kuril-Japan-Izu-Mariana-Yap	143.5281	23.0423	129.2	23.02	18.77
kisz–43b	Kamchatka-Kuril-Japan-Izu-Mariana-Yap	143.8128	23.3626	129.2	15.99	5
kisz–44a	Kamchatka-Kuril-Japan-Izu-Mariana-Yap	144.2230	22.5240	134.6	28.24	18.56
kisz–44b	Kamchatka-Kuril-Japan-Izu-Mariana-Yap	144.5246	22.8056	134.6	15.74	5
kisz–45a	Kamchatka-Kuril-Japan-Izu-Mariana-Yap	145.0895	21.8866	125.8	36.73	22.79
kisz–45b	Kamchatka-Kuril-Japan-Izu-Mariana-Yap	145.3171	22.1785	125.8	20.84	5
kisz–46a	Kamchatka-Kuril-Japan-Izu-Mariana-Yap	145.6972	21.3783	135.9	30.75	20.63
kisz–46b	Kamchatka-Kuril-Japan-Izu-Mariana-Yap	145.9954	21.6469	135.9	18.22	5
kisz–47a	Kamchatka-Kuril-Japan-Izu-Mariana-Yap	146.0406	20.9341	160.1	29.87	19.62
kisz–47b	Kamchatka-Kuril-Japan-Izu-Mariana-Yap	146.4330	21.0669	160.1	17	5
kisz–48a	Kamchatka-Kuril-Japan-Izu-Mariana-Yap	146.3836	20.0690	158	32.75	19.68
kisz–48b	Kamchatka-Kuril-Japan-Izu-Mariana-Yap	146.7567	20.2108	158	17.07	5
kisz–49a	Kamchatka-Kuril-Japan-Izu-Mariana-Yap	146.6689	19.3123	164.5	25.07	21.41
kisz–49b	Kamchatka-Kuril-Japan-Izu-Mariana-Yap	147.0846	19.4212	164.5	19.16	5
kisz–50a	Kamchatka-Kuril-Japan-Izu-Mariana-Yap	146.9297	18.5663	172.1	22	22.1
kisz–50b	Kamchatka-Kuril-Japan-Izu-Mariana-Yap	147.3650	18.6238	172.1	20	5
kisz–51a	Kamchatka-Kuril-Japan-Izu-Mariana-Yap	146.9495	17.7148	175.1	22.06	22.04
kisz–51b	Kamchatka-Kuril-Japan-Izu-Mariana-Yap	147.3850	17.7503	175.1	19.93	5
kisz–52a	Kamchatka-Kuril-Japan-Izu-Mariana-Yap	146.9447	16.8869	180	25.51	18.61
kisz–52b	Kamchatka-Kuril-Japan-Izu-Mariana-Yap	147.3683	16.8869	180	15.79	5
kisz–53a	Kamchatka-Kuril-Japan-Izu-Mariana-Yap	146.8626	16.0669	185.2	27.39	18.41

107

Segment	Description	Longitude(^{o}E)	Latitude(^{o}N)	Strike(^{o})	Dip(^{o})	Depth (km)
kisz–53b	Kamchatka-Kuril-Japan-Izu-Mariana-Yap	147.2758	16.0309	185.2	15.56	5
kisz–54a	Kamchatka-Kuril-Japan-Izu-Mariana-Yap	146.7068	15.3883	199.1	28.12	20.91
kisz–54b	Kamchatka-Kuril-Japan-Izu-Mariana-Yap	147.0949	15.2590	199.1	18.56	5
kisz–55a	Kamchatka-Kuril-Japan-Izu-Mariana-Yap	146.4717	14.6025	204.3	29.6	26.27
kisz–55b	Kamchatka-Kuril-Japan-Izu-Mariana-Yap	146.8391	14.4415	204.3	25.18	5
kisz–56a	Kamchatka-Kuril-Japan-Izu-Mariana-Yap	146.1678	13.9485	217.4	32.04	26.79
kisz–56b	Kamchatka-Kuril-Japan-Izu-Mariana-Yap	146.4789	13.7170	217.4	25.84	5
kisz–57a	Kamchatka-Kuril-Japan-Izu-Mariana-Yap	145.6515	13.5576	235.8	37	24.54
kisz–57b	Kamchatka-Kuril-Japan-Izu-Mariana-Yap	145.8586	13.2609	235.8	23	5
kisz–58a	Kamchatka-Kuril-Japan-Izu-Mariana-Yap	144.9648	12.9990	237.8	37.72	24.54
kisz–58b	Kamchatka-Kuril-Japan-Izu-Mariana-Yap	145.1589	12.6984	237.8	23	5
kisz–59a	Kamchatka-Kuril-Japan-Izu-Mariana-Yap	144.1799	12.6914	242.9	34.33	22.31
kisz–59b	Kamchatka-Kuril-Japan-Izu-Mariana-Yap	144.3531	12.3613	242.9	20.25	5
kisz–60a	Kamchatka-Kuril-Japan-Izu-Mariana-Yap	143.3687	12.3280	244.9	30.9	20.62
kisz–60b	Kamchatka-Kuril-Japan-Izu-Mariana-Yap	143.5355	11.9788	244.9	18.2	5
kisz–61a	Kamchatka-Kuril-Japan-Izu-Mariana-Yap	142.7051	12.1507	261.8	35.41	25.51
kisz–61b	Kamchatka-Kuril-Japan-Izu-Mariana-Yap	142.7582	11.7883	261.8	24.22	5
kisz–62a	Kamchatka-Kuril-Japan-Izu-Mariana-Yap	141.6301	11.8447	245.7	39.86	34.35
kisz–62b	Kamchatka-Kuril-Japan-Izu-Mariana-Yap	141.7750	11.5305	245.7	35.94	5
kisz–63a	Kamchatka-Kuril-Japan-Izu-Mariana-Yap	140.8923	11.5740	256.2	42	38.46
kisz–63b	Kamchatka-Kuril-Japan-Izu-Mariana-Yap	140.9735	11.2498	256.2	42	5
kisz–64a	Kamchatka-Kuril-Japan-Izu-Mariana-Yap	140.1387	11.6028	269.6	42.48	38.77
kisz–64b	Kamchatka-Kuril-Japan-Izu-Mariana-Yap	140.1410	11.2716	269.6	42.48	5
kisz–65a	Kamchatka-Kuril-Japan-Izu-Mariana-Yap	139.4595	11.5883	288.7	44.16	39.83
kisz–65b	Kamchatka-Kuril-Japan-Izu-Mariana-Yap	139.3541	11.2831	288.7	44.16	5
kisz–66a	Kamchatka-Kuril-Japan-Izu-Mariana-Yap	138.1823	11.2648	193.1	45	40.36
kisz–66b	Kamchatka-Kuril-Japan-Izu-Mariana-Yap	138.4977	11.1929	193.1	45	5
kisz–67a	Kamchatka-Kuril-Japan-Izu-Mariana-Yap	137.9923	10.3398	189.8	45	40.36
kisz–67b	Kamchatka-Kuril-Japan-Izu-Mariana-Yap	138.3104	10.2856	189.8	45	5
kisz–68a	Kamchatka-Kuril-Japan-Izu-Mariana-Yap	137.7607	9.6136	201.7	45	40.36
kisz–68b	Kamchatka-Kuril-Japan-Izu-Mariana-Yap	138.0599	9.4963	201.7	45	5
kisz–69a	Kamchatka-Kuril-Japan-Izu-Mariana-Yap	137.4537	8.8996	213.5	45	40.36
kisz–69b	Kamchatka-Kuril-Japan-Izu-Mariana-Yap	137.7215	8.7241	213.5	45	5
kisz–70a	Kamchatka-Kuril-Japan-Izu-Mariana-Yap	137.0191	8.2872	226.5	45	40.36
kisz–70b	Kamchatka-Kuril-Japan-Izu-Mariana-Yap	137.2400	8.0569	226.5	45	5
kisz–71a	Kamchatka-Kuril-Japan-Izu-Mariana-Yap	136.3863	7.9078	263.9	45	40.36
kisz–71b	Kamchatka-Kuril-Japan-Izu-Mariana-Yap	136.4202	7.5920	263.9	45	5
kisz–72a	Kamchatka-Kuril-Japan-Izu-Mariana-Yap	135.6310	7.9130	276.9	45	40.36
kisz–72b	Kamchatka-Kuril-Japan-Izu-Mariana-Yap	135.5926	7.5977	276.9	45	5
kisz–73a	Kamchatka-Kuril-Japan-Izu-Mariana-Yap	134.3296	7.4541	224	45	40.36
kisz–73b	Kamchatka-Kuril-Japan-Izu-Mariana-Yap	134.5600	7.2335	224	45	5
kisz–74a	Kamchatka-Kuril-Japan-Izu-Mariana-Yap	133.7125	6.8621	228.1	45	40.36
kisz–74b	Kamchatka-Kuril-Japan-Izu-Mariana-Yap	133.9263	6.6258	228.1	45	5
kisz–75a	Kamchatka-Kuril-Japan-Izu-Mariana-Yap	133.0224	6.1221	217.7	45	40.36
kisz–75b	Kamchatka-Kuril-Japan-Izu-Mariana-Yap	133.2751	5.9280	217.7	45	5
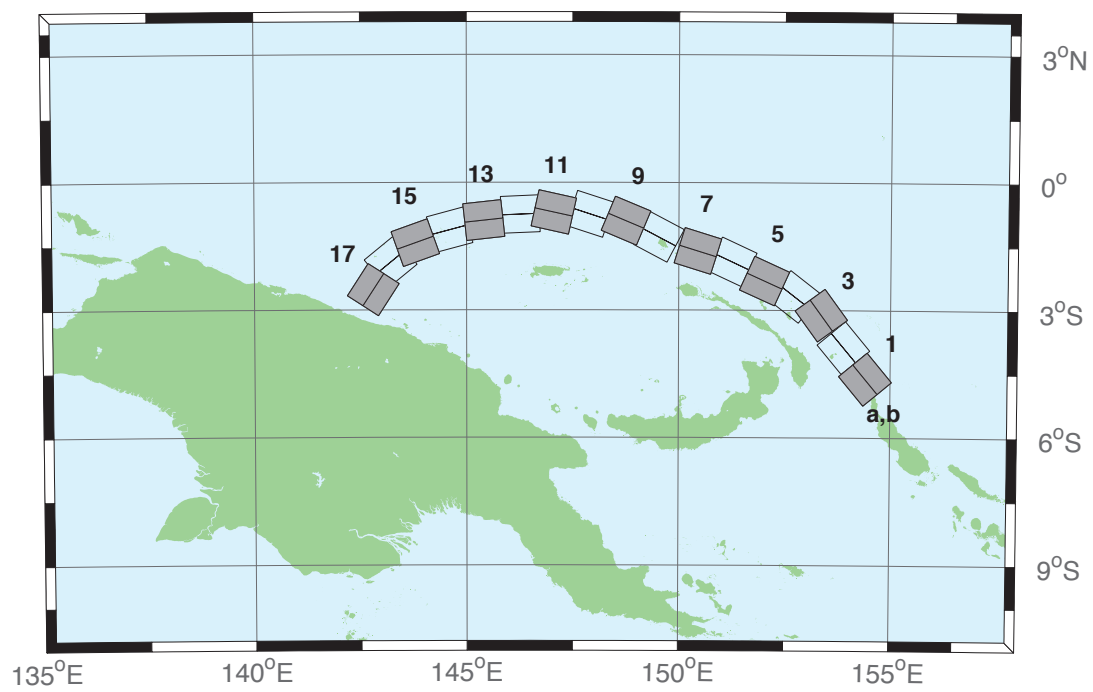
Figure B.6: Manus–Oceanic Convergent Boundary unit sources.

Table B.6: Earthquake parameters for Manus–Oceanic Convergent Boundary unit sources.

Segment	Description	Longitude(^{o}E)	Latitude(^{o}N)	Strike(^{o})	Dip(^{o})	Depth (km)
mosz–1a	Manus–Oceanic Convergent Boundary	154.0737	-4.8960	140.2	15	15.88
mosz–1b	Manus–Oceanic Convergent Boundary	154.4082	-4.6185	140.2	15	2.94
mosz–2a	Manus–Oceanic Convergent Boundary	153.5589	-4.1575	140.2	15	15.91
mosz–2b	Manus–Oceanic Convergent Boundary	153.8931	-3.8800	140.2	15	2.97
mosz–3a	Manus–Oceanic Convergent Boundary	153.0151	-3.3716	143.9	15	16.64
mosz–3b	Manus–Oceanic Convergent Boundary	153.3662	-3.1160	143.9	15	3.7
mosz–4a	Manus–Oceanic Convergent Boundary	152.4667	-3.0241	127.7	15	17.32
mosz–4b	Manus–Oceanic Convergent Boundary	152.7321	-2.6806	127.7	15	4.38
mosz–5a	Manus–Oceanic Convergent Boundary	151.8447	-2.7066	114.3	15	17.57
mosz–5b	Manus–Oceanic Convergent Boundary	152.0235	-2.3112	114.3	15	4.63
mosz–6a	Manus–Oceanic Convergent Boundary	151.0679	-2.2550	115	15	17.66
mosz–6b	Manus–Oceanic Convergent Boundary	151.2513	-1.8618	115	15	4.72
mosz–7a	Manus–Oceanic Convergent Boundary	150.3210	-2.0236	107.2	15	17.73
mosz–7b	Manus–Oceanic Convergent Boundary	150.4493	-1.6092	107.2	15	4.79
mosz–8a	Manus–Oceanic Convergent Boundary	149.3226	-1.6666	117.8	15	17.83
mosz–8b	Manus–Oceanic Convergent Boundary	149.5251	-1.2829	117.8	15	4.89
mosz–9a	Manus–Oceanic Convergent Boundary	148.5865	-1.3017	112.7	15	17.84
mosz–9b	Manus–Oceanic Convergent Boundary	148.7540	-0.9015	112.7	15	4.9
mosz–10a	Manus–Oceanic Convergent Boundary	147.7760	-1.1560	108	15	17.78
mosz–10b	Manus–Oceanic Convergent Boundary	147.9102	-0.7434	108	15	4.84
mosz–11a	Manus–Oceanic Convergent Boundary	146.9596	-1.1226	102.5	15	17.54
mosz–11b	Manus–Oceanic Convergent Boundary	147.0531	-0.6990	102.5	15	4.6
mosz–12a	Manus–Oceanic Convergent Boundary	146.2858	-1.1820	87.48	15	17.29
mosz–12b	Manus–Oceanic Convergent Boundary	146.2667	-0.7486	87.48	15	4.35
mosz–13a	Manus–Oceanic Convergent Boundary	145.4540	-1.3214	83.75	15	17.34
mosz–13b	Manus–Oceanic Convergent Boundary	145.4068	-0.8901	83.75	15	4.4
mosz–14a	Manus–Oceanic Convergent Boundary	144.7151	-1.5346	75.09	15	17.21
mosz–14b	Manus–Oceanic Convergent Boundary	144.6035	-1.1154	75.09	15	4.27
mosz–15a	Manus–Oceanic Convergent Boundary	143.9394	-1.8278	70.43	15	16.52
mosz–15b	Manus–Oceanic Convergent Boundary	143.7940	-1.4190	70.43	15	3.58
mosz–16a	Manus–Oceanic Convergent Boundary	143.4850	-2.2118	50.79	15	15.86
mosz–16b	Manus–Oceanic Convergent Boundary	143.2106	-1.8756	50.79	15	2.92
mosz–17a	Manus–Oceanic Convergent Boundary	143.1655	-2.7580	33	15	16.64
mosz–17b	Manus–Oceanic Convergent Boundary	142.8013	-2.5217	33	15	3.7
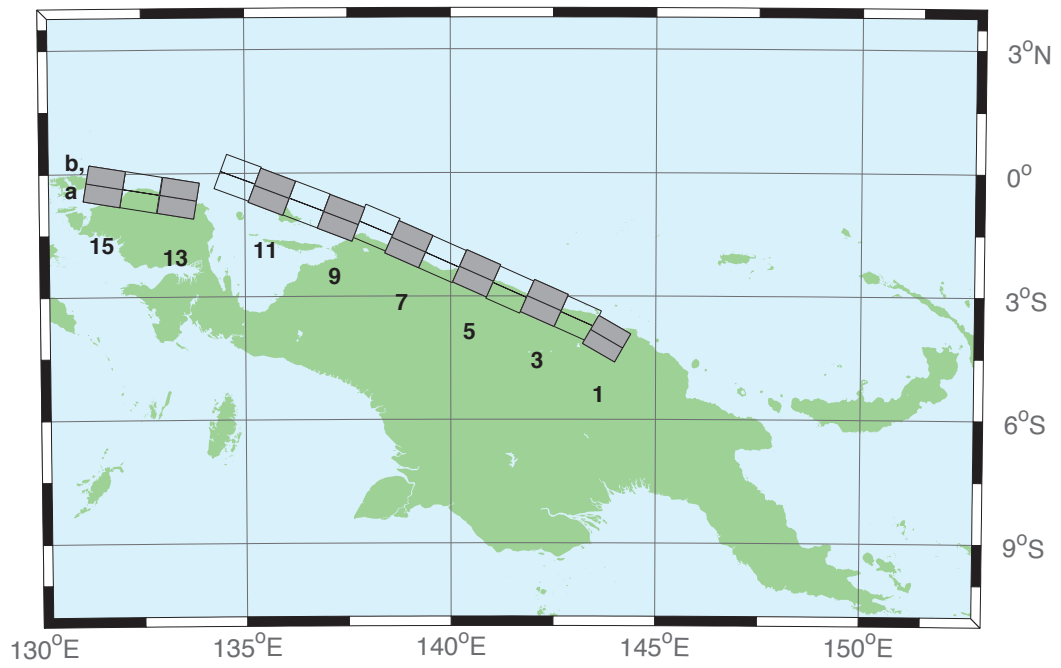
Figure B.7: New Guinea Subduction Zone unit sources.

Table B.7: Earthquake parameters for New Guinea Subduction Zone unit sources.

Segment	Description	Longitude(^{o}E)	Latitude(^{o}N)	Strike(^{o})	Dip(^{o})	Depth (km)
ngsz–1a	New Guinea	143.6063	-4.3804	120	29	25.64
ngsz–1b	New Guinea	143.8032	-4.0402	120	29	1.4
ngsz–2a	New Guinea	142.9310	-3.9263	114	27.63	20.1
ngsz–2b	New Guinea	143.0932	-3.5628	114	21.72	1.6
ngsz–3a	New Guinea	142.1076	-3.5632	114	20.06	18.73
ngsz–3b	New Guinea	142.2795	-3.1778	114	15.94	5
ngsz–4a	New Guinea	141.2681	-3.2376	114	21	17.76
ngsz–4b	New Guinea	141.4389	-2.8545	114	14.79	5
ngsz–5a	New Guinea	140.4592	-2.8429	114	21.26	16.14
ngsz–5b	New Guinea	140.6296	-2.4605	114	12.87	5
ngsz–6a	New Guinea	139.6288	-2.4960	114	22.72	15.4
ngsz–6b	New Guinea	139.7974	-2.1175	114	12	5
ngsz–7a	New Guinea	138.8074	-2.1312	114	21.39	15.4
ngsz–7b	New Guinea	138.9776	-1.7491	114	12	5
ngsz–8a	New Guinea	138.0185	-1.7353	113.1	18.79	15.14
ngsz–8b	New Guinea	138.1853	-1.3441	113.1	11.7	5
ngsz–9a	New Guinea	137.1805	-1.5037	111	15.24	13.23
ngsz–9b	New Guinea	137.3358	-1.0991	111	9.47	5
ngsz–10a	New Guinea	136.3418	-1.1774	111	13.51	11.09
ngsz–10b	New Guinea	136.4983	-0.7697	111	7	5
ngsz–11a	New Guinea	135.4984	-0.8641	111	11.38	12.49
ngsz–11b	New Guinea	135.6562	-0.4530	111	8.62	5
ngsz–12a	New Guinea	134.6759	-0.5216	110.5	10	13.68
ngsz–12b	New Guinea	134.8307	-0.1072	110.5	10	5
ngsz–13a	New Guinea	133.3065	-1.0298	99.5	10	13.68
ngsz–13b	New Guinea	133.3795	-0.5935	99.5	10	5
ngsz–14a	New Guinea	132.4048	-0.8816	99.5	10	13.68
ngsz–14b	New Guinea	132.4778	-0.4453	99.5	10	5
ngsz–15a	New Guinea	131.5141	-0.7353	99.5	10	13.68
ngsz–15b	New Guinea	131.5871	-0.2990	99.5	10	5
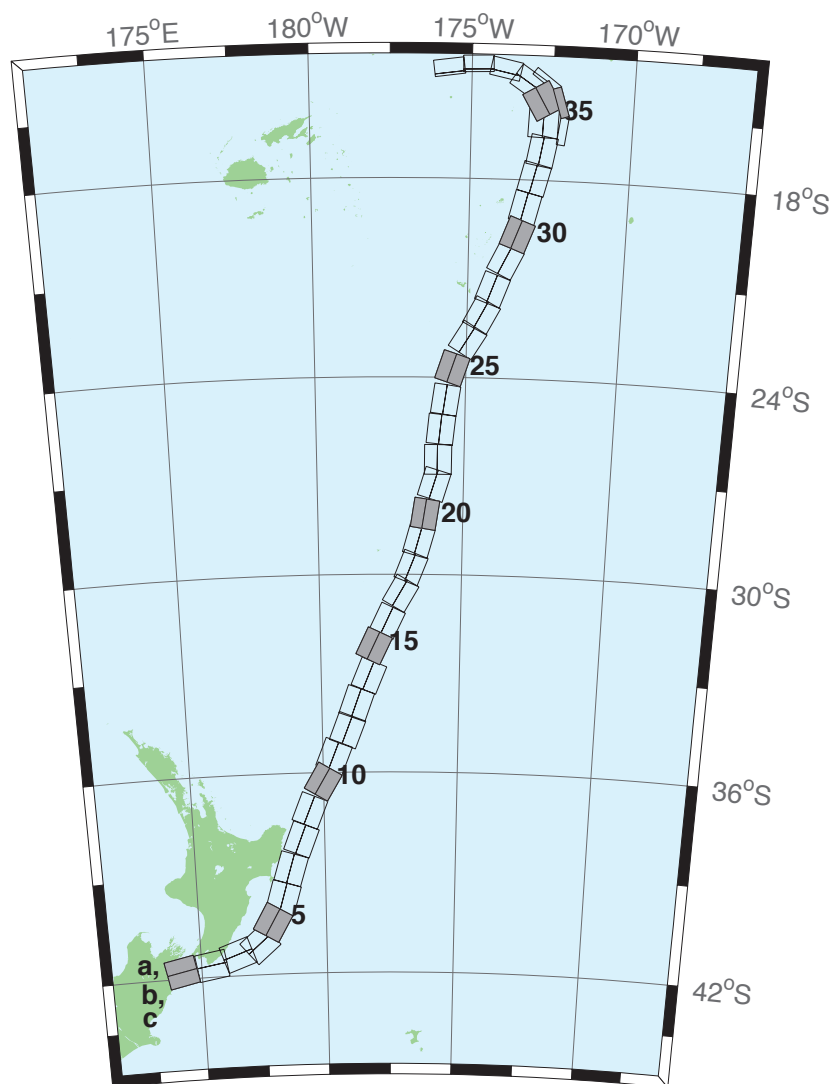
Figure B.8: New Zealand–Kermadec–Tonga Subduction Zone unit sources.

Table B.8: Earthquake parameters for New Zealand–Kermadec–Tonga Subduction Zone unit sources.

Segment	Description	Longitude(°E)	Latitude(°N)	Strike(°)	Dip(°)	Depth (km)
ntsz–1a	New Zealand–Kermadec–Tonga	174.0985	-41.3951	258.6	24	25.34
ntsz–1b	New Zealand–Kermadec–Tonga	174.2076	-41.7973	258.6	24	5
ntsz–2a	New Zealand–Kermadec–Tonga	175.3289	-41.2592	260.6	29.38	23.17
ntsz–2b	New Zealand–Kermadec–Tonga	175.4142	-41.6454	260.6	21.31	5
ntsz–3a	New Zealand–Kermadec–Tonga	176.2855	-40.9950	250.7	29.54	21.74
ntsz–3b	New Zealand–Kermadec–Tonga	176.4580	-41.3637	250.7	19.56	5
ntsz–4a	New Zealand–Kermadec–Tonga	177.0023	-40.7679	229.4	24.43	18.87
ntsz–4b	New Zealand–Kermadec–Tonga	177.3552	-41.0785	229.4	16.1	5
ntsz–5a	New Zealand–Kermadec–Tonga	177.4114	-40.2396	210	18.8	19.29
ntsz–5b	New Zealand–Kermadec–Tonga	177.8951	-40.4525	210	16.61	5
ntsz–6a	New Zealand–Kermadec–Tonga	177.8036	-39.6085	196.7	18.17	15.8
ntsz–6b	New Zealand–Kermadec–Tonga	178.3352	-39.7310	196.7	12.48	5
ntsz–7a	New Zealand–Kermadec–Tonga	178.1676	-38.7480	197	28.1	17.85
ntsz–7b	New Zealand–Kermadec–Tonga	178.6541	-38.8640	197	14.89	5
ntsz–8a	New Zealand–Kermadec–Tonga	178.6263	-37.8501	201.4	31.47	18.78
ntsz–8b	New Zealand–Kermadec–Tonga	179.0788	-37.9899	201.4	16	5
ntsz–9a	New Zealand–Kermadec–Tonga	178.9833	-36.9770	202.2	29.58	20.02
ntsz–9b	New Zealand–Kermadec–Tonga	179.4369	-37.1245	202.2	17.48	5
ntsz–10a	New Zealand–Kermadec–Tonga	179.5534	-36.0655	210.6	32.1	20.72
ntsz–10b	New Zealand–Kermadec–Tonga	179.9595	-36.2593	210.6	18.32	5
ntsz–11a	New Zealand–Kermadec–Tonga	179.9267	-35.3538	201.7	25	16.09
ntsz–11b	New Zealand–Kermadec–Tonga	180.3915	-35.5040	201.7	12.81	5
ntsz–12a	New Zealand–Kermadec–Tonga	180.4433	-34.5759	201.2	25	15.46
ntsz–12b	New Zealand–Kermadec–Tonga	180.9051	-34.7230	201.2	12.08	5
ntsz–13a	New Zealand–Kermadec–Tonga	180.7990	-33.7707	199.8	25.87	19.06
ntsz–13b	New Zealand–Kermadec–Tonga	181.2573	-33.9073	199.8	16.33	5
ntsz–14a	New Zealand–Kermadec–Tonga	181.2828	-32.9288	202.4	31.28	22.73
ntsz–14b	New Zealand–Kermadec–Tonga	181.7063	-33.0751	202.4	20.77	5
ntsz–15a	New Zealand–Kermadec–Tonga	181.4918	-32.0035	205.4	32.33	22.64
ntsz–15b	New Zealand–Kermadec–Tonga	181.8967	-32.1665	205.4	20.66	5
ntsz–16a	New Zealand–Kermadec–Tonga	181.9781	-31.2535	205.5	34.29	23.59
ntsz–16b	New Zealand–Kermadec–Tonga	182.3706	-31.4131	205.5	21.83	5
ntsz–17a	New Zealand–Kermadec–Tonga	182.4819	-30.3859	210.3	37.6	25.58
ntsz–17b	New Zealand–Kermadec–Tonga	182.8387	-30.5655	210.3	24.3	5
ntsz–18a	New Zealand–Kermadec–Tonga	182.8176	-29.6545	201.6	37.65	26.13
ntsz–18b	New Zealand–Kermadec–Tonga	183.1985	-29.7856	201.6	25	5
ntsz–19a	New Zealand–Kermadec–Tonga	183.0622	-28.8739	195.7	34.41	26.13
ntsz–19b	New Zealand–Kermadec–Tonga	183.4700	-28.9742	195.7	25	5
ntsz–20a	New Zealand–Kermadec–Tonga	183.2724	-28.0967	188.8	38	26.13
ntsz–20b	New Zealand–Kermadec–Tonga	183.6691	-28.1508	188.8	25	5
ntsz–21a	New Zealand–Kermadec–Tonga	183.5747	-27.1402	197.1	32.29	24.83
ntsz–21b	New Zealand–Kermadec–Tonga	183.9829	-27.2518	197.1	23.37	5
ntsz–22a	New Zealand–Kermadec–Tonga	183.6608	-26.4975	180	29.56	18.63
ntsz–22b	New Zealand–Kermadec–Tonga	184.0974	-26.4975	180	15.82	5
ntsz–23a	New Zealand–Kermadec–Tonga	183.7599	-25.5371	185.8	32.42	20.56
ntsz–23b	New Zealand–Kermadec–Tonga	184.1781	-25.5752	185.8	18.13	5
ntsz–24a	New Zealand–Kermadec–Tonga	183.9139	-24.6201	188.2	33.31	23.73
ntsz–24b	New Zealand–Kermadec–Tonga	184.3228	-24.6734	188.2	22	5
ntsz–25a	New Zealand–Kermadec–Tonga	184.1266	-23.5922	198.5	29.34	19.64
ntsz–25b	New Zealand–Kermadec–Tonga	184.5322	-23.7163	198.5	17.03	5
ntsz–26a	New Zealand–Kermadec–Tonga	184.6613	-22.6460	211.7	30.26	19.43
ntsz–26b	New Zealand–Kermadec–Tonga	185.0196	-22.8497	211.7	16.78	5
ntsz–27a	New Zealand–Kermadec–Tonga	185.0879	-21.9139	207.9	31.73	20.67
ntsz–27b	New Zealand–Kermadec–Tonga	185.4522	-22.0928	207.9	18.27	5
ntsz–28a	New Zealand–Kermadec–Tonga	185.4037	-21.1758	200.5	32.44	21.76
ntsz–28b	New Zealand–Kermadec–Tonga	185.7849	-21.3084	200.5	19.58	5
ntsz–29a	New Zealand–Kermadec–Tonga	185.8087	-20.2629	206.4	32.47	20.4
ntsz–29b	New Zealand–Kermadec–Tonga	186.1710	-20.4312	206.4	17.94	5
ntsz–30a	New Zealand–Kermadec–Tonga	186.1499	-19.5087	200.9	32.98	22.46
ntsz–30b	New Zealand–Kermadec–Tonga	186.5236	-19.6432	200.9	20.44	5

Segment	Description	Longitude(°E)	Latitude(°N)	Strike(°)	Dip(°)	Depth (km)
ntsz–31a	New Zealand–Kermadec–Tonga	186.3538	-18.7332	193.9	34.41	21.19
ntsz–31b	New Zealand–Kermadec–Tonga	186.7339	-18.8221	193.9	18.89	5
ntsz–32a	New Zealand–Kermadec–Tonga	186.5949	-17.8587	194.1	30	19.12
ntsz–32b	New Zealand–Kermadec–Tonga	186.9914	-17.9536	194.1	16.4	5
ntsz–33a	New Zealand–Kermadec–Tonga	186.8172	-17.0581	190	33.15	23.34
ntsz–33b	New Zealand–Kermadec–Tonga	187.2047	-17.1237	190	21.52	5
ntsz–34a	New Zealand–Kermadec–Tonga	186.7814	-16.2598	182.1	15	13.41
ntsz–34b	New Zealand–Kermadec–Tonga	187.2330	-16.2759	182.1	9.68	5
ntsz–34c	New Zealand–Kermadec–Tonga	187.9697	-16.4956	7.62	57.06	6.571
ntsz–35a	New Zealand–Kermadec–Tonga	186.8000	-15.8563	149.8	15	12.17
ntsz–35b	New Zealand–Kermadec–Tonga	187.1896	-15.6384	149.8	8.24	5
ntsz–35c	New Zealand–Kermadec–Tonga	187.8776	-15.6325	342.4	57.06	6.571
ntsz–36a	New Zealand–Kermadec–Tonga	186.5406	-15.3862	123.9	40.44	36.72
ntsz–36b	New Zealand–Kermadec–Tonga	186.7381	-15.1025	123.9	39.38	5
ntsz–36c	New Zealand–Kermadec–Tonga	187.3791	-14.9234	307	57.06	6.571
ntsz–37a	New Zealand–Kermadec–Tonga	185.9883	-14.9861	102	68.94	30.99
ntsz–37b	New Zealand–Kermadec–Tonga	186.0229	-14.8282	102	31.32	5
ntsz–38a	New Zealand–Kermadec–Tonga	185.2067	-14.8259	88.4	80	26.13
ntsz–38b	New Zealand–Kermadec–Tonga	185.2044	-14.7479	88.4	25	5
ntsz–39a	New Zealand–Kermadec–Tonga	184.3412	-14.9409	82.55	80	26.13
ntsz–39b	New Zealand–Kermadec–Tonga	184.3307	-14.8636	82.55	25	5
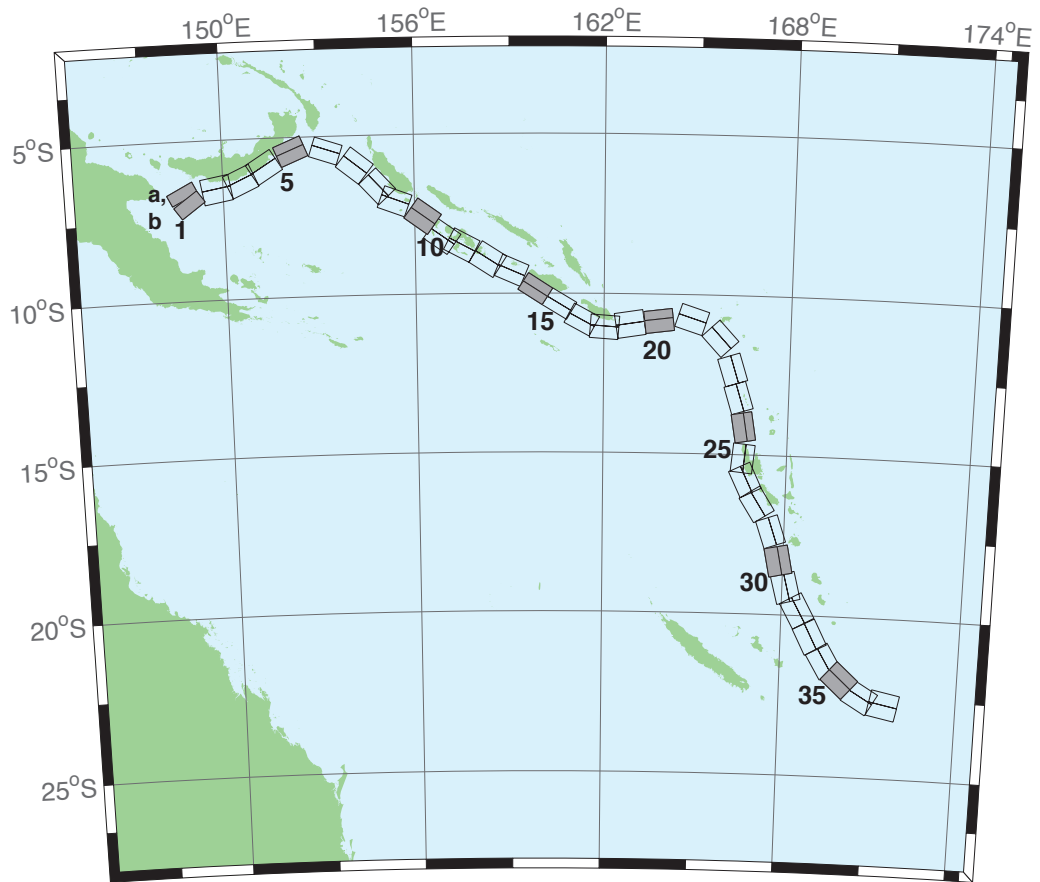
Figure B.9: New Britain–Solomons–Vanuatu Zone unit sources.

Table B.9: Earthquake parameters for New Britain–Solomons–Vanuatu Subduction Zone unit sources.

Segment	Description	Longitude(°E)	Latitude(°N)	Strike(°)	Dip(°)	Depth (km)
nvsz–1a	New Britain–Solomons–Vanuatu	148.6217	-6.4616	243.2	32.34	15.69
nvsz–1b	New Britain–Solomons–Vanuatu	148.7943	-6.8002	234.2	12.34	5
nvsz–2a	New Britain–Solomons–Vanuatu	149.7218	-6.1459	260.1	35.1	16.36
nvsz–2b	New Britain–Solomons–Vanuatu	149.7856	-6.5079	260.1	13.13	5
nvsz–3a	New Britain–Solomons–Vanuatu	150.4075	-5.9659	245.7	42.35	18.59
nvsz–3b	New Britain–Solomons–Vanuatu	150.5450	-6.2684	245.7	15.77	5
nvsz–4a	New Britain–Solomons–Vanuatu	151.1095	-5.5820	238.2	42.41	23.63
nvsz–4b	New Britain–Solomons–Vanuatu	151.2851	-5.8639	238.2	21.88	5
nvsz–5a	New Britain–Solomons–Vanuatu	152.0205	-5.1305	247.7	49.22	32.39
nvsz–5b	New Britain–Solomons–Vanuatu	152.1322	-5.4020	247.7	33.22	5
nvsz–6a	New Britain–Solomons–Vanuatu	153.3450	-5.1558	288.6	53.53	33.59
nvsz–6b	New Britain–Solomons–Vanuatu	153.2595	-5.4089	288.6	34.87	5
nvsz–7a	New Britain–Solomons–Vanuatu	154.3814	-5.6308	308.3	39.72	19.18
nvsz–7b	New Britain–Solomons–Vanuatu	154.1658	-5.9017	308.3	16.48	5
nvsz–8a	New Britain–Solomons–Vanuatu	155.1097	-6.3511	317.2	45.33	22.92
nvsz–8b	New Britain–Solomons–Vanuatu	154.8764	-6.5656	317.2	21	5
nvsz–9a	New Britain–Solomons–Vanuatu	155.5027	-6.7430	290.5	48.75	22.92
nvsz–9b	New Britain–Solomons–Vanuatu	155.3981	-7.0204	290.5	21	5
nvsz–10a	New Britain–Solomons–Vanuatu	156.4742	-7.2515	305.9	36.88	27.62
nvsz–10b	New Britain–Solomons–Vanuatu	156.2619	-7.5427	305.9	26.9	5
nvsz–11a	New Britain–Solomons–Vanuatu	157.0830	-7.8830	305.4	32.97	29.72
nvsz–11b	New Britain–Solomons–Vanuatu	156.8627	-8.1903	305.4	29.63	5
nvsz–12a	New Britain–Solomons–Vanuatu	157.6537	-8.1483	297.9	37.53	28.57
nvsz–12b	New Britain–Solomons–Vanuatu	157.4850	-8.4630	297.9	28.13	5
nvsz–13a	New Britain–Solomons–Vanuatu	158.5089	-8.5953	302.7	33.62	23.02
nvsz–13b	New Britain–Solomons–Vanuatu	158.3042	-8.9099	302.7	21.12	5
nvsz–14a	New Britain–Solomons–Vanuatu	159.1872	-8.9516	293.3	38.44	34.06
nvsz–14b	New Britain–Solomons–Vanuatu	159.0461	-9.2747	293.3	35.54	5
nvsz–15a	New Britain–Solomons–Vanuatu	159.9736	-9.5993	302.8	46.69	41.38
nvsz–15b	New Britain–Solomons–Vanuatu	159.8044	-9.8584	302.8	46.69	5
nvsz–16a	New Britain–Solomons–Vanuatu	160.7343	-10.0574	301	46.05	41
nvsz–16b	New Britain–Solomons–Vanuatu	160.5712	-10.3246	301	46.05	5
nvsz–17a	New Britain–Solomons–Vanuatu	161.4562	-10.5241	298.4	40.12	37.22
nvsz–17b	New Britain–Solomons–Vanuatu	161.2900	-10.8263	298.4	40.12	5
nvsz–18a	New Britain–Solomons–Vanuatu	162.0467	-10.6823	274.1	40.33	29.03
nvsz–18b	New Britain–Solomons–Vanuatu	162.0219	-11.0238	274.1	28.72	5
nvsz–19a	New Britain–Solomons–Vanuatu	162.7818	-10.5645	261.3	34.25	24.14
nvsz–19b	New Britain–Solomons–Vanuatu	162.8392	-10.9315	261.3	22.51	5
nvsz–20a	New Britain–Solomons–Vanuatu	163.7222	-10.5014	262.9	50.35	26.3
nvsz–20b	New Britain–Solomons–Vanuatu	163.7581	-10.7858	262.9	25.22	5
nvsz–21a	New Britain–Solomons–Vanuatu	164.9445	-10.4183	287.9	40.31	23.3
nvsz–21b	New Britain–Solomons–Vanuatu	164.8374	-10.7442	287.9	21.47	5
nvsz–22a	New Britain–Solomons–Vanuatu	166.0261	-11.1069	317.1	42.39	20.78
nvsz–22b	New Britain–Solomons–Vanuatu	165.7783	-11.3328	317.1	18.4	5
nvsz–23a	New Britain–Solomons–Vanuatu	166.5179	-12.2260	342.4	47.95	22.43
nvsz–23b	New Britain–Solomons–Vanuatu	166.2244	-12.3171	342.4	20.4	5
nvsz–24a	New Britain–Solomons–Vanuatu	166.7236	-13.1065	342.6	47.13	28.52
nvsz–24b	New Britain–Solomons–Vanuatu	166.4241	-13.1979	342.6	28.06	5
nvsz–25a	New Britain–Solomons–Vanuatu	166.8914	-14.0785	350.3	54.1	31.16
nvsz–25b	New Britain–Solomons–Vanuatu	166.6237	-14.1230	350.3	31.55	5
nvsz–26a	New Britain–Solomons–Vanuatu	166.9200	-15.1450	365.6	50.46	29.05
nvsz–26b	New Britain–Solomons–Vanuatu	166.6252	-15.1170	365.6	28.75	5
nvsz–27a	New Britain–Solomons–Vanuatu	167.0053	-15.6308	334.2	44.74	25.46
nvsz–27b	New Britain–Solomons–Vanuatu	166.7068	-15.7695	334.2	24.15	5
nvsz–28a	New Britain–Solomons–Vanuatu	167.4074	-16.3455	327.5	41.53	22.44
nvsz–28b	New Britain–Solomons–Vanuatu	167.1117	-16.5264	327.5	20.42	5
nvsz–29a	New Britain–Solomons–Vanuatu	167.9145	-17.2807	341.2	49.1	24.12
nvsz–29b	New Britain–Solomons–Vanuatu	167.6229	-17.3757	341.2	22.48	5
nvsz–30a	New Britain–Solomons–Vanuatu	168.2220	-18.2353	348.6	44.19	23.99
nvsz–30b	New Britain–Solomons–Vanuatu	167.8895	-18.2991	348.6	22.32	5

Table B.9 – continued

Segment	Description	Longitude(^{o}E)	Latitude(^{o}N)	Strike(^{o})	Dip(^{o})	Depth (km)
nvsz–31a	New Britain–Solomons–Vanuatu	168.5022	-19.0510	345.6	42.2	22.26
nvsz–31b	New Britain–Solomons–Vanuatu	168.1611	-19.1338	345.6	20.2	5
nvsz–32a	New Britain–Solomons–Vanuatu	168.8775	-19.6724	331.1	42.03	21.68
nvsz–32b	New Britain–Solomons–Vanuatu	168.5671	-19.8338	331.1	19.49	5
nvsz–33a	New Britain–Solomons–Vanuatu	169.3422	-20.4892	332.9	40.25	22.4
nvsz–33b	New Britain–Solomons–Vanuatu	169.0161	-20.6453	332.9	20.37	5
nvsz–34a	New Britain–Solomons–Vanuatu	169.8304	-21.2121	329.1	39	22.73
nvsz–34b	New Britain–Solomons–Vanuatu	169.5086	-21.3911	329.1	20.77	5
nvsz–35a	New Britain–Solomons–Vanuatu	170.3119	-21.6945	311.9	39	22.13
nvsz–35b	New Britain–Solomons–Vanuatu	170.0606	-21.9543	311.9	20.03	5
nvsz–36a	New Britain–Solomons–Vanuatu	170.9487	-22.1585	300.4	39.42	23.5
nvsz–36b	New Britain–Solomons–Vanuatu	170.7585	-22.4577	300.4	21.71	5
nvsz–37a	New Britain–Solomons–Vanuatu	171.6335	-22.3087	281.3	30	22.1
nvsz–37b	New Britain–Solomons–Vanuatu	171.5512	-22.6902	281.3	20	5
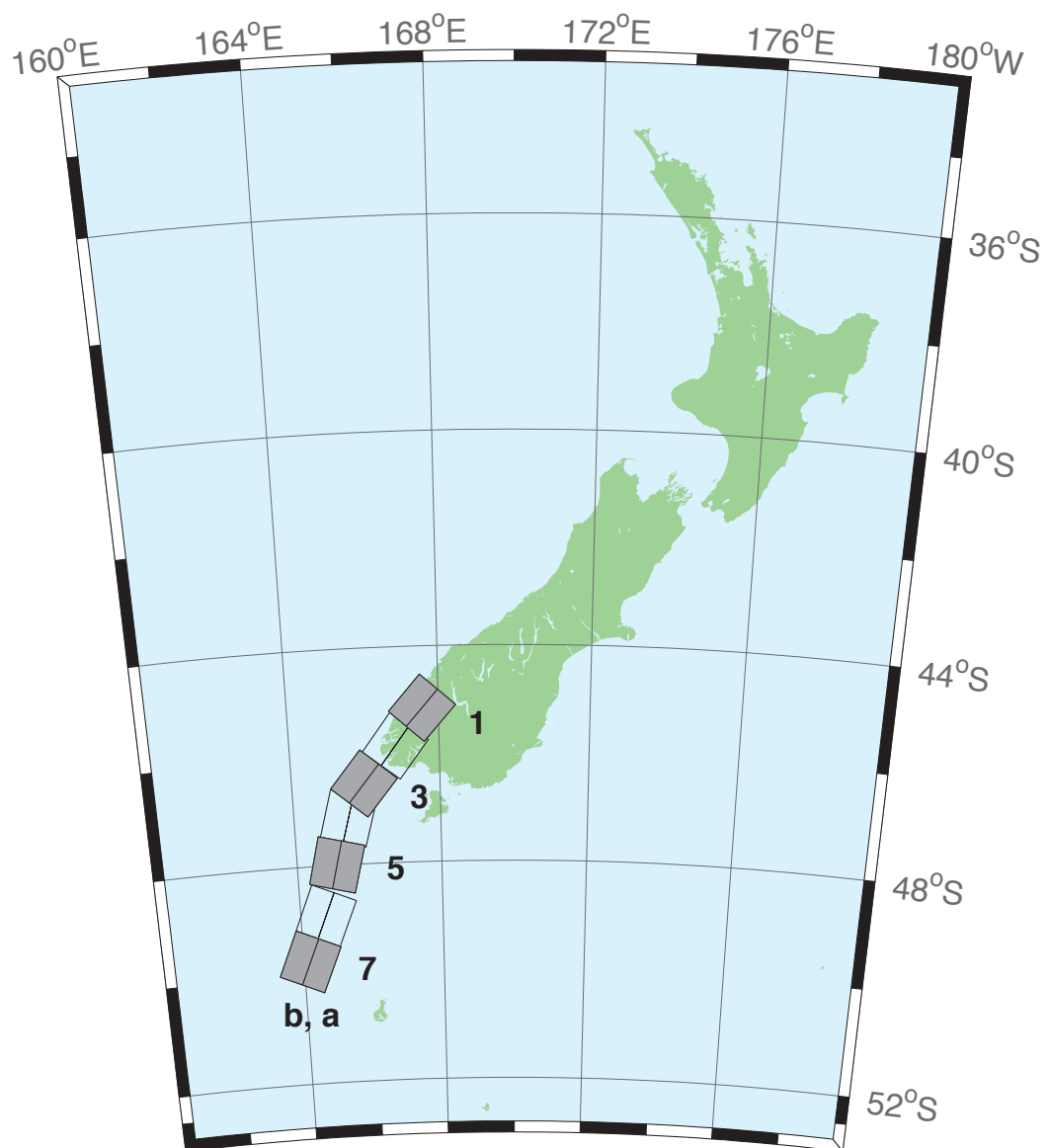
Figure B.10: New Zealand–Puysegur Zone unit sources.

Table B.10: Earthquake parameters for New Zealand–Puysegur Subduction Zone unit sources.

Segment	Description	Longitude(^{o}E)	Latitude(^{o}N)	Strike(^{o})	Dip(^{o})	Depth (km)
nzsz–1a	New Zealand–Puysegur	168.0294	-45.4368	41.5	15	17.94
nzsz–1b	New Zealand–Puysegur	167.5675	-45.1493	41.5	15	5
nzsz–2a	New Zealand–Puysegur	167.3256	-46.0984	37.14	15	17.94
nzsz–2b	New Zealand–Puysegur	166.8280	-45.8365	37.14	15	5
nzsz–3a	New Zealand–Puysegur	166.4351	-46.7897	39.53	15	17.94
nzsz–3b	New Zealand–Puysegur	165.9476	-46.5136	39.53	15	5
nzsz–4a	New Zealand–Puysegur	166.0968	-47.2583	15.38	15	17.94
nzsz–4b	New Zealand–Puysegur	165.4810	-47.1432	15.38	15	5
nzsz–5a	New Zealand–Puysegur	165.7270	-48.0951	13.94	15	17.94
nzsz–5b	New Zealand–Puysegur	165.0971	-47.9906	13.94	15	5
nzsz–6a	New Zealand–Puysegur	165.3168	-49.0829	22.71	15	17.94
nzsz–6b	New Zealand–Puysegur	164.7067	-48.9154	22.71	15	5
nzsz–7a	New Zealand–Puysegur	164.8017	-49.9193	23.25	15	17.94
nzsz–7b	New Zealand–Puysegur	164.1836	-49.7480	23.25	15	5
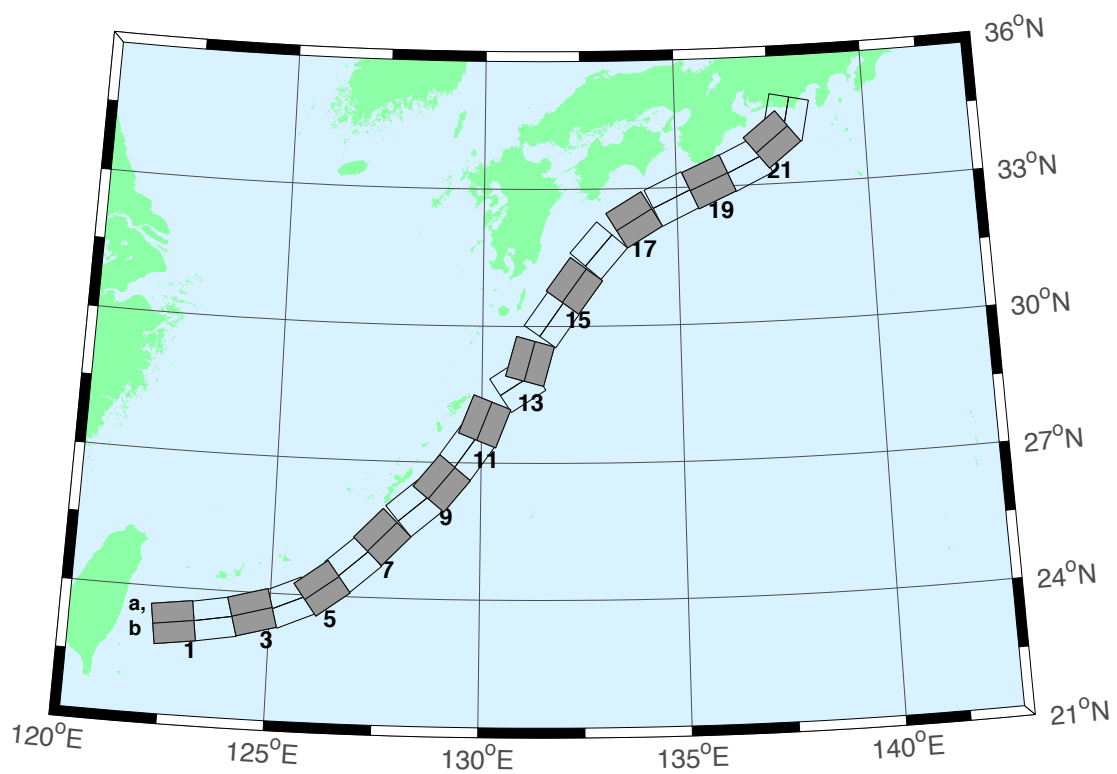
Figure B.11: Ryukyu–Kyushu–Nankai Zone unit sources.

Table B.11: Earthquake parameters for Ryukyu–Kyushu–Nankai Subduction Zone unit sources.

Segment	Description	Longitude(°E)	Latitude(°N)	Strike(°)	Dip(°)	Depth (km)
rnsz–1a	Ryukyu–Kyushu–Nankai	122.6672	23.6696	262	14	11.88
rnsz–1b	Ryukyu–Kyushu–Nankai	122.7332	23.2380	262	10	3.2
rnsz–2a	Ryukyu–Kyushu–Nankai	123.5939	23.7929	259.9	18.11	12.28
rnsz–2b	Ryukyu–Kyushu–Nankai	123.6751	23.3725	259.9	10	3.6
rnsz–3a	Ryukyu–Kyushu–Nankai	124.4604	23.9777	254.6	19.27	14.65
rnsz–3b	Ryukyu–Kyushu–Nankai	124.5830	23.5689	254.6	12.18	4.1
rnsz–4a	Ryukyu–Kyushu–Nankai	125.2720	24.2102	246.8	18	20.38
rnsz–4b	Ryukyu–Kyushu–Nankai	125.4563	23.8177	246.8	16	6.6
rnsz–5a	Ryukyu–Kyushu–Nankai	125.9465	24.5085	233.6	18	20.21
rnsz–5b	Ryukyu–Kyushu–Nankai	126.2241	24.1645	233.6	16	6.43
rnsz–6a	Ryukyu–Kyushu–Nankai	126.6349	25.0402	228.7	17.16	19.55
rnsz–6b	Ryukyu–Kyushu–Nankai	126.9465	24.7176	228.7	15.16	6.47
rnsz–7a	Ryukyu–Kyushu–Nankai	127.2867	25.6343	224	15.85	17.98
rnsz–7b	Ryukyu–Kyushu–Nankai	127.6303	25.3339	224	13.56	6.26
rnsz–8a	Ryukyu–Kyushu–Nankai	128.0725	26.3146	229.7	14.55	14.31
rnsz–8b	Ryukyu–Kyushu–Nankai	128.3854	25.9831	229.7	9.64	5.94
rnsz–9a	Ryukyu–Kyushu–Nankai	128.6642	26.8177	219.2	15.4	12.62
rnsz–9b	Ryukyu–Kyushu–Nankai	129.0391	26.5438	219.2	8	5.66
rnsz–10a	Ryukyu–Kyushu–Nankai	129.2286	27.4879	215.2	17	12.55
rnsz–10b	Ryukyu–Kyushu–Nankai	129.6233	27.2402	215.2	8.16	5.45
rnsz–11a	Ryukyu–Kyushu–Nankai	129.6169	28.0741	201.3	17	12.91
rnsz–11b	Ryukyu–Kyushu–Nankai	130.0698	27.9181	201.3	8.8	5.26
rnsz–12a	Ryukyu–Kyushu–Nankai	130.6175	29.0900	236.7	16.42	13.05
rnsz–12b	Ryukyu–Kyushu–Nankai	130.8873	28.7299	236.7	9.57	4.74
rnsz–13a	Ryukyu–Kyushu–Nankai	130.7223	29.3465	195.2	20.25	15.89
rnsz–13b	Ryukyu–Kyushu–Nankai	131.1884	29.2362	195.2	12.98	4.66
rnsz–14a	Ryukyu–Kyushu–Nankai	131.3467	30.3899	215.1	22.16	19.73
rnsz–14b	Ryukyu–Kyushu–Nankai	131.7402	30.1507	215.1	17.48	4.71
rnsz–15a	Ryukyu–Kyushu–Nankai	131.9149	31.1450	216	15.11	16.12
rnsz–15b	Ryukyu–Kyushu–Nankai	132.3235	30.8899	216	13.46	4.48
rnsz–16a	Ryukyu–Kyushu–Nankai	132.5628	31.9468	220.9	10.81	10.88
rnsz–16b	Ryukyu–Kyushu–Nankai	132.9546	31.6579	220.9	7.19	4.62
rnsz–17a	Ryukyu–Kyushu–Nankai	133.6125	32.6956	239	10.14	12.01
rnsz–17b	Ryukyu–Kyushu–Nankai	133.8823	32.3168	239	8.41	4.7
rnsz–18a	Ryukyu–Kyushu–Nankai	134.6416	33.1488	244.7	10.99	14.21
rnsz–18b	Ryukyu–Kyushu–Nankai	134.8656	32.7502	244.5	10.97	4.7
rnsz–19a	Ryukyu–Kyushu–Nankai	135.6450	33.5008	246.5	14.49	14.72
rnsz–19b	Ryukyu–Kyushu–Nankai	135.8523	33.1021	246.5	11.87	4.44
rnsz–20a	Ryukyu–Kyushu–Nankai	136.5962	33.8506	244.8	15	14.38
rnsz–20b	Ryukyu–Kyushu–Nankai	136.8179	33.4581	244.8	12	3.98
rnsz–21a	Ryukyu–Kyushu–Nankai	137.2252	34.3094	231.9	15	15.4
rnsz–21b	Ryukyu–Kyushu–Nankai	137.5480	33.9680	231.9	12	5
rnsz–22a	Ryukyu–Kyushu–Nankai	137.4161	34.5249	192.3	15	15.4
rnsz–22b	Ryukyu–Kyushu–Nankai	137.9301	34.4327	192.3	12	5

Appendix C

SIFT Testing

Authors: Lindsey Wright, Diego Arcas

C.1   Purpose

Forecast models are tested with synthetic tsunami events covering a range of tsunami source locations. Testing is also done with selected historical tsunami events when available.

The purpose of forecast model testing is three-fold. The first objective is to assure that the results obtained with NOAA's tsunami forecast system, which has been released to the Tsunami Warning Centers for operational use, are consistent those obtained by the researcher during the development of the forecast model. The second objective is to test the forecast model for consistency, accuracy, time efficiency, and quality of results over a range of possible tsunami locations and magnitudes. The third objective is to identify bugs and issues in need of resolution by the researcher who developed the Forecast Model or by the forecast software development team before the next version release to NOAA's two Tsunami Warning Centers.

Local hardware and software applications, and tools familiar to the researcher(s), are used to run the Method of Splitting Tsunamis (MOST) model during the forecast model development. The test results presented in this report lend confidence that the model performs as developed and produces the same results when initiated within the forecast application in an operational setting as those produced by the researcher during the forecast model development. The test results assure those who rely on the Santa Monica tsunami forecast model that consistent results are produced irrespective of system.

C.2   Testing Procedure

The general procedure for forecast model testing is to run a set of synthetic tsunami scenarios and a selected set of historical tsunami events through the forecast system application and compare the results with those obtained by the researcher during the forecast model development and presented in the Tsunami Forecast Model Report. Specific steps taken to test the model include:

1. Identification of testing scenarios, including the standard set of synthetic events, appropriate historical events, and customized synthetic scenarios that may have been used by

the researcher(s) in developing the forecast model.

2. Creation of new events to represent customized synthetic scenarios used by the researcher(s) in developing the forecast model, if any.

3. Submission of test model runs with the forecast system, and export of the results from A, B, and C grids, along with time series.

4. Recording applicable metadata, including the specific version of the forecast system used for testing.

5. Examination of forecast model results from the forecast system for instabilities in both time series and plot results.

6. Comparison of forecast model results obtained through the forecast system with those obtained during the forecast model development.

7. Summarization of results with specific mention of quality, consistency, and time efficiency.

8. Reporting of issues identified to modeler and forecast software development team.

9. Retesting the forecast models in the forecast system when reported issues have been addressed or explained.

Synthetic model runs were tested on a DELL PowerEdge R510 computer equipped with two Xeon E5670 processors at 2.93 Ghz, each with 12 MBytes of cache and 32GB memory. The processors are hex core and support hyperthreading, resulting in the computer performing as a 24 processor core machine. Additionally, the testing computer supports 10 Gigabit Ethernet for fast network connections. This computer configuration is similar or the same as the configurations of the computers installed at the Tsunami Warning Centers so the compute times should only vary slightly.

C.3   Results

The Santa Monica forecast model was tested with NOAA's tsunami forecast system version 3.2.

The Santa Monica forecast model was tested with four synthetic scenarios and one historical tsunami event. Test results from the forecast system and comparisons with the results obtained during the forecast model development are shown numerically in Table C.1 and graphically in Figures C.1 to C.5. The results show that the forecast model is stable and robust, with consistent and high quality results across geographically distributed tsunami sources and mega-event tsunami magnitudes. The model run time (wall clock time) was under 15.30 minutes for 8 hours of simulation time, and under 7.68 minutes for 4 hours. This run time is well within the 10 minute run time for 4 hours of simulation time and satisfies time efficiency requirements.

Four synthetic events were run on the Santa Monica forecast model. The modeled scenarios were stable for all cases tested, with no instabilities or ringing. Results show that the largest modeled amplitude was 251 centimeters (cm) and originated in the New Zealand-Kermadec-Tonga (NTSZ 30-39) source. Amplitudes greater than 100 cm were recorded for 3 of the 4 test

sources. The smallest signal of 54 cm was recorded at the Aleutian-Alaska-Cascadia (ACSZ 56-65) source. Direct comparisons of output from the forecast tool with results of both the Tohoku 2011 historical event and available development synthetic events, demonstrated that the wave pattern were nearly identical in shape, pattern and amplitude.

(a) A Grid

(b) B Grid

(c) C Grid

(d)
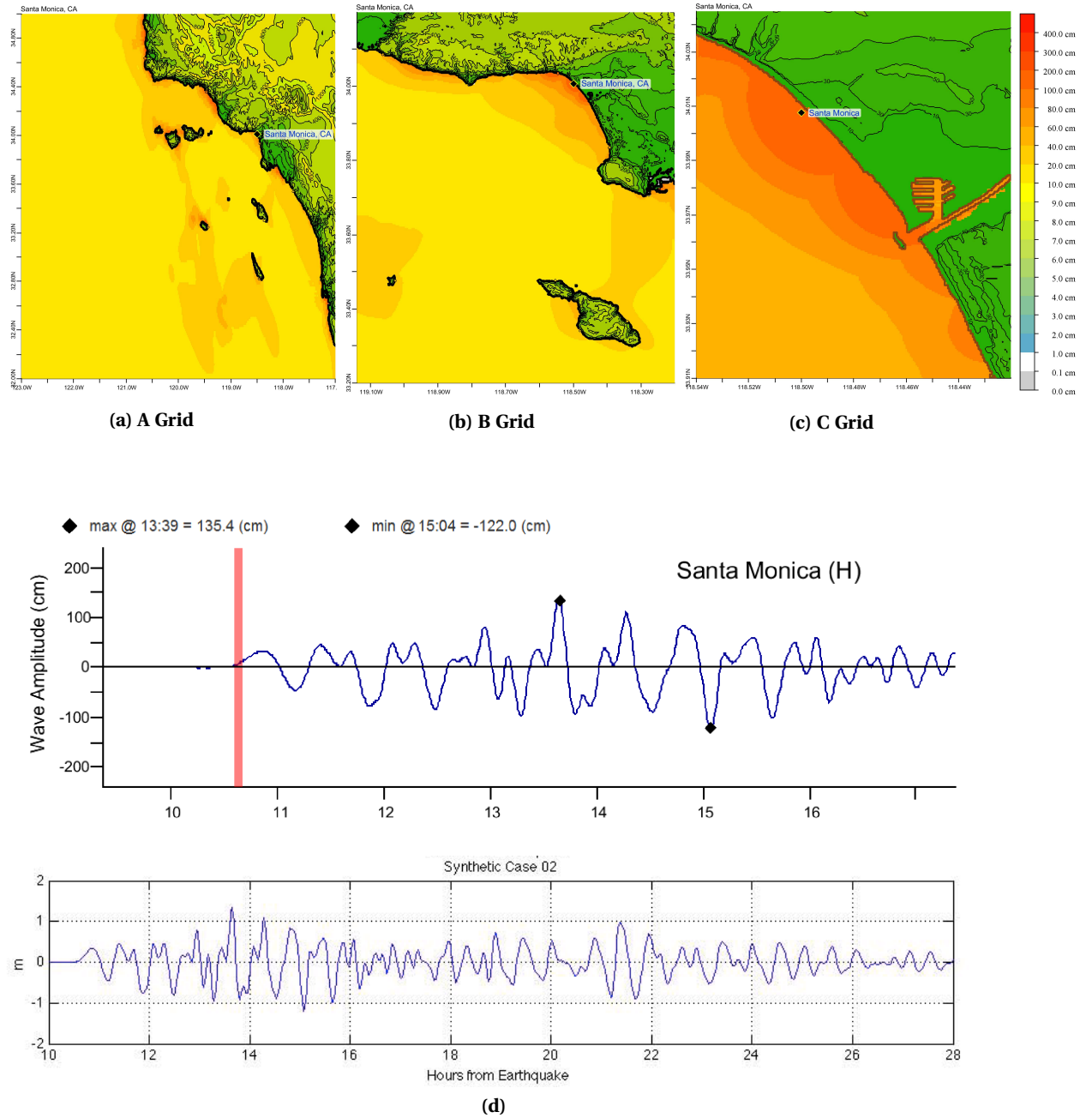
Figure C.1: Response of the Santa Monica, CA forecast model to synthetic scenario KISZ 22-31 (alpha=25). Maximum sea surface elevation for (a) A-grid, b) B-grid, c) C-grid. Sea surface elevation time series at the C-grid warning point (d). The lower time series plot is the result obtained during model development and is shown for comparison with test results.

(a) A Grid

(b) B Grid

(c) C Grid

(d)
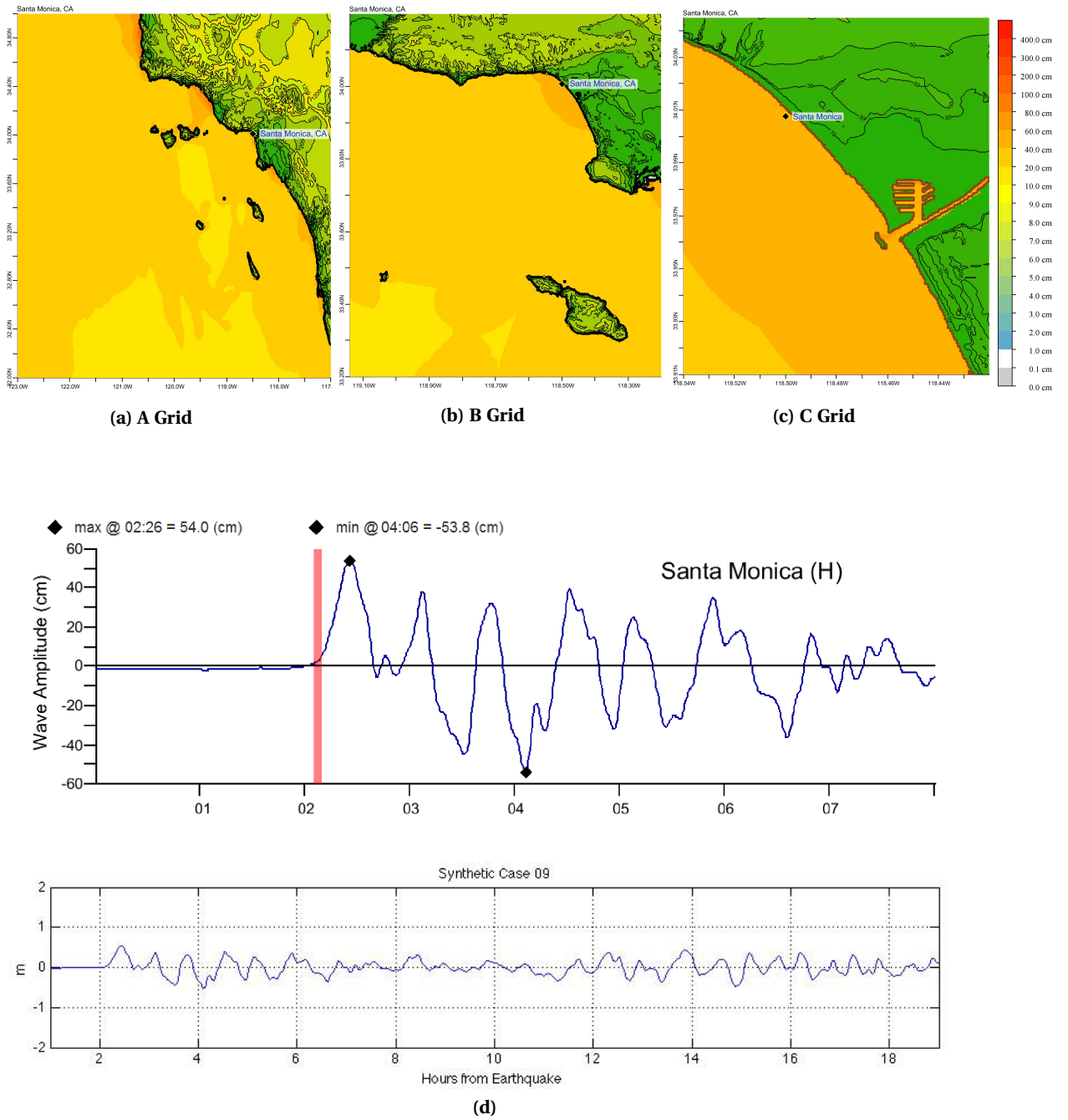
Figure C.2: Response of the Santa Monica, CA forecast model to synthetic scenario ACSZ 56-65 (alpha=25). Maximum sea surface elevation for (a) A-grid, b) B-grid, c) C-grid. Sea surface elevation time series at the C-grid warning point (d). The lower time series plot is the result obtained during model development and is shown for comparison with test results.

(a) A Grid   **(b) B Grid**   **(c) C Grid**

(d)
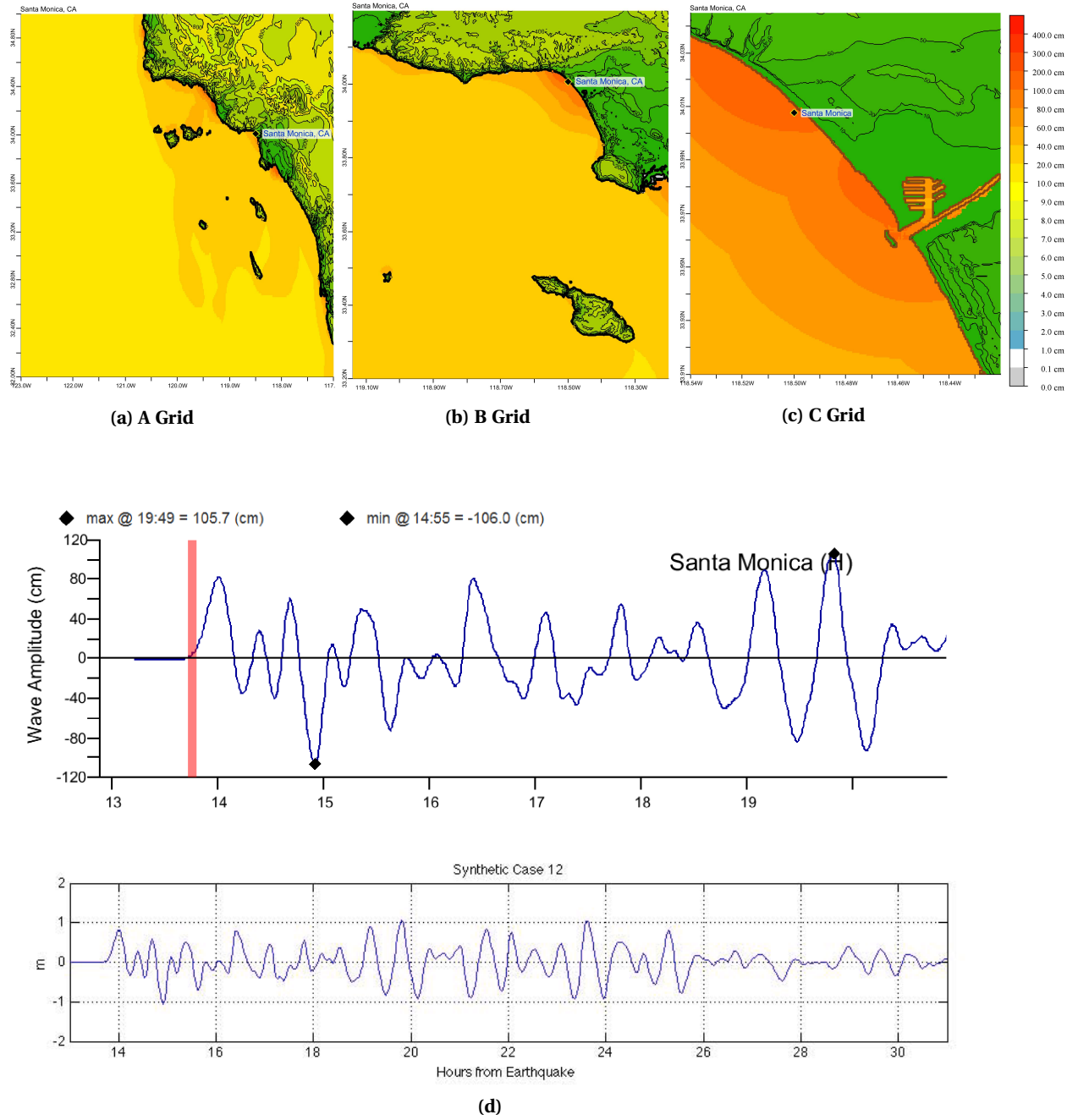
Figure C.3: Response of the Santa Monica, CA forecast model to synthetic scenario CSSZ 89-98 (alpha=25). Maximum sea surface elevation for (a) A-grid, b) B-grid, c) C-grid. Sea surface elevation time series at the C-grid warning point (d). The lower time series plot is the result obtained during model development and is shown for comparison with test results.

(a) A Grid   **(b) B Grid**   **(c) C Grid**

(d)
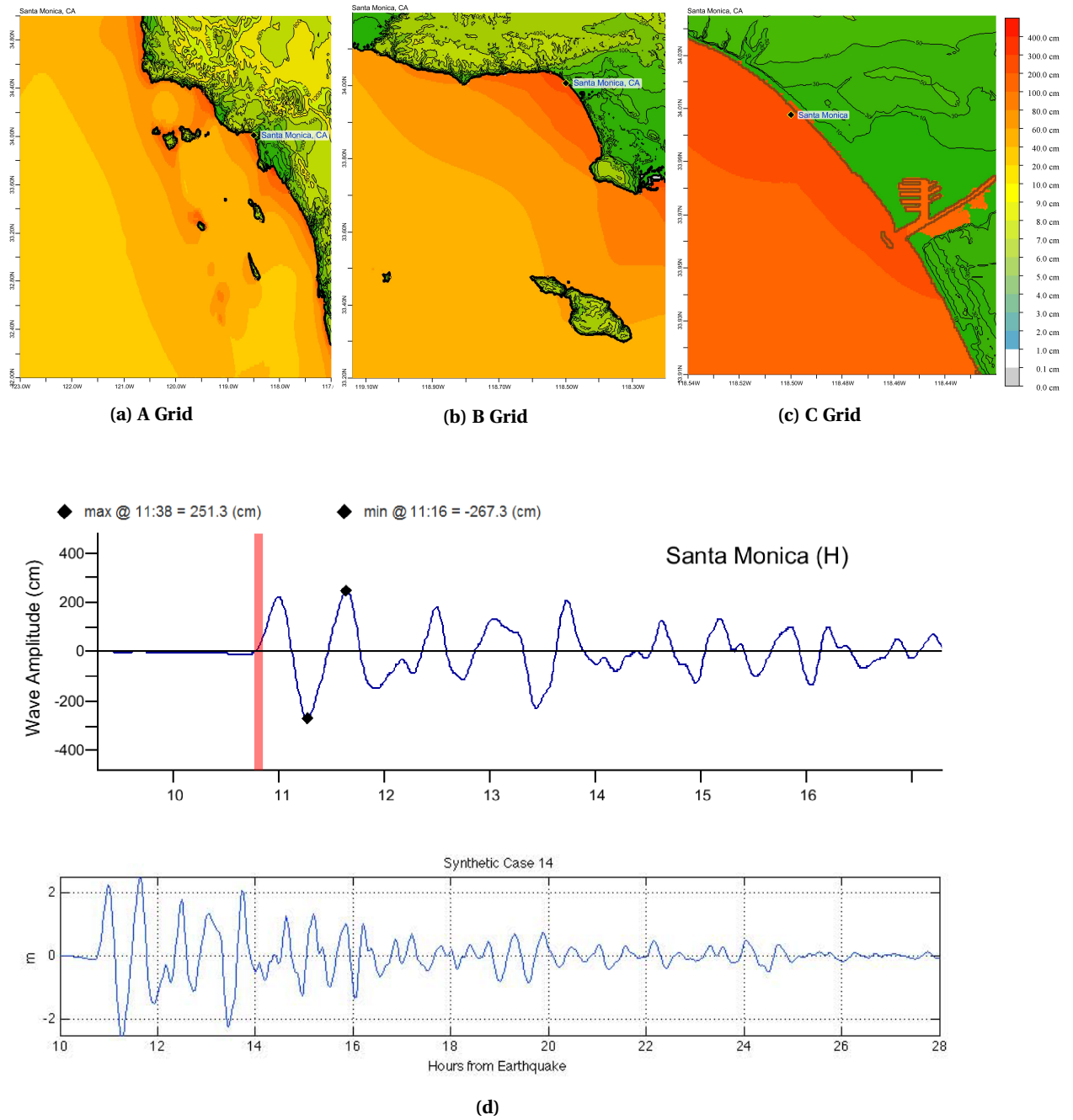
Figure C.4: Response of the Santa Monica forecast model to synthetic scenario NTSZ 30-39 (alpha=25). Maximum sea surface elevation for (a) A-grid, b) B-grid, c) C-grid. Sea surface elevation time series at the C-grid warning point (d). The lower time series plot is the result obtained during model development and is shown for comparison with test results.

(a) A Grid   (b) B Grid   (c) C Grid

(d)
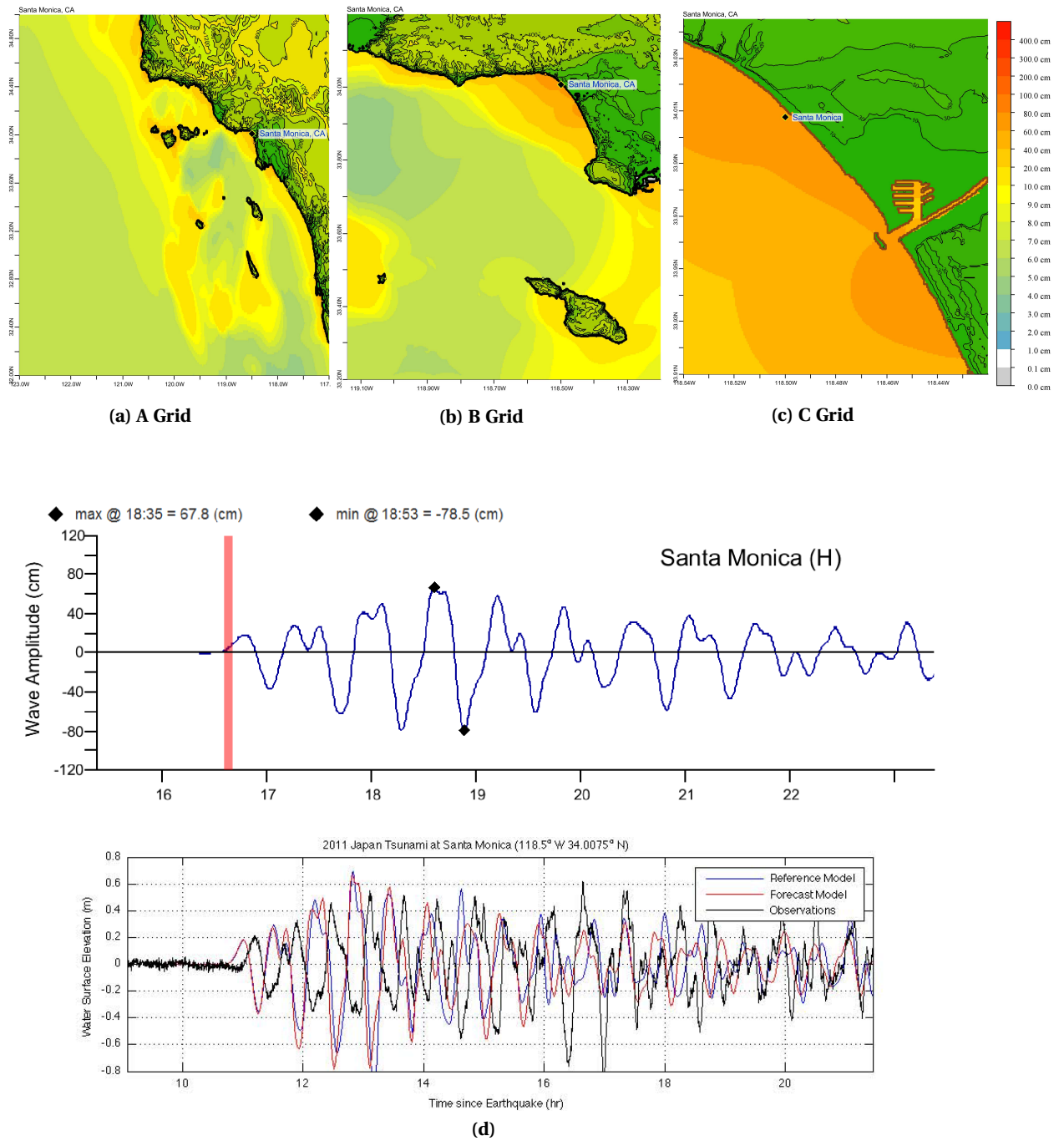
Figure C.5: Response of the Santa Monica forecast model to the 2011 Tohoku tsunami. Maximum sea surface elevation for (a) A-grid, b) B-grid, c) C-grid. Sea surface elevation time series at the C-grid warning point (d). The lower time series plot is the result obtained during model development and is shown for comparison with test results.

Table 1. Table of maximum and minimum amplitudes (cm) at the Santa Monica, California warning point for synthetic and historical events tested using SIFT 3.2 and obtained during development.

Scenario Name	Source Zone	Tsunami Source	α [m]	SIFT Max (cm)	Development Max (cm)	SIFT Min (cm)	Development Min (cm)
Mega-tsunami Scenarios							
KISZ 22-31	Kamchatka-Yap-Mariana-Izu-Bonin	A22-A31, B22-B31	25	135.4	133	-122.0	-120
ACSZ 56-65	Aleutian-Alaska-Cascadia	A56-A65, B56-B65	25	54	87	-53.8	-78
CSSZ 89-98	Central and South America	A89-A98, B89-B98	25	105.7	105	-106.0	-106
NTSZ 30-39	New Zealand-Kermadec-Tonga	A30-A39, B30-B39	25	251.3	248	-267.3	-267
Historical Events							
Tohoku 2011	Kamchatka-Yap-Mariana-Izu-Bonin			67.8		-78.5	

Table C.1: Table of maximum and minimum amplitudes at Santa Monica, California warning point for synthetic and historical events tested using SIFT.

Appendix D

Supplementary Material

D.1   Propagation Pattern
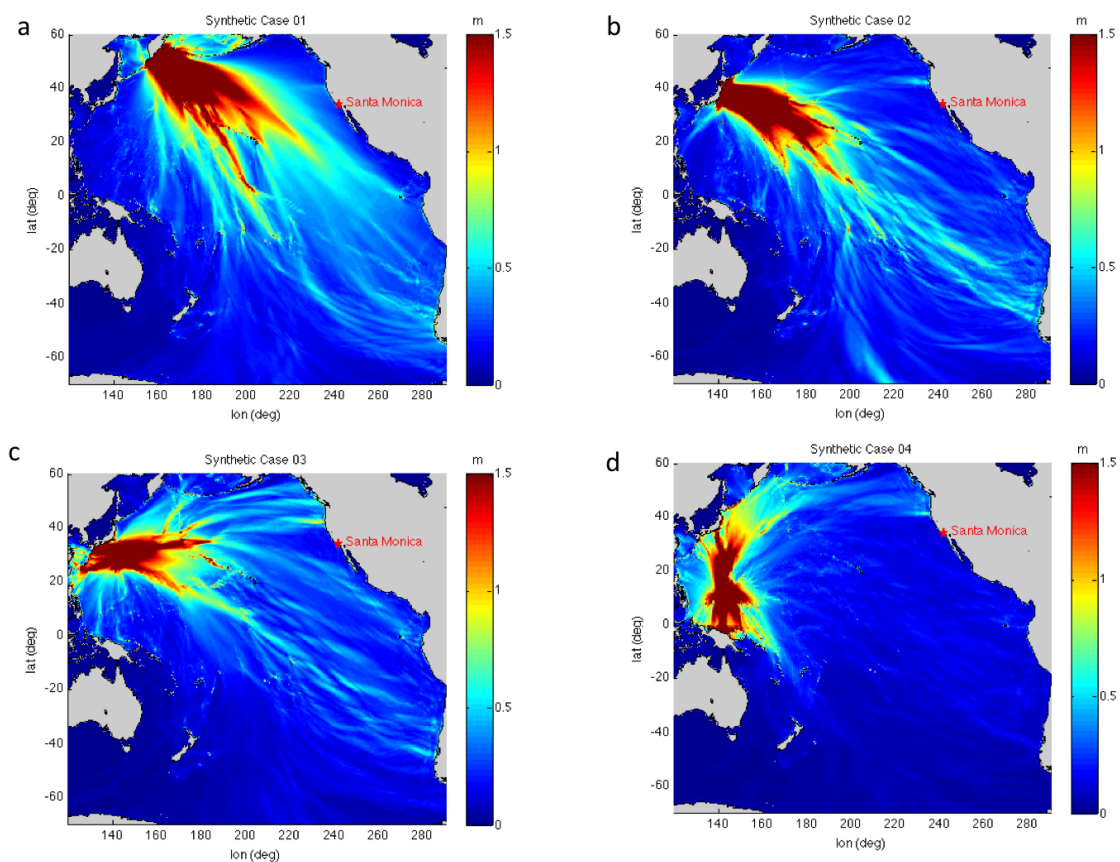
Figure D.1: Energy propagation patterns throughout the Pacific Ocean of the 19 synthetic tsunami scenarios used during the Santa Monica, CA forecast model development. Upper left panel is Case 1 of Table 3, upper right panel is case 2, lower left is case 3 and lower right is case 4.
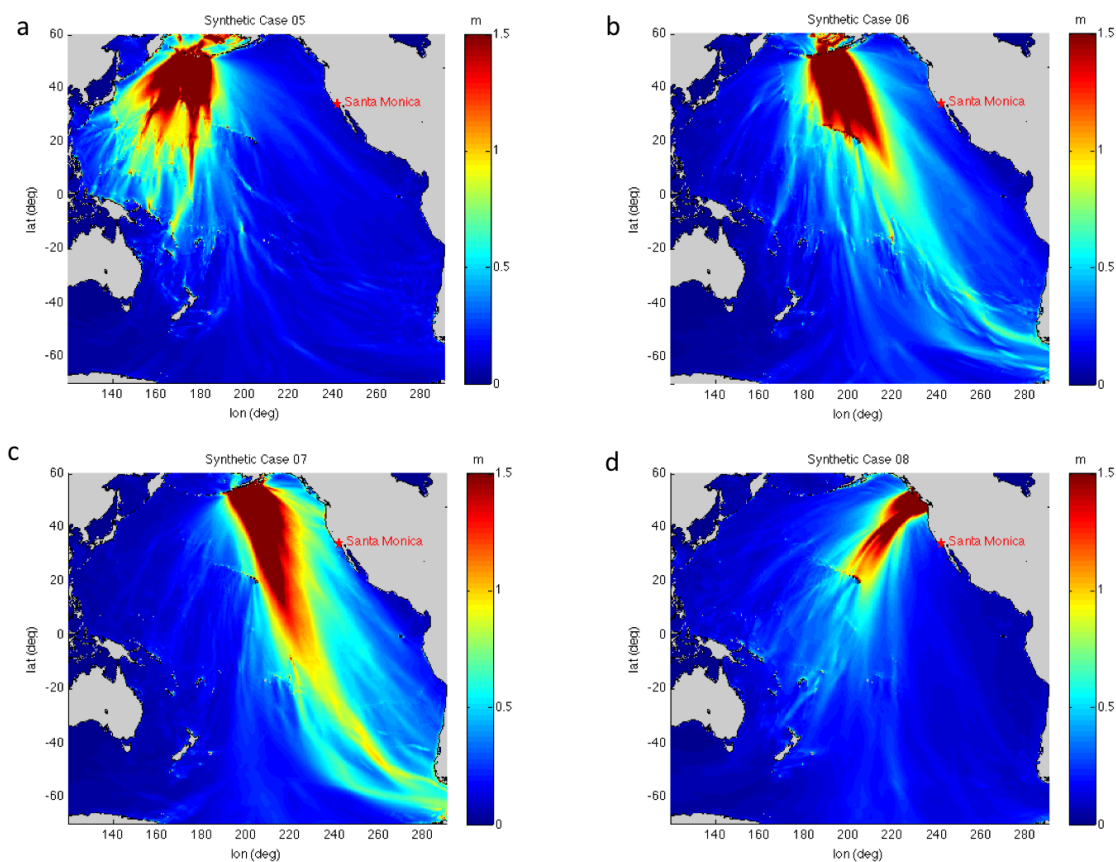
Figure D.2: Energy propagation patterns throughout the Pacific Ocean of the 19 synthetic tsunami scenarios used during the Santa Monica, CA forecast model development. Upper left panel is Case 5 of Table 3, upper right panel is case 6, lower left is case 7 and lower right is case 8.
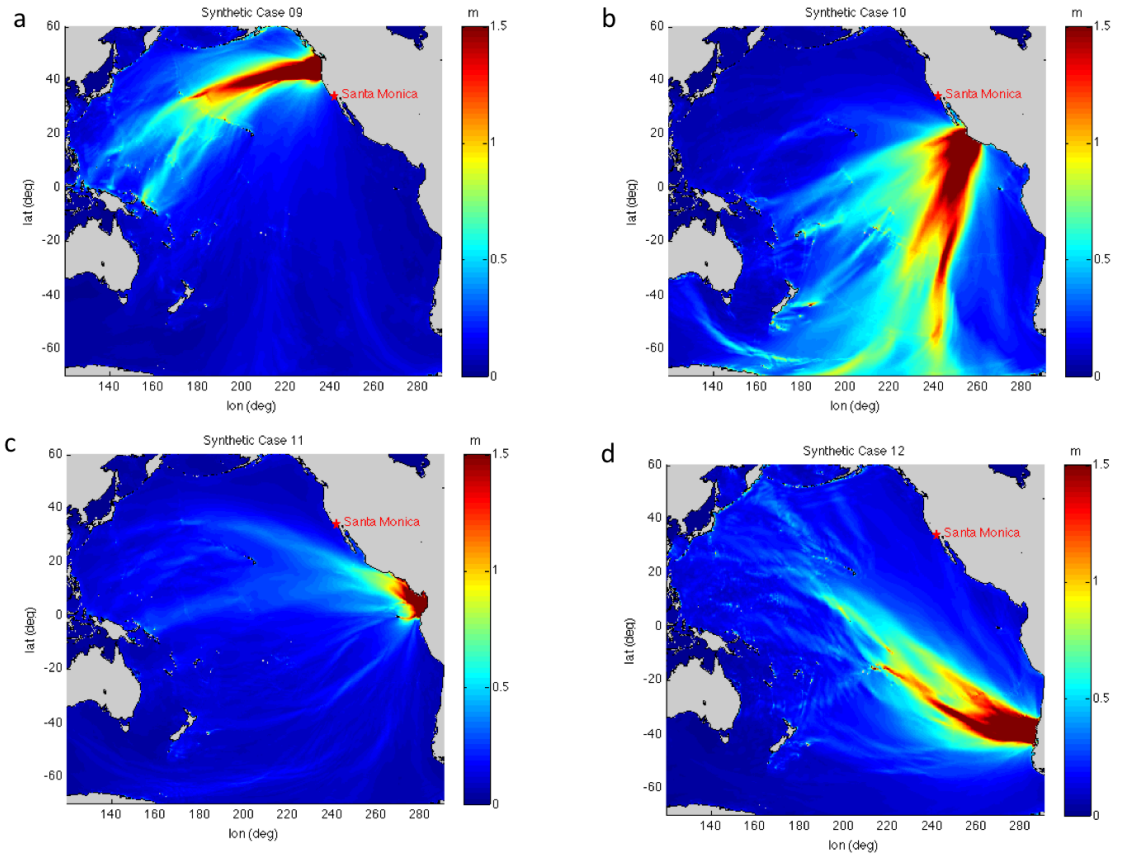
Figure D.3: Energy propagation patterns throughout the Pacific Ocean of the 19 synthetic tsunami scenarios used during the Santa Monica, CA forecast model development. Upper left panel is Case 9 of Table 3, upper right panel is case 10, lower left is case 11 and lower right is case 12.
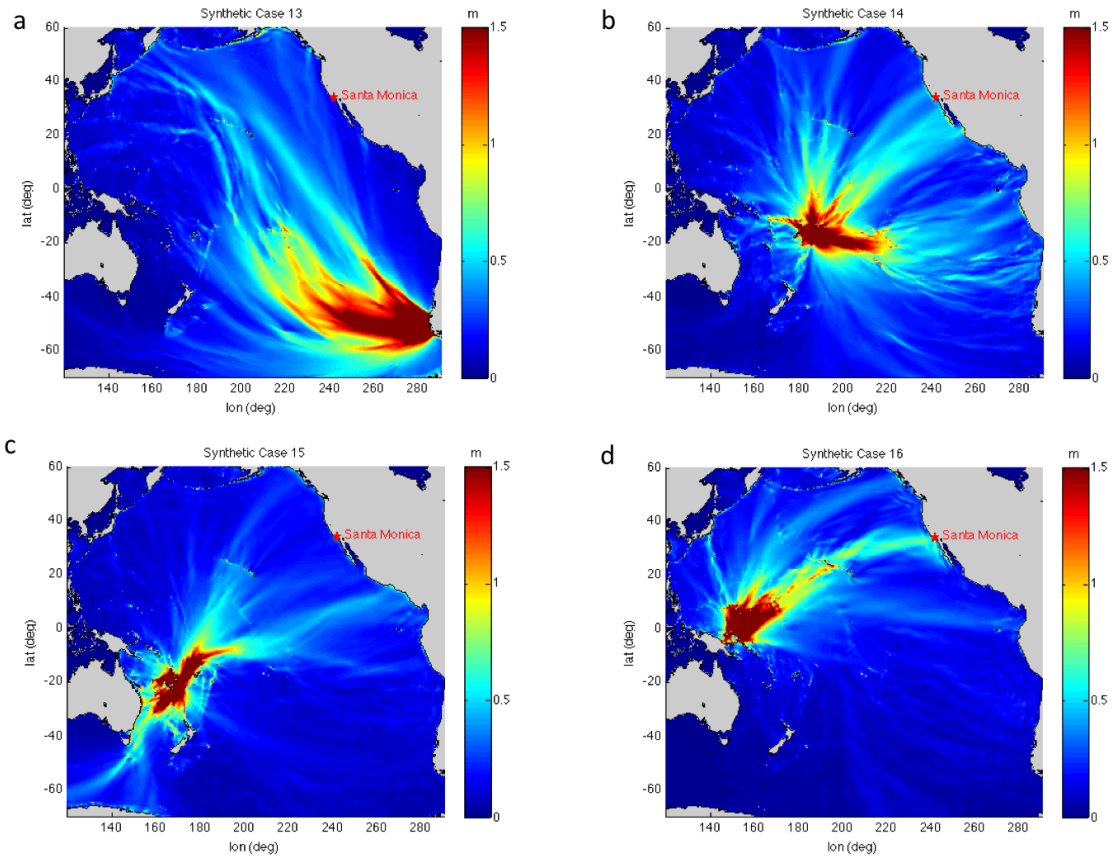
Figure D.4: Energy propagation patterns throughout the Pacific Ocean of the 19 synthetic tsunami scenarios used during the Santa Monica, CA forecast model development. Upper left panel is Case 13 of Table 3, upper right panel is case 14, lower left is case 15 and lower right is case 16. Synthetic scenario 16 represents the worst case scenario for Santa Monica, due to energy directivity effects.
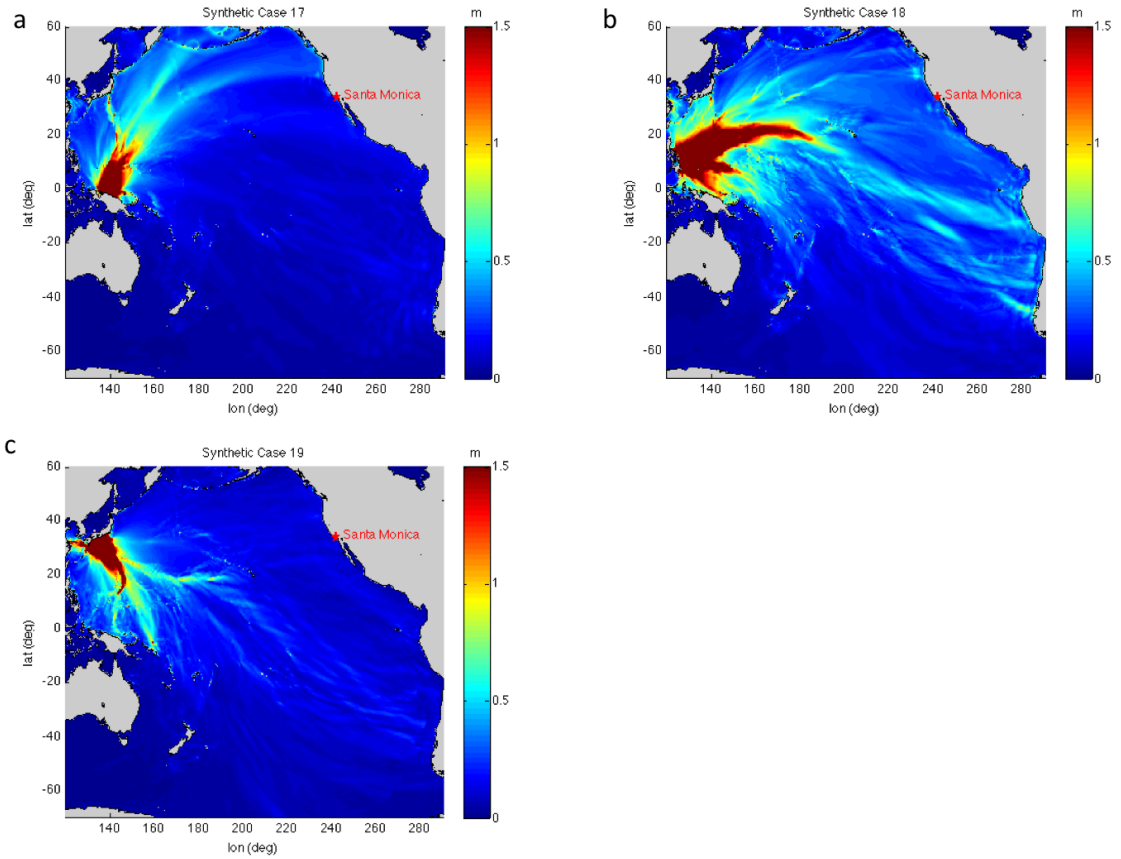
Figure D.5: Energy propagation patterns throughout the Pacific Ocean of the 19 synthetic tsunami scenarios used during the Santa Monica, CA forecast model development. Upper left panel is Case 17 of Table 3, upper right panel is case 18 and lower left is case 19.

D.2 Santa Monica Area Tsunami Inundation Maps (State of California).

California Emergency Management Agency
California Geological Survey
University of Southern California

Tsunami Inundation Map for Emergency Planning
Venice Quadrangle

State of California
County of Los Angeles

METHOD OF PREPARATION

Initial tsunami modeling was performed by the University of Southern California (USC) Tsunami Research Center funded through the California Emergency Management Agency (CalEMA) by the National Tsunami Hazard Mitigation Program. The tsunami modeling process utilized the MOST (Method of Splitting Tsunami) computational program (Version 0), which allows for wave evolution over a variable bathymetry and topography used for the inundation mapping (Titov and Gonzalez, 1997; Titov and Synolakis, 1998).

The bathymetric/topographic data that were used in the tsunami models consist of a series of nested grids. Near-shore grids with a 3 arc-second (75- to 90-meters) resolution or higher, were adjusted to "Mean High Water" sea-level conditions, representing a conservative sea level for the intended use of the tsunami modeling and mapping.

A suite of tsunami source events was selected for modeling, representing realistic local and distant earthquakes and hypothetical extreme undersea, near-shore landslides (Table 1). Local tsunami sources that were considered include offshore reverse-thrust faults, restraining bends on strike-slip fault zones and large submarine landslides capable of significant seafloor displacement and tsunami generation. Distant tsunami sources that were considered include great subduction zone events that are known to have occurred historically (1960 Chile and 1964 Alaska earthquakes) and others which can occur around the Pacific Ocean "Ring of Fire."

In order to enhance the result from the 75- to 90-meter inundation grid data, a method was developed utilizing higher-resolution digital topographic data (3- to 10-meters resolution) that better defines the location of the maximum inundation line (U.S. Geological Survey, 1993; Intermap, 2003; NOAA, 2004). The location of the enhanced inundation line was determined by using digital imagery and terrain data on a GIS platform with consideration given to historic inundation information (Lander, et al., 1993). This information was verified, where possible, by field work coordinated with local county personnel.

The accuracy of the inundation line shown on these maps is subject to limitations in the accuracy and completeness of available terrain and tsunami source information, and the current understanding of tsunami generation and propagation phenomena as expressed in the models. Thus, although an attempt has been made to identify a credible upper bound to inundation at any location along the coastline, it remains possible that actual inundation could be greater in a major tsunami event.

This map does not represent inundation from a single scenario event. It was created by combining inundation results for an ensemble of source events affecting a given region (Table 1). For this reason, all of the inundation region in a particular area will not likely be inundated during a single tsunami event.

References:

Intermap Technologies, Inc., 2003, Intermap product handbook and quick start guide: Intermap NEXTmap document on 5-meter resolution data, 112 p.

Lander, J.F., Lockridge, P.A., and Kozuch, M.J., 1993, Tsunamis Affecting the West Coast of the United States 1806-1992: National Geophysical Data Center Key to Geophysical Record Documentation No. 29, NOAA, NESDIS, NGDC, 242 p.

National Atmospheric and Oceanic Administration (NOAA), 2004, Interferometric Synthetic Aperture Radar (IfSAR) Digital Elevation Models from GeoSAR platform (EarthData): 3-meter resolution data.

Titov, V.V., and Gonzalez, F.I., 1997, Implementation and Testing of the Method of Tsunami Splitting (MOST): NOAA Technical Memorandum ERL PMEL – 112, 11 p.

Titov, V.V., and Synolakis, C.E., 1998, Numerical modeling of tidal wave runup: Journal of Waterways, Port, Coastal and Ocean Engineering, ASCE, 124 (4), pp 157-171.

U.S. Geological Survey, 1993, Digital Elevation Models: National Mapping Program, Technical Instructions, Data Users Guide 5, 48 p.

TSUNAMI INUNDATION MAP
FOR EMERGENCY PLANNING

State of California ~ County of Los Angeles
VENICE QUADRANGLE

March 1, 2009

SCALE 1:24,000

Table 1: Tsunami sources modeled for the Los Angeles County coastline.

Sources (M = moment magnitude used in modeled event)		Areas of Inundation Map Coverage and Sources Used		
		Malibu	Santa Monica	Los Angeles Harbor
Local Sources	Anacapa-Dume Fault	X	X	
	Catalina Fault	X		X
	Channel Island Thrust Fault			X
	Newport-Inglewood Fault			X
	Santa Monica Fault	X	X	
	Palos Verdes Landslide #1			X
	Palos Verdes Landslide #2			X
Distant Sources	Cascadia Subduction Zone #2 (M9.2)		X	X
	Central Aleutians Subduction Zone#1 (M8.9)		X	X
	Central Aleutians Subduction Zone#2 (M8.9)		X	X
	Central Aleutians Subduction Zone#3 (M9.2)	X	X	X
	Chile North Subduction Zone (M9.4)	X	X	X
	1960 Chile Earthquake (M9.5)		X	X
	1964 Alaska Earthquake (M9.2)	X	X	X
	Japan Subduction Zone #2 (M8.8)		X	X
	Kuril Islands Subduction Zone #2 (M8.9)		X	X
	Kuril Islands Subduction Zone #3 (M8.9)		X	X
	Kuril Islands Subduction Zone #4 (M8.8)		X	X

MAP EXPLANATION

~~~ Tsunami Inundation Line

▨ Tsunami Inundation Area

PURPOSE OF THIS MAP

This tsunami inundation map was prepared to assist cities and counties in identifying their tsunami hazard. It is intended for local jurisdictional, coastal evacuation planning uses only. This map, and the information presented herein, is not a legal document and does not meet disclosure requirements for real estate transactions nor for any other regulatory purpose.

The inundation map has been compiled with best currently available scientific information. The inundation line represents the maximum considered tsunami runup from a number of extreme, yet realistic, tsunami sources. Tsunamis are rare events; due to a lack of known occurrences in the historical record, this map includes no information about the probability of any tsunami affecting any area within a specific period of time.

Please refer to the following websites for additional information on the construction and/or intended use of the tsunami inundation map:

State of California Emergency Management Agency, Earthquake and Tsunami Program:
http://www.oes.ca.gov/WebPage/oeswebsite.nsf/Content/B1EC51BA2159317688257419F005EBD80?OpenDocument

University of Southern California – Tsunami Research Center:
http://www.usc.edu/dept/tsunamis/2005/index.php

State of California Geological Survey Tsunami Information:
http://www.conservation.ca.gov/cgs/geologic_hazards/Tsunami/index.htm

National Oceanic and Atmospheric Agency Center for Tsunami Research (MOST model):
http://nctr.pmel.noaa.gov/time/background/models.html

MAP BASE

Topographic base maps prepared by U.S. Geological Survey as part of the 7.5-minute Quadrangle Map Series (originally 1:24,000 scale). Tsunami inundation line boundaries may reflect updated digital orthophotographic and topographic data that can differ significantly from contours shown on the base map.

DISCLAIMER

The California Emergency Management Agency (CalEMA), the University of Southern California (USC), and the California Geological Survey (CGS) make no representation or warranties regarding the accuracy of this inundation map nor the data from which the map was derived. Neither the State of California nor USC shall be liable under any circumstances for any direct, indirect, special, incidental or consequential damages with respect to any claim by any user or any third party on account of or arising from the use of this map.

Figure D.6: Tsunami inundation map for emergency planning (Venice Quadrangle), The tsunami inundation area represents the combined maximum inundation extent of a set of 18 historical and artificial scenarios.

Figure D.7: Tsunami inundation map for emergency planning (Beverly Hills Quadrangle), The tsunami inundation area represents the combined maximum inundation extent of a set of 18 historical and artificial scenarios.

California Emergency Management Agency
California Geological Survey
University of Southern California

Tsunami Inundation Map for Emergency Planning
Topanga Quadrangle

State of California
County of Los Angeles

METHOD OF PREPARATION

Initial tsunami modeling was performed by the University of Southern California (USC) Tsunami Research Center funded through the California Emergency Management Agency (CalEMA) by the National Tsunami Hazard Mitigation Program. The tsunami modeling process utilized the MOST (Method of Splitting Tsunami) computational program (Version 0), which allows for wave evolution over a variable bathymetry and topography used for the inundation mapping (Titov and Gonzalez, 1997; Titov and Synolakis, 1998).

The bathymetric/topographic data that were used in the tsunami models consist of a series of nested grids. Near-shore grids with a 3 arc-second (75- to 90-meters) resolution or higher, were adjusted to "Mean High Water" sea-level conditions, representing a conservative sea level for the intended use of the tsunami modeling and mapping.

A suite of tsunami source events was selected for modeling, representing realistic local and distant earthquakes and hypothetical extreme undersea, near-shore landslides (Table 1). Local tsunami sources that were considered include offshore reverse-thrust faults, restraining bends on strike-slip fault zones and large submarine landslides capable of significant seafloor displacement and tsunami generation. Distant tsunami sources that were considered include great subduction zone events that are known to have occurred historically (1960 Chile and 1964 Alaska earthquakes) and others which can occur around the Pacific Ocean "Ring of Fire."

In order to enhance the result from the 75- to 90-meter inundation grid data, a method was developed utilizing higher-resolution digital topographic data (3- to 10-meters resolution) that better defines the location of the maximum inundation line (U.S. Geological Survey, 1993; Intermap, 2003; NOAA, 2004). The location of the enhanced inundation line was determined by using digital imagery and terrain data on a GIS platform with consideration given to historic inundation information (Lander, et al., 1993). This information was verified, where possible, by field work coordinated with local county personnel.

The accuracy of the inundation line shown on these maps is subject to limitations in the accuracy and completeness of available terrain and tsunami source information, and the current understanding of tsunami generation and propagation phenomena as expressed in the models. Thus, although an attempt has been made to identify a credible upper bound to inundation at any location along the coastline, it remains possible that actual inundation could be greater in a major tsunami event.

This map does not represent inundation from a single scenario event. It was created by combining inundation results for an ensemble of source events affecting a given region (Table 1). For this reason, all of the inundation region in a particular area will not likely be inundated during a single tsunami event.

References:

Intermap Technologies, Inc., 2003, Intermap product handbook and quick start guide: Intermap NEXTmap document on 5-meter resolution data, 112 p.

Lander, J.F., Lockridge, P.A., and Kozuch, M.J., 1993, Tsunamis Affecting the West Coast of the United States 1806-1992: National Geophysical Data Center Key to Geophysical Record Documentation No. 29, NOAA, NESDIS, NGDC, 242 p.

National Atmospheric and Oceanic Administration (NOAA), 2004, Interferometric Synthetic Aperture Radar (IfSAR) Digital Elevation Models from GeoSAR platform (EarthData): 3-meter resolution data.

Titov, V.V., and Gonzalez, F.I., 1997, Implementation and Testing of the Method of Tsunami Splitting (MOST): NOAA Technical Memorandum ERL PMEL – 112, 11 p.

Titov, V.V., and Synolakis, C.E., 1998, Numerical modeling of tidal wave runup: Journal of Waterways, Port, Coastal and Ocean Engineering, ASCE, 124 (4), pp 157-171.

U.S. Geological Survey, 1993, Digital Elevation Models: National Mapping Program, Technical Instructions, Data Users Guide 5, 48 p.

TSUNAMI INUNDATION MAP FOR EMERGENCY PLANNING

State of California ~ County of Los Angeles
TOPANGA QUADRANGLE

March 1, 2009

SCALE 1:24,000

Table 1: Tsunami sources modeled for the Los Angeles County coastline.

Sources (M = moment magnitude used in modeled event)		Areas of Inundation Map Coverage and Sources Used		
		Malibu	Santa Monica	Los Angeles Harbor
Local Sources	Anacapa-Dume Fault	X	X	
	Catalina Fault	X	X	X
	Channel Island Thrust Fault		X	
	Newport-Inglewood Fault			X
	Santa Monica Fault	X	X	
	Palos Verdes Landslide #1		X	X
	Palos Verdes Landslide #2		X	X
Distant Sources	Cascadia Subduction Zone #2 (M9.2)		X	X
	Central Aleutians Subduction Zone#1 (M8.9)		X	X
	Central Aleutians Subduction Zone#2 (M8.9)		X	X
	Central Aleutians Subduction Zone#3 (M9.2)		X	X
	Chile North Subduction Zone (M9.4)	X	X	X
	1960 Chile Earthquake (M9.5)		X	X
	1964 Alaska Earthquake (M9.2)	X	X	X
	Japan Subduction Zone #2 (M8.5)		X	X
	Kuril Islands Subduction Zone #2 (M8.9)		X	X
	Kuril Islands Subduction Zone #3 (M8.8)		X	X
	Kuril Islands Subduction Zone #4 (M8.8)		X	X

Cal EMA   CGS CALIFORNIA GEOLOGICAL SURVEY   USC UNIVERSITY OF SOUTHERN CALIFORNIA

MAP EXPLANATION

Tsunami Inundation Line
Tsunami Inundation Area

PURPOSE OF THIS MAP

This tsunami inundation map was prepared to assist cities and counties in identifying their tsunami hazard. It is intended for local jurisdictional, coastal evacuation planning uses only. This map, and the information presented herein, is not a legal document and does not meet disclosure requirements for real estate transactions nor for any other regulatory purposes.

The inundation map has been compiled with best currently available scientific information. The inundation line represents the maximum considered tsunami runup from a number of extreme, yet realistic, tsunami sources. Tsunamis are rare events; due to a lack of known occurrences in the historical record, this map includes no information about the probability of any tsunami affecting any area within a specific period of time.

Please refer to the following websites for additional information on the construction and/or intended use of the tsunami inundation map:

State of California Emergency Management Agency, Earthquake and Tsunami Program:
http://www.oes.ca.gov/WebPage/oeswebsite.nsf/Content/B1EC51BA215931768825741F005E8D80?OpenDocument

University of Southern California – Tsunami Research Center:
http://www.usc.edu/dept/tsunamis/2005/index.php

State of California Geological Survey Tsunami Information:
http://www.conservation.ca.gov/cgs/geologic_hazards/Tsunami/index.htm

National Oceanic and Atmospheric Agency Center for Tsunami Research (MOST model):
http://nctr.pmel.noaa.gov/time/background/models.html

MAP BASE

Topographic base maps prepared by U.S. Geological Survey as part of the 7.5-minute Quadrangle Map Series (originally 1:24,000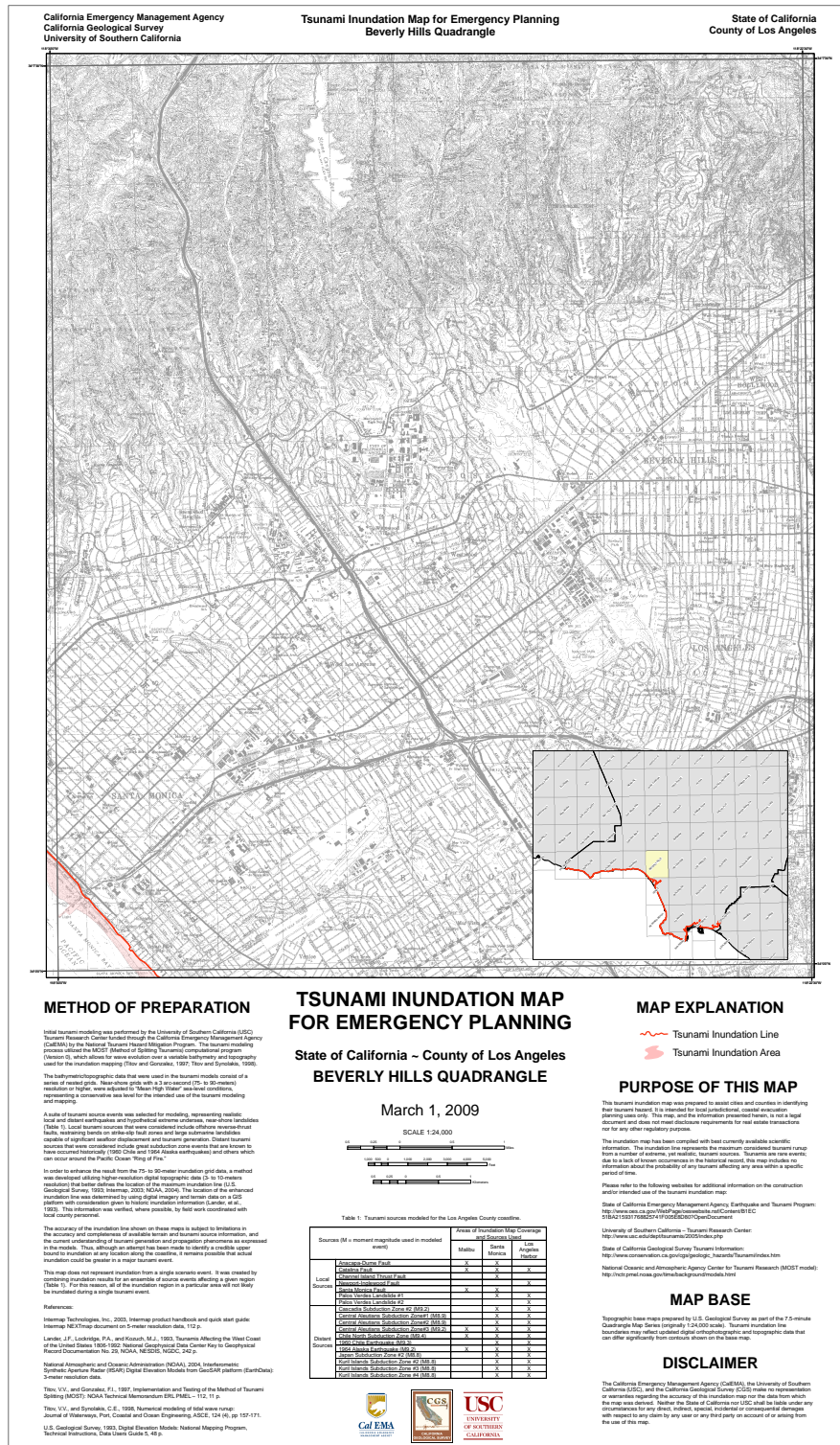 scale). Tsunami inundation line boundaries may reflect updated digital orthophotographic and topographic data that can differ significantly from contours on the base map.

DISCLAIMER

The California Emergency Management Agency (CalEMA), the University of Southern California (USC), and the California Geological Survey (CGS) make no representation or warranties regarding the accuracy of this inundation map nor the data from which the map was derived. Neither the State of California nor USC shall be liable under any circumstances for any direct, indirect, special, incidental or consequential damages with respect to any claim by any user or any third party on account of or arising from the use of this map.

Figure D.8: Tsunami inundation map for emergency planning (Topanga Quadrangle), The tsunami inundation area represents the combined maximum inundation extent of a set of 18 historical and artificial scenarios.

143